AD-A129 652 THE INFLUENCE OF IMPURITIES IN TUNGSTEN AND MATRIX COMPOSITION ON THE TUN..(U) TECHNISCHE UNIV VIENNA (AUSTRIA) INST FUER CHEMISCHE TECHNOLO.. B LUX ET AL. 1/2

UNCLASSIFIED OCT 82 DAJA37-80-C-0008 F/G 11/6 NL

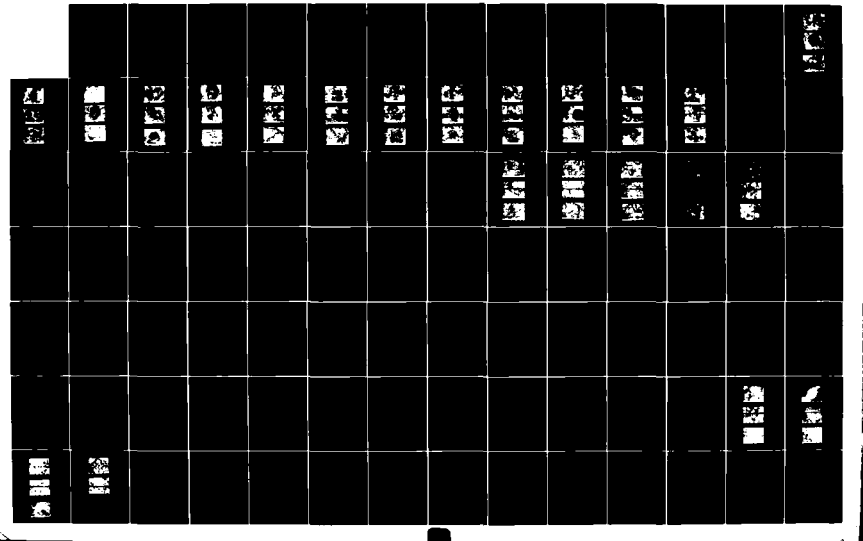

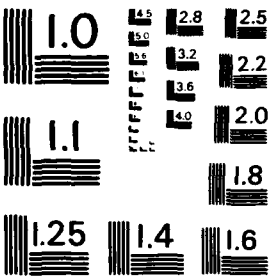

(14)

The Influence of Impurities in Tungsten and Matrix Composition on the Tungsten-Matrix Interfacial Properties of Heavy Metal Alloys

Contract No. DAJA - 80 - C - 0008

The Influence of Impurities in Tungsten and Matrix Composition on the Tungsten-Matrix Interfacial Properties of Heavy Metal Alloys

Final Technical Report

covering the period

November 1979 - November 1982

B.Lux, W.J.Huppmann, G.Jangg, H.Danninger, W.Pisan
Institut für Chemische Technologie Anorganischer Stoffe
TU Vienna

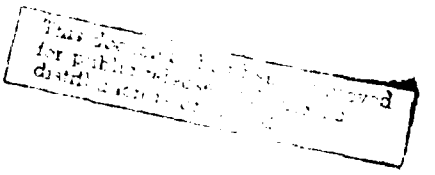

UNCLASSIFIED

SECURITY CLASSIFICATION OF THIS PAGE (When Data Entered)

R&D 2751-MS

REPORT DOCUMENTATION PAGE

READ INSTRUCTIONS BEFORE COMPLETING FORM

1. REPORT NUMBER	2. GOVT ACCESSION NO. AD-A129652 / 3. RECIPIENT'S CATALOG NUMBER
4. TITLE (and Subtitle) The Influence of Impurities in Tungsten and Matrix Composition on the Tungsten-Matrix Interfacial Properties of Heavy Metal Alloys	5. TYPE OF REPORT & PERIOD COVERED Final Technical Report Nov 79 - Nov 82
	6. PERFORMING ORG. REPORT NUMBER
7. AUTHOR(s) B. Lux, W.J. Huppmann, G. Jangg, H. Danninger, W. Pisan	8. CONTRACT OR GRANT NUMBER(s) DAJA37-80-C-0008
9. PERFORMING ORGANIZATION NAME AND ADDRESS Institut für Chemische Technologie anorganischer Stoffe Technische Universität Wien Getreidemarkt 9, A-1060 Vienna	10. PROGRAM ELEMENT, PROJECT, TASK AREA & WORK UNIT NUMBERS 6.11.02A 1T16 1102BH57-04
11. CONTROLLING OFFICE NAME AND ADDRESS USARDSG-UK Box 65 FPO New York 09510	12. REPORT DATE October 1982
	13. NUMBER OF PAGES 135
14. MONITORING AGENCY NAME & ADDRESS(if different from Controlling Office)	15. SECURITY CLASS. (of this report) Unclassified
	15a. DECLASSIFICATION/DOWNGRADING SCHEDULE

16. DISTRIBUTION STATEMENT (of this Report)

Approved for public release; distribution unlimited

17. DISTRIBUTION STATEMENT (of the abstract entered in Block 20, if different from Report)

18. SUPPLEMENTARY NOTES

19. KEY WORDS (Continue on reverse side if necessary and identify by block number)

Tungsten heavy metals, liquid phase sintering, starting W powders, pore formation by impurities, influence of the sintering cycle, sintering time.

20. ABSTRACT (Continue on reverse side if necessary and identify by block number)

The mechanical properties of tungsten heavy metals are strongly influenced by the quality of the starting materials, especially the powders. Powders that are too coarse result in highly porous heavy metals, regardless of the sintering conditions, as, due to insufficient distribution of the binder melt, liquid phase sintering occurs only locally. A second, although different, type of porosity is caused by traces of alkaline metals or rare earths, the pores in this case being formed during liquid phase sintering. These

DD FORM 1 JAN 73 1473 EDITION OF 1 NOV 65 IS OBSOLETE

UNCLASSIFIED

SECURITY CLASSIFICATION OF THIS PAGE (When Data Entered)

20. (continued)

elements apparently promote reduction of oxide traces and Ostwald ripening of the resulting micropores. The influence of most other impurities is less pronounced but could be identified by statistical evaluation.

Another important parameter is the sintering cycle. An optimal sintering cycle affords sufficient pre-reduction before liquid phase sintering and yields a fine, homogeneous microstructure. Too short a time for liquid phase sintering results in inhomogeneous material with insufficient ductility. Too long a sintering time results in grain coarsening and in considerable microporosity, which is apparently caused by the same mechanism as with alkaline metals, i.e. reduction of oxide traces, though at a much slower rate.

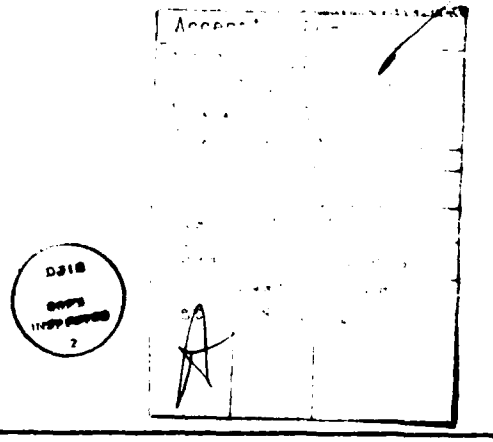

1. Introduction

The two-phase alloys commonly known as "Tungsten Heavy Metals" are a successful combination of the heavy and strong but relatively brittle bcc W grains and a highly ductile fcc Ni-Fe-W binder. High density - almost that of pure W - and strength combined with excellent ductility are the principal advantages of these alloys. Depending on binder content, densities ranging from 17,1 (with 10& binder) to 18,5 (with 3% binder) are attained; a further increase in W content does not yield a corresponding increase in density as the resulting material is porous (1). The tensile strength is usually between 950 and 1000 N/mm^2, and, most important of all, the elongation ranges from $< 5\%$ for 97% W to $> 20\%$ for 90% W. However, the properties, especially the ductility, depend very much on several parameters, the most important of which are:

a) formation of the appropriate microstructure during the sintering process, which is influenced mainly by the sintering parameters temperature and time

b) absence of certain impurities which appear to cause strong embrittlement of the heavy metals by lowering the interphase strength between W grains and binder or by causing pore formation.

The sensitivity of the heavy metals towards those parameters is probably responsible for certain difficulties encountered in the reproducibility of the properties; slight changes in the sintering parameters or starting materials can cause considerable deterioration of the mechanical properties, esp. of the ductility.

The first group of problems is mainly a function of furnace control, esp. furnace temperature and temperature distribution within the sintering boats and even within the samples. The problems encountered with impurities, however, are more difficult to identify, as there are several sources for detrimental elements:

1) Impurities contained in the starting powders W, Ni, Fe. As both Ni and Fe of "carbonyl quality" are used, they are relatively pure. Further their amount in the heavy metals is much lower than that of W, so that the impurities contained in the W powders are of much greater importance.

2) Impurities brought into the material during blending and compaction. In this stage contamination can be easily avoided by proper precautions.

3) Residues from cracked pressing lubricant not removedduring de-waxing. By using suitable pressing lubricants and carefully optimizing the de-waxing stage of the sintering cycle,at least with smaller samples the pressing lubricant can be completely removed.

4) Impurities from the sintering atmosphere absorbed by the heavy metals during sintering.

Earlier experiments (2,3) had shown that the most pronounced deterioration of the mechanical properties is caused by oxygen. During storage, the surface of the powders - W, Ni and Fe - are inadvertently oxidized. During liquid phase sintering the oxides are to some extent reduced by H_2, and the resulting H_2O tends to form pores and blisters which weaken the material; remaining oxygen is concentrated at the phase boundaries were it weakens interphase strength and causes the material to fail at very low degrees of deformation ($< 2\%$). This contamination, however, can easily be identified by SEM investigation of the fracture surfaces; it is characterized by intergranular fracture and esp. by W spheres from which the binder has completely peeled off without leaving any traces. Careful prereduction of the compacts at temperatures $>1000^{\circ}C$ before liquid phase sintering, however, is sufficient to obtain reasonably oxygen-free material.

Further test proved that heavy metals are also sensitive to hydrogen embrittlement: due to the strong influence of the temperature on the solubility of hydrogen both in W and Ni-Fe, rapid cooling may trap hydrogen in the heavy metals. Heat treatment in vacuum or even slow cooling permits the surplus hydrogen to escape, more than doubling the elongation.

Formation of brittle intermetallic phases by slow cooling, as described by several authors (4,5), was not observed. The decrease in ductility through rapid cooling was more pronounced the higher the temperature from which the samples were quenched; below 800°C no detrimental effect was observed (6; see also 7).

First experiments with intentionally doped W powders had shown that Na in particular promotes formation of pores and often even externally visible blisters which considerably weaken the material. Certain impurities, e.g. Al can also be harmful, while many other dopants investigated had no effect on the properties (1,3,6). With this in mind, the extension of the work to include new dopants, and in particular combinations of various additives was regarded to be of principal importance. The excellent reproducibility attained with the developed sintering cycle would enable identification of even slight effects from the doping additives. However, further investigation of the sintering process was also interesting, because it was hoped that more detailed knowledge could lead to better explanations for several as yet unclear effects which had been observed.

2. Starting materials

All W powders investigated were specially prepared and supplied to us by an Austrian tungsten manufacturer. In accordance with the intentions of the program, W powders with various doping additives were produced. The elements selected for doping were mainly those present in varying quantities in the usual industrial W powder grades.

All dopants were added to the tungstate solution before precipitation of APT, thus ensuring homogeneous distribution. The reduction parameters - temperature, humidity of the hydrogen atmosphere - were selected for powders of ~3 µm average grain size, as usually used for the production of W heavy metals. Due to the promoting effect of several elements on grain growth during H_2 reduction e.g. Na, Li (8,9) the powders containing those elements were considerably coarser with grain sizes up to >20 µm, as shown both by Fisher SSS and sedimentation (see attached sheets). The chemical compositions of the powders as supplied by the manufacturer are shown in Tab. 1. The purity of the W powders themselves is very satisfactory, the impurity level generally being lower than 20 ppm and in some cases even < 10 ppm. By comparing the amount of dopant added before reduction to the real content in the W powder as analyzed after reduction, the evaporation of some elements during reduction is clearly shown (9).

The compacting and sintering behaviour of the W powders is also influenced considerably by parameters not identified by Fisher SSS or sedimentation, e.g. grain shape and tendency to form agglomerates. Therefore all powders were also investigated by SEM; representative photos are shown in Fig. 1-37.

Besides the differences in grain size and grain size distribution as shown by Fisher SSS and the sedimentation sheets, the differences in grain shape are noteworthy. In some cases clear-facetted crystals are observed (e.g. with the powders containing Li and Na) while other final materials are roughly irregular or even almost spherical (e.g. the powders doped with Al or K). The powders containing Al also exhibit surface contaminants which were shown by EEDS to consist of Al_2O_3.

Regarding the agglomerates, almost all powders contain certain amount of agglomerates, although they are of the rather different form. The powders containing alkaline metals in particular exhibit very dense, compact agglomerates; as shown

Table 1: Chemical Analysis of the W-powders (contents in ppm)

	Additive	C	O_2	P	Al	Ca	Co	Cr	Cu	Fe	K	Mg	Mo	Na	Ni	Si	V
5o3		2o	24o	21	< 1o	< 1o				12			< 2o	26	< 1o	< 2o	
E 2	25o Na	7	13o	42	< 1o	< 1o				< 1o			< 2o	2o	< 1o	< 2c	
E 5	25o Li	4	63o	44	< 1o	< 1o				< 1o			< 2o	< 1o	< 1o	< 2o	
E 8	188 Ca	15	28o	43	< 1o	22o				< 1o			< 2o	< 1o	< 1o	< 2o	
E 11	25o B	24	76o	48	< 1o	< 1o				< 1o			< 2o	22	< 1o	< 2o	
E 14	25o Al	17	47o	37	288	< 1o				< 1o			< 2o	22	< 1o	< 2o	
E 17	1oo Si	11	47o	24	< 1o	12	< 1o	< 2o	< 1o	12	14	< 1o	< 2o	48	< 1o	96	< 25
E 21	14o Na, 1oo P	24	31o	93	< 1o	< 1o	< 1o	< 2o	< 1o	< 1o	< 1o	< 1o	< 2o	24	< 1o	< 2o	< 25
E 24	1oo As, Sb, Bi	15	64o	31	< 1o	12	< 1o	< 2o	< 1o	24	< 1o	< 1o	< 2o	26	12	< 2o	< 25
E 27	1oo U	11	45o	29	< 1o	16	< 1o	< 2o	< 1o	< 1o	< 1o	< 1o	< 2o	18	< 1o	< 2o	< 25
E 3o	188 Na, 1o6 Al 113 U, 5oo F	14	22o	52	64	< 1o				12			< 2o	48	< 1o	< 2o	
E 33		11	31o	49	< 1o	< 1o				< 1o			< 2o	14	< 1o	< 2o	
E 36	1oo Na	13	24o	3o	< 1o	12	< 1c	< 2o	< 1o	< 1o	14	< 1o	< 2o	22	< 1o	< 2o	< 25
E 39	5o Na	6	27o	23	< 1o	16	< 1o	< 2o	< 1o	< 1o	1o	< 1o	< 2o	22	< 1o	< 2o	< 25
E 45	1oo Li	4	53o	36	< 1o	< 1o	< 1o	< 2o	< 1o	< 1o	< 1o	< 1o	< 2o	< 1o	< 1o	< 2o	

Table 1 (continued)

	Addition	grain size (um)	C	O	P	Al	Ca	Co	Cr	Cu	Fe	K	Mg	Mo	Na	Ni	Si	V	Dopant
640		3,00	20	240		23					16			60	18	<10	<20		
E 48	200 Na	25,10	7	30	16	<10	<10	<10	<20	<10	16	16	<10	<20	<10	<10	<20	<25	10 Na
E 51	200 Li	40,00	22	450	51	<10	<10	<10	<20	<10	12	30	<10	<20	<10	<10	<20	<25	193 Li
E 56	200 Al	11,95	12	200	31	<10	<10	<10	<20	<10	16	20	<10	<20	<10	<10	<20	<25	116 Al
E 61	Impure Blue Oxide	18,00	8	200	47	116	<10	<10	<20	<10	20	16	<10	<20	12	<10	<20	<25	20 F
E 63	200 K	4,58	2	160	33	<10	<10	<10	<20	<10	14	<10	<10	<20	<10	<10	<20	<25	10 K
E 67	100 K	4,90	10	140	30	<10	<10	<10	<20	<10	<10	<10	<10	<20	<10	<10	<20	<25	10 K
E 71	50 K	3,95	10	180	31	<10	<10	<10	<20	<10	<10	<10	<10	<20	<10	<10	<20	<25	10 K
E 75	200 Na, 120 Si	5,80	17	330	28	<10	<10	<10	<20	<10	<10	<10	<10	<20	64	<10	100	<25	64Na,100Si
E 83	100 Na, 80 F	5,20	5	140	31	<10	<10	<10	<20	<10	12	<10	<10	<20	20	<10	<20	<25	20Na, 20F
E 87	150 Mg	3,01	9	310	29	<10	<10	<10	<20	<10	<10	<10	200	<20	16	<10	<20	<25	200 Mg
E 91	200 Ba	3,35	8	250	28	<10	<10	<10	<20	<10	<10	<10	<10	<20	<10	<10	<20	<25	
E 95																			
E 99	100 Zn	3,75	11	200	25	<10	<10	<10	<20	<10	<10	<10	<10	<20	14	<10	<20	<25	
E103	100 Cu	3,19	24	290	29	<10	<10	<10	<20	132	<10	<10	<10	<20	14	<10	<20	<25	132 Cu
E107	100 Ni	3,18	6	210	27	<10	<10	<10	<20	<10	12	<10	<10	<20	12	152	<20	<25	152 Si
E111	Rare Earths 84 Ce	3,40	19	230	29	<10	<10	<10	<20	<10	<10	<10	<10	<20	10	<10	<20	<25	
E115	100 P	3,13	19	250	83	<10	<10	<10	<20	<10	<10	<10	<10	<20	14	<10	<20	<25	83 P

these agglomerates formed during reduction when small particles were cemented together by molten tungsten bronzes; the high strength and density of these objects is thus hardly surprising. On the other hand Al is particular effective in inhibiting the agglomerates or at least in making them less compact since it inhibits in the formation of tungsten bronzes (10,11). The amount of agglomerates, their size and their strength are not only of academic interest. They may cause incorrect results for grain size measurements in that abnormally large sizes would be measured, while for liquid phase sintering, esp. for the solution-repricipitation mechanism, the radius of the individual grain determines the tendency to be dissolved in the binder In Ref.(1) three powder were shown to be much finer than indicated by Fisher SSS; measuring the grain size by means of SEM photos revealed a grain size just under 1 µm rather than the 3 µm measured by both Fisher SSS and sedimentation.

For the binder elements Ni and Fe powders of "carbonyl quality" with average grain size of ~5 µm were used; to avoid binder inhomogeneities in the heavy metals, particles >45 µm were screened off. Without this separation step a considerably increased scatter in the measured values, particularly in those for elongation, had been observed.

3. Investigation of the sintering process

As stated above, the formation of the appropriate microstructure is of decisive importance for the properties of W heavy metals. Due to various grain growth mechanisms, e.g. solution, reprecipitation and coalescence (12,13), both grain size and grain shape change considerably during sintering; thus the sintering time is probably one of the most important parameter for the microstructure. The investigation of the changes in the microstructure during sintering and of the effects on the mechanical properties was regarded as necessary in order to set a standard against

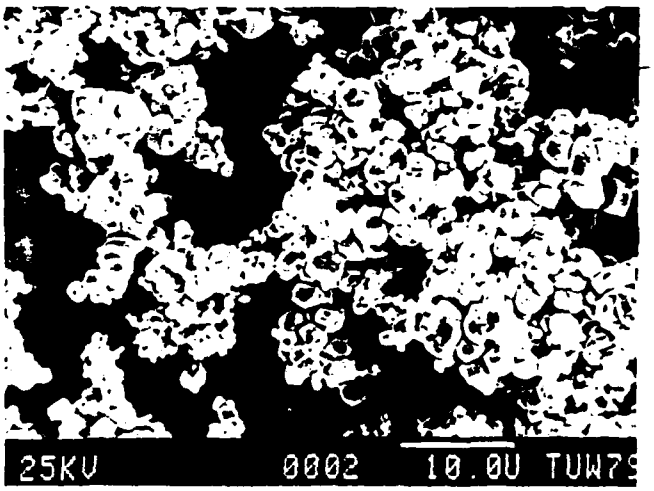

Fig.1
undoped standard powder 503/79

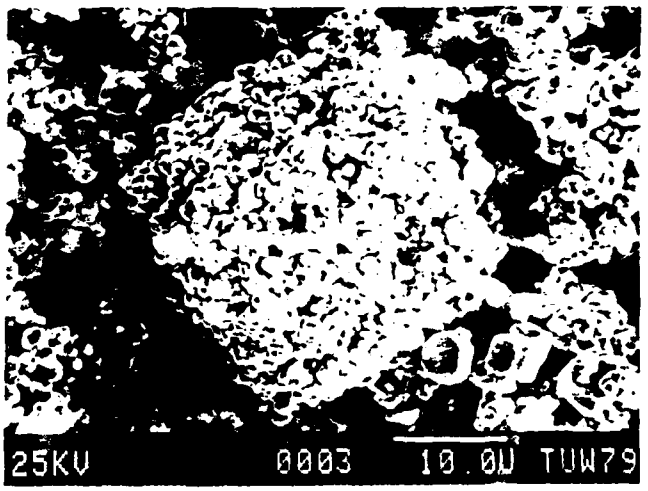

Fig.2
W503/79
typical agglomerate

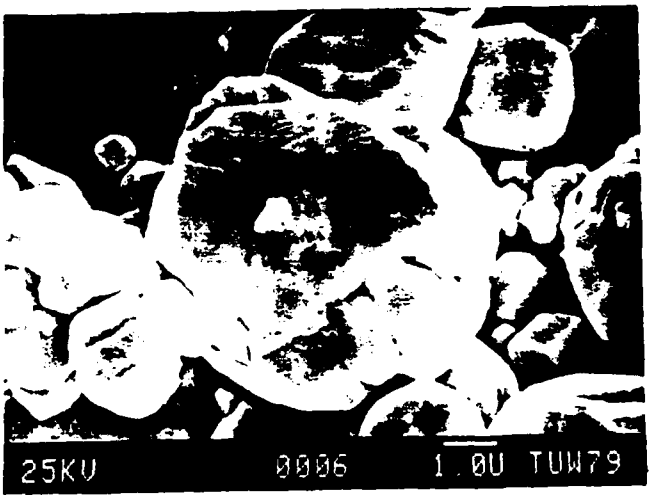

Fig.3
W503/79
grain shape of the standard powder

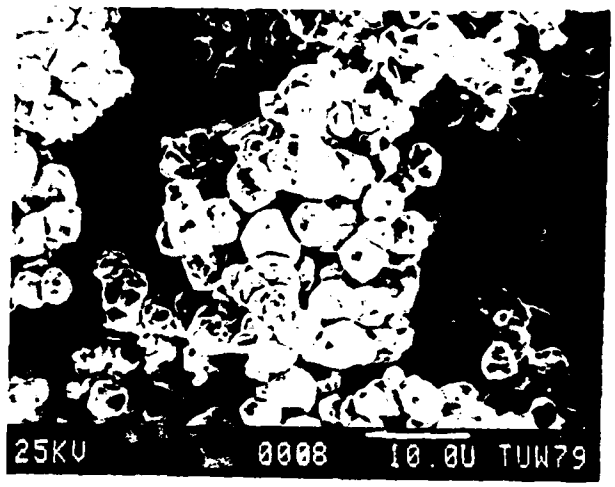

Fig.4
E2W
(W powder doped with 250ppm Na)

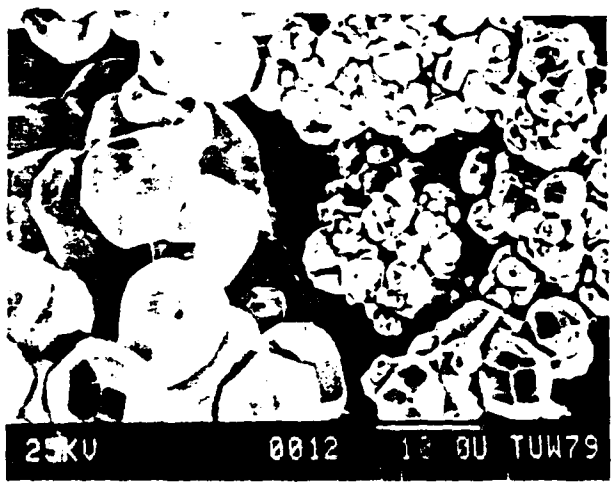

Fig.5
E5W
(250ppm Li)

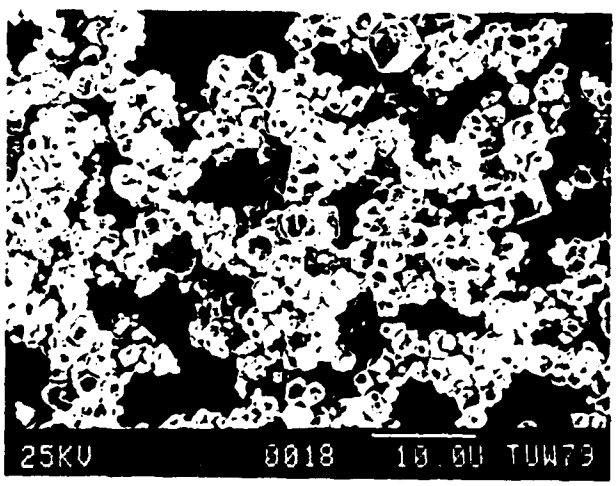

Fig.6
E8W
(188ppm Ca)

Fig.7
E11W
(W powder doped
with 250ppm B)

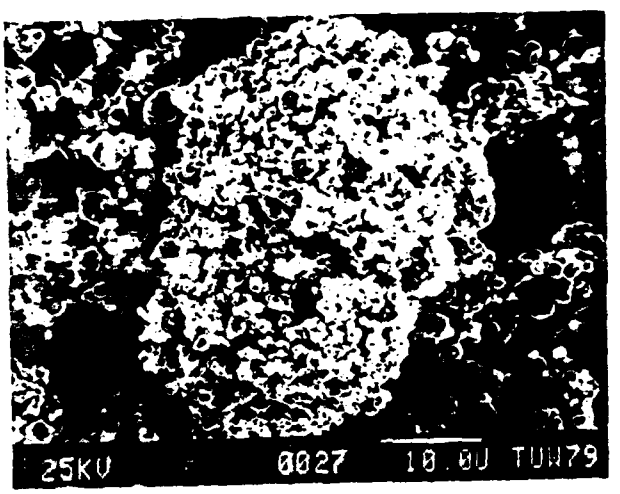

Fig.8
E14W
(Dopant 250ppm Al)

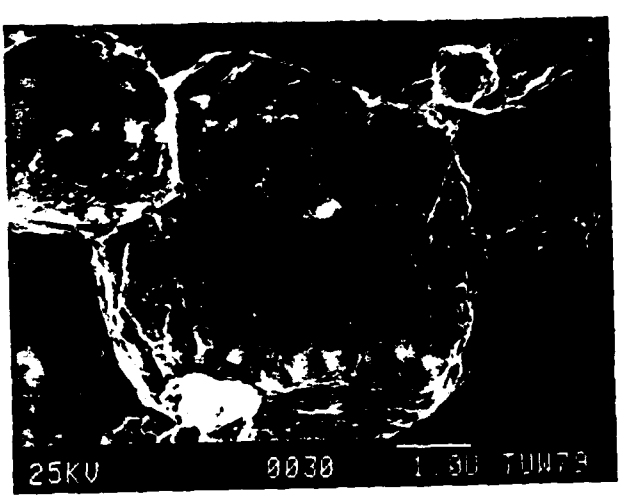

Fig.9
E14W
grains covered
with small
Al_2O_3 particles

Fig.10
E17W
W powder doped with 100ppm Si

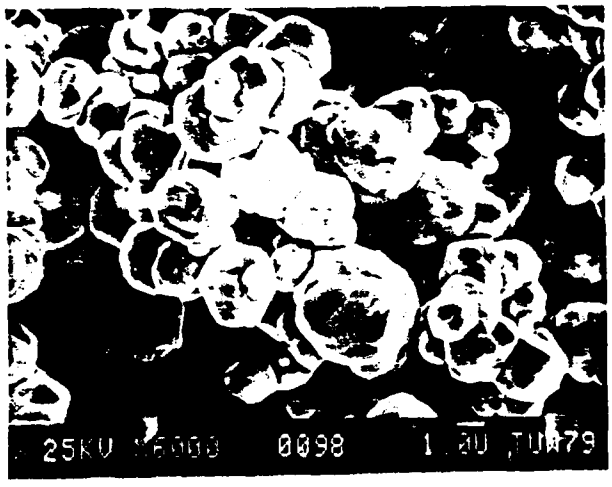

Fig.11
E 21W
(doped with 140ppm Na, 100 ppm P)

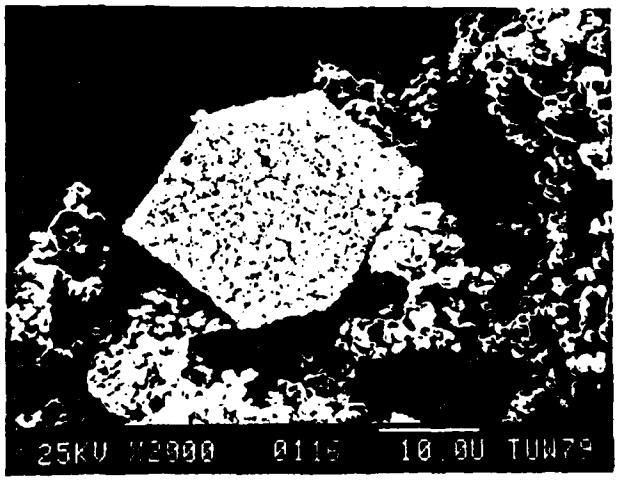

Fig.12
E24W
doped with As,Sb, Bi (100ppm each) characteristic pseudomorphous structure)

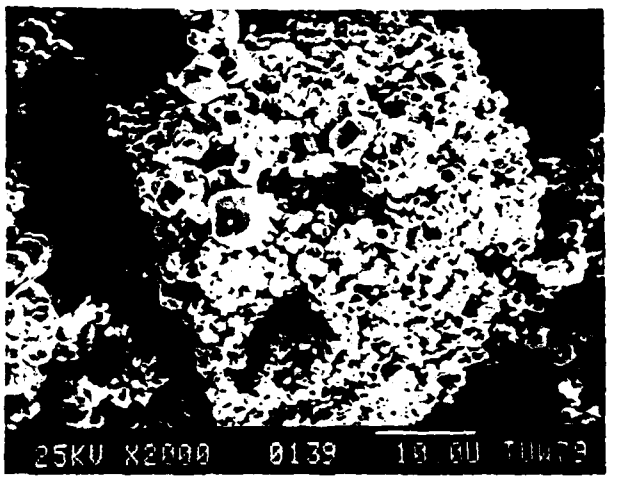

Fig.13
E27W
W powder doped with 100ppm U

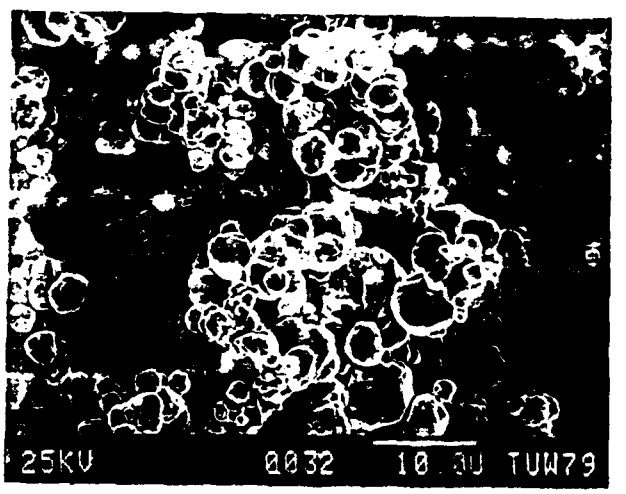

Fig.14
E30W
W powder prepared from impure blue oxide

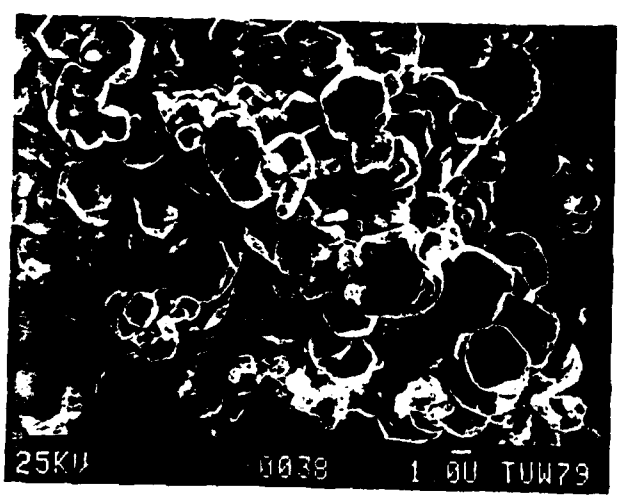

Fig.15
E33W
undoped W powder

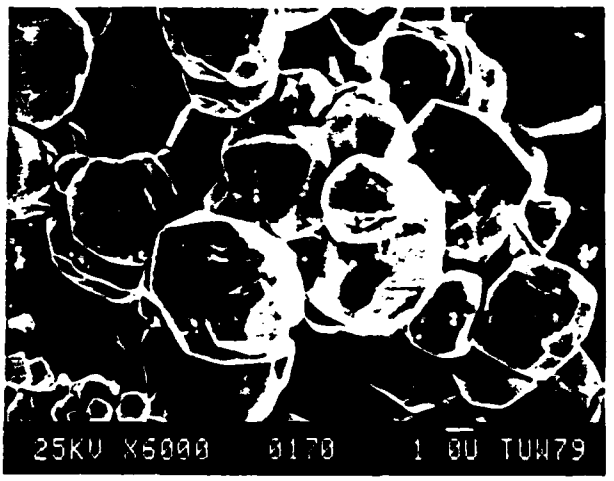

Fig.16
E36W
W powder doped
with 100ppm Na

Fig.17
E39W
Dopant 50ppm Na

Fig.18
E45W
W powder doped
with 100ppm Li;
very coarse powder

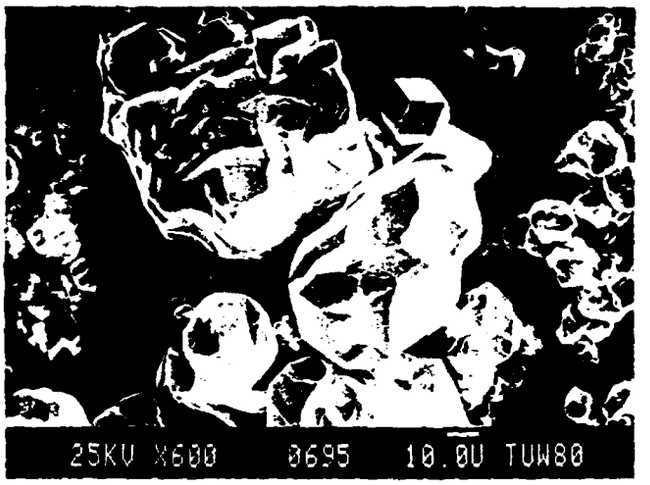

Fig.19
E48W
W powder doped with 200ppm Na; coarse powder

Fig.20
E51W
W powder doped with 200ppm Li; extremely coarse powder

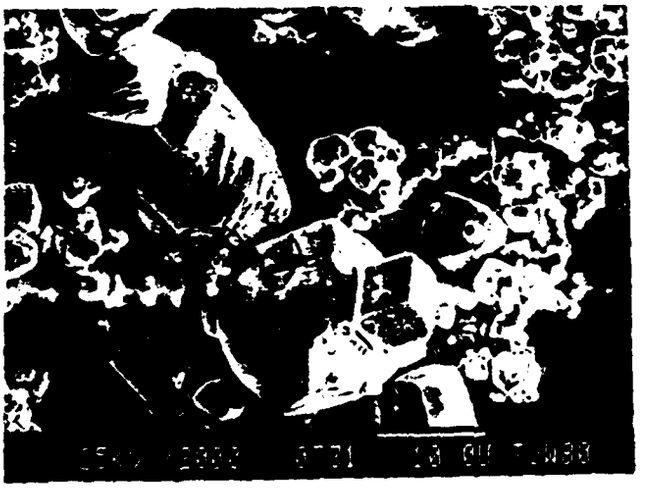

Fig.21
E56W
doped with 200ppm Al; surface contaminated with Al_2O_3

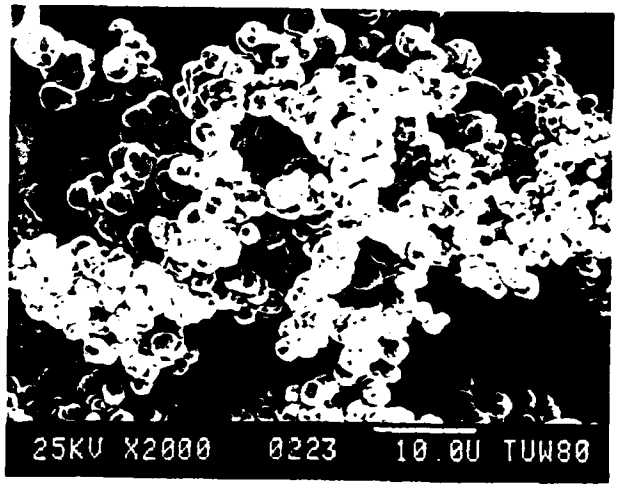

Fig.22
E63W
W powder doped
with 200ppm K

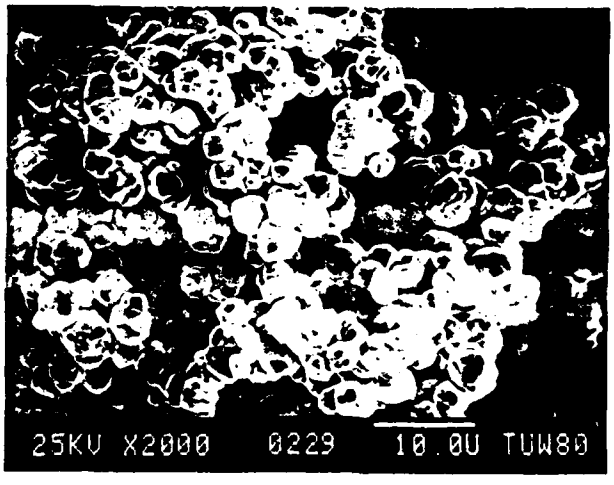

Fig.23
E67W
doped with
100ppm K

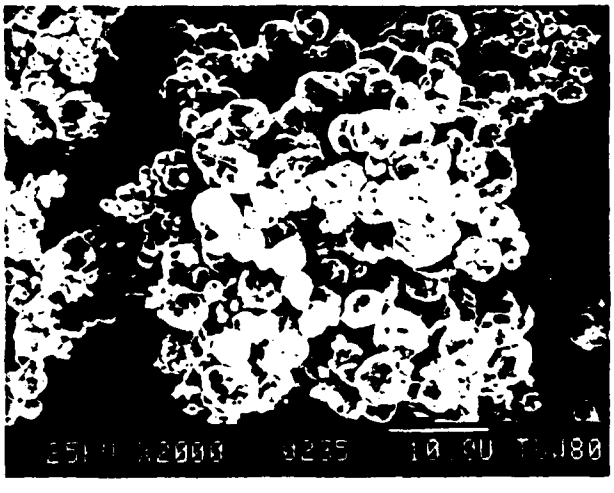

Fig.24
E71W
doped with
50ppm K

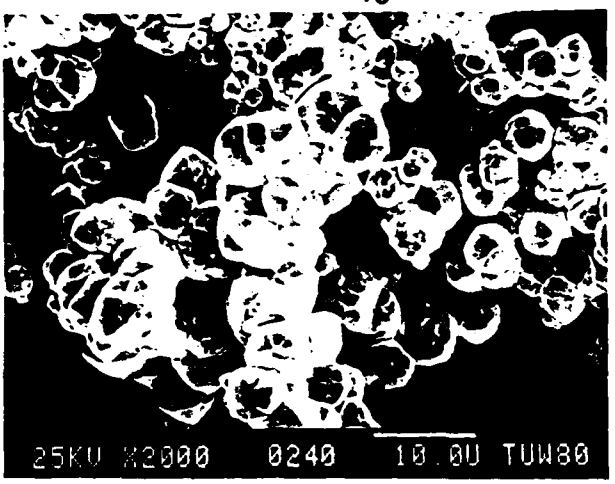

Fig.25
E79W
W powder doped with 200ppm Na, 120ppm Si

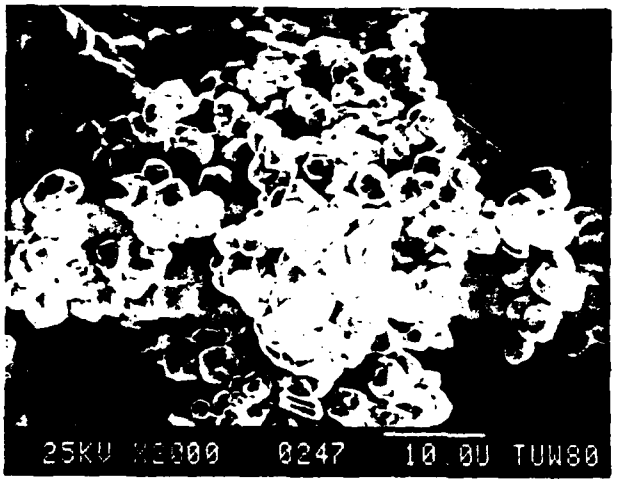

Fig.26
E83W
doped with 100ppm Na, 80ppm F

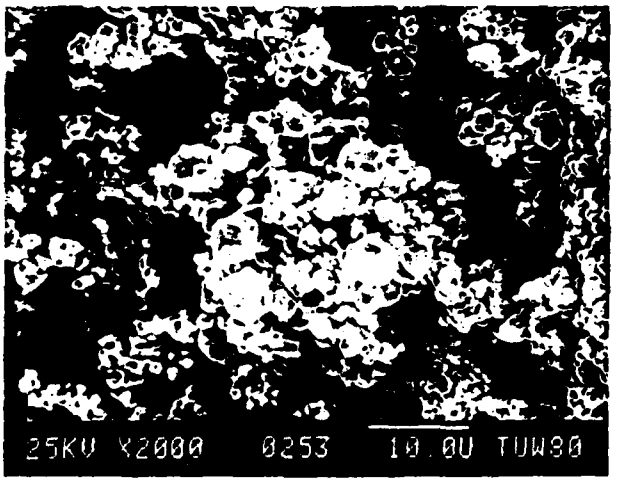

Fig.27
E87W
doped with 150ppm Mg

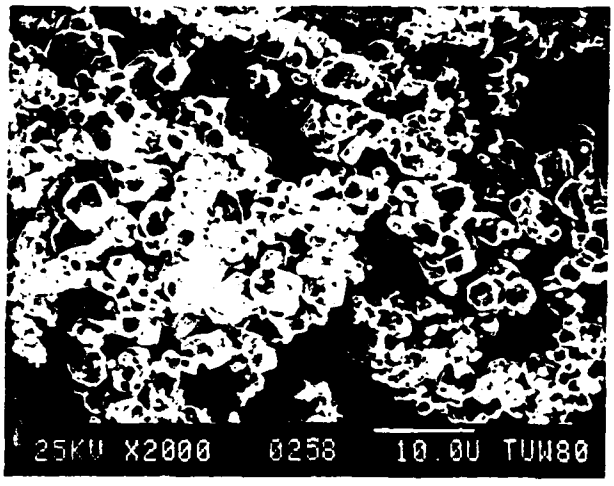

Fig.28
E91W
W powder doped
with 200ppm Ba

Fig.29
E95W
doped with
100ppm Sn

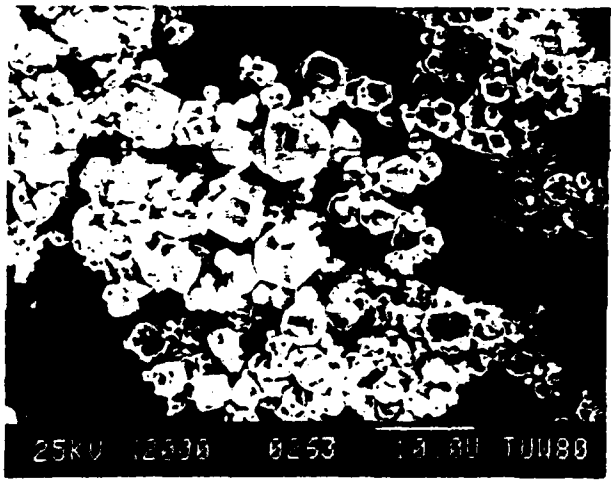

Fig.30
E99W
doped with
100ppm Zn

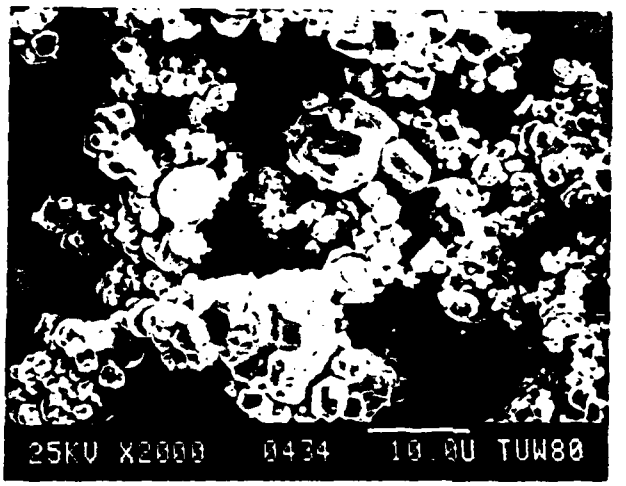

Fig.31
E103W
W powder doped with 100ppm Cu

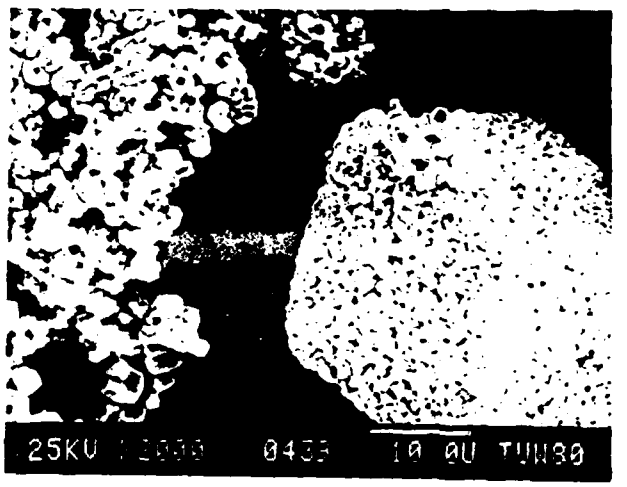

Fig.32
E107W
doped with 100ppm Ni; very dense agglomerates

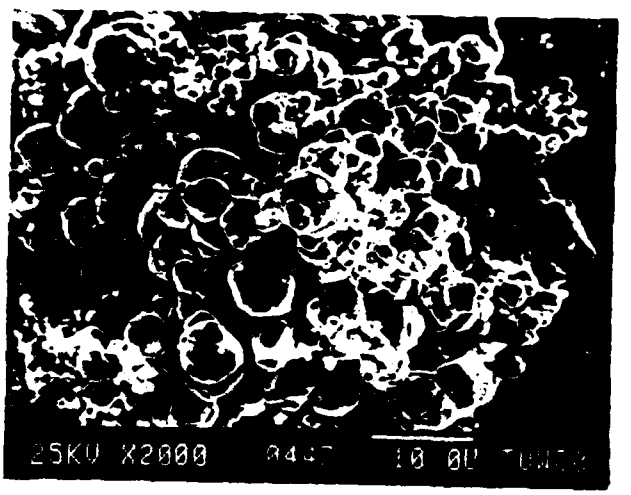

Fig.33
E111W
doped with rare earths

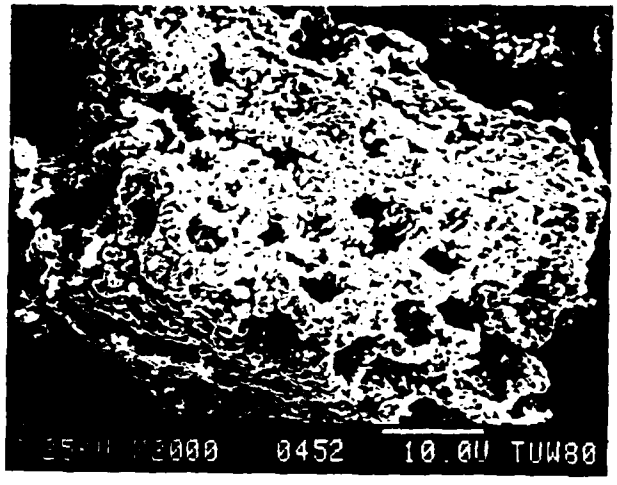

Fig.34
E115W
W powder doped
with 100ppm P

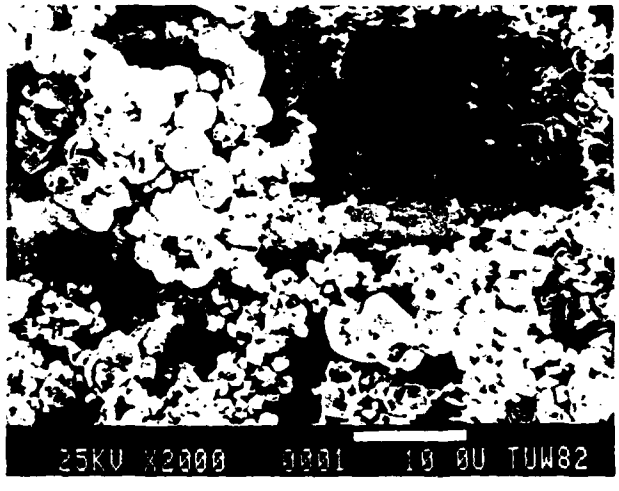

Fig.35a
W640/81
standard W powder
(undoped)

Fig.35b
W640/81
typical
agglomerates

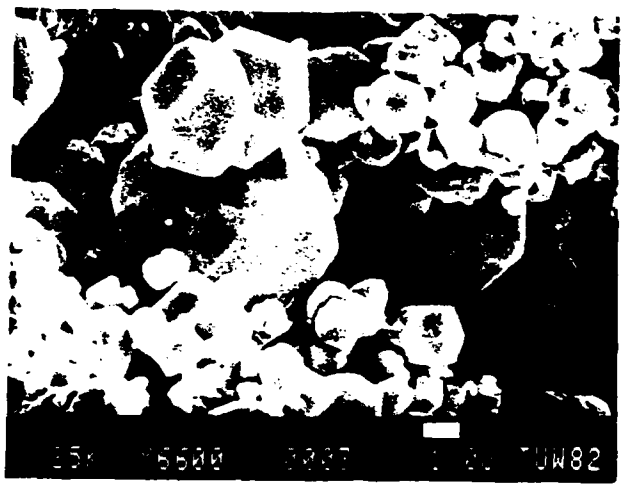

Fig.35c
W640/81
standard powder;
shape of individual grains

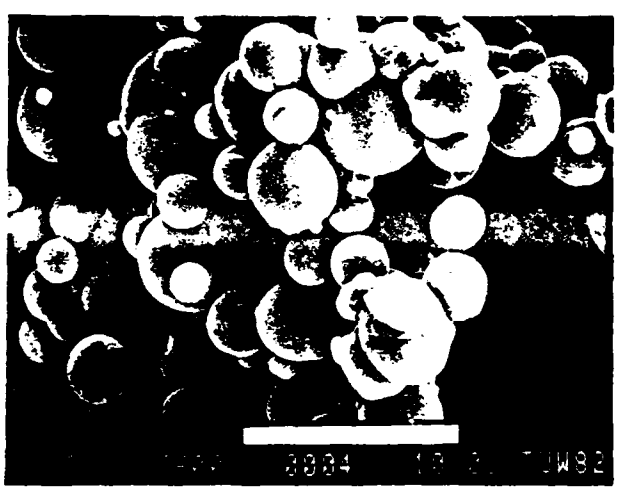

Fig.36
Carbonyl Fe

Fig.37
Carbonyl Ni

which the experiments with doped powders could be correctly compared and evaluated. It was thought possible that the doping elements in the W powder would influence not only the properties of the heavy metals but also the sintering process; sufficient knowledge about the sintering process thus might make it possible to identify and explain special effects caused by the dopants.

3.1 Experimental procedures

The experiments were carried out with heavy metals of the standard composition 90 wt% W - 6,7 wt% Ni - 3,3 wt% Fe and 1% camphor as pressing lubricant; the W powder used was the standard powder W 640/81 of ~3 µm average grain size. The Ni and Fe powders were the 'Carbonyl powders' - average grain size 5 µm - described in the last chapter. After 3 hrs mixing in cyclohexane the solvent was partially evaporated and the still somewhat damp powder was granulated through a 0,8 mm mesh sieve and then dried. The granulate was compacted in a pressing tool for standard tensile strength bars (MPIF standard 10-63). The excellent flow characteristics of the granulate resulting in uniform filling of the die so that pressing faults were completely avoided. The tensile strength bars were sintered in a high temperature furnace with an Mo heat conducting coil at a temperature of 1475°C; the sintering atmosphere was technical hydrogen with a flow rate of 2 l/min. As mentioned above, a pre-reduction treatment to reduce any oxides in the powders as well as slow cooling after liquid phase sintering are necessary to avoid embrittlement of the heavy metals. Fig.38 shows the temperature-time diagram for the sintering cycle. Pre-reduction was carried out by slowly heating the samples from 500°C to 1400°C and then keeping them at 1400°C for 1 hr. After a short rest in a somewhat cooler zone of the furnace to enable the heating zone to reach sintering temperature the samples were liquid phase sintered for the desired length of time and then the furnace was simply switched off, the samples cooling down to 500°C within 14 hrs. The short inter-cooling was regarded necessary for exact control of the sintering time; it does not affect the mechanical properties of the heavy metals.

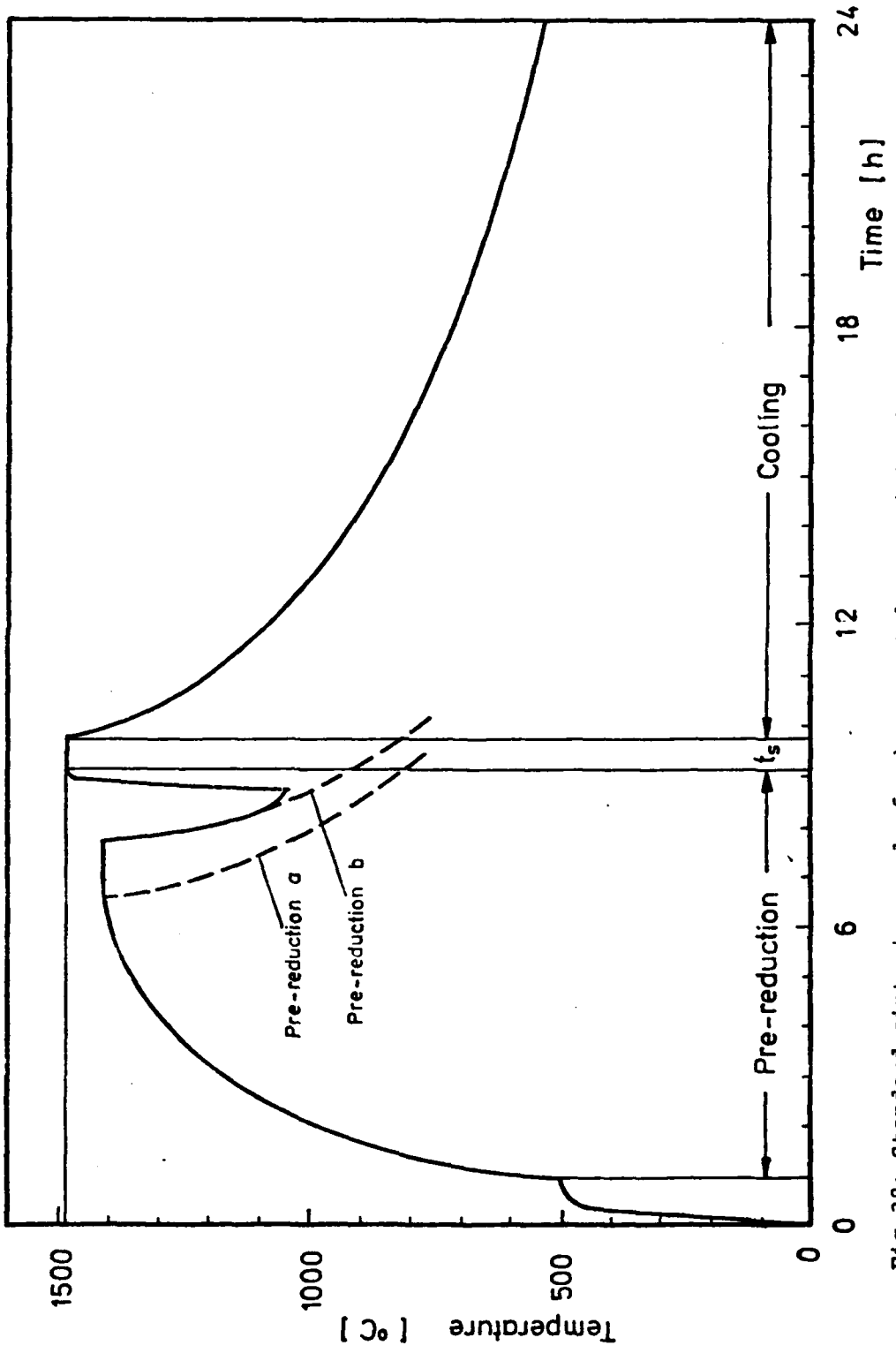

Fig.38: Standard sintering cycle for heavy metals containing 90%W

While the sintering temperature was held constant at 1475±5°C, the sintering time was varied from 1-120 min. To control the state of the material before liquid phase sintering, samples in different states of pre-reduction (a,b in Fig.38) were also investigated. The mechanical properties of the samples thus produced are shown in Table 2.

3.2 Experimental results

Surprisingly, even after short pre-reduction and before reaching liquid phase sintering very high density was attained and the porosity was already below 3%. After extended prereduction (b in Fig.38) practically full density was achieved. Apparently, at those temperatures solid state sintering is very rapid. The binder materials probably act as promotors for the sintering of W (14), the driving force being the saturation of W with the binder materials (15). During liquid phase sintering there are almost no changes in density; only after very long sintering times (> 60 min) could a slight decrease in density be measured. This may be attributable to the formation of pores, as already described for longer sintering times by Churn and Yoon (16).

The high density of pre-reduced samples also explains their quite good tensile strength; in accordance with the increase in density, extended pre-reduction also increases tensile strength. Although the density is equal to that of liquid phase sintered material, the tensile strength is still considerably lower. The stress-strain diagrams show that with these samples only elastic deformation occurs, the tensile strength being identical to the yield strength, and the samples are not strengthened further by work hardening. After melting of the liquid phase the tensile strength increases rapidly, the maximum value being attained after only 5 min where it remains nearly constant up to 60 min. This is followed by rapid decreases at 90 and 120 min, an effect attributable to the above mentioned pores.

Table 2: Mechanical properties of W heavy metals (90%W - 6,7% Ni - 3,3% Fe) sintered at 1475°C for different lengths of time. Average values from 4 samples

Sintering time (min)	Density (g/cm^3)	Tensile strength (MPa)	Elongation (%)	Mean grain size (µm)
0	16,652	725	0	-
0 pre-reduction extended by 1h at 1400°C	17,057	833	0	-
1	17,073	861	4,8	7,0
2	17,104	867	4,5	-
3	17,084	904	7,3	10,6
5	17,060	990	16,3	13,8
10	17,109	954	19,4	16,2
15	17,125	961	19,2	16,9
30	17,080	954	27,3	18,6
45	17,069	946	26,4	25,2
60	17,082	933	16,5	23,3
90	17,0313	769	6,6	31,0
120	17,039	774	5,9	35,0

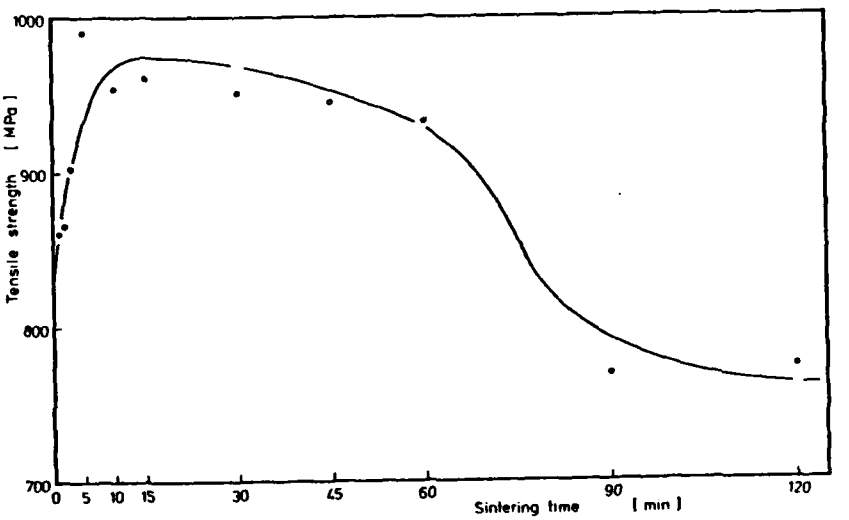

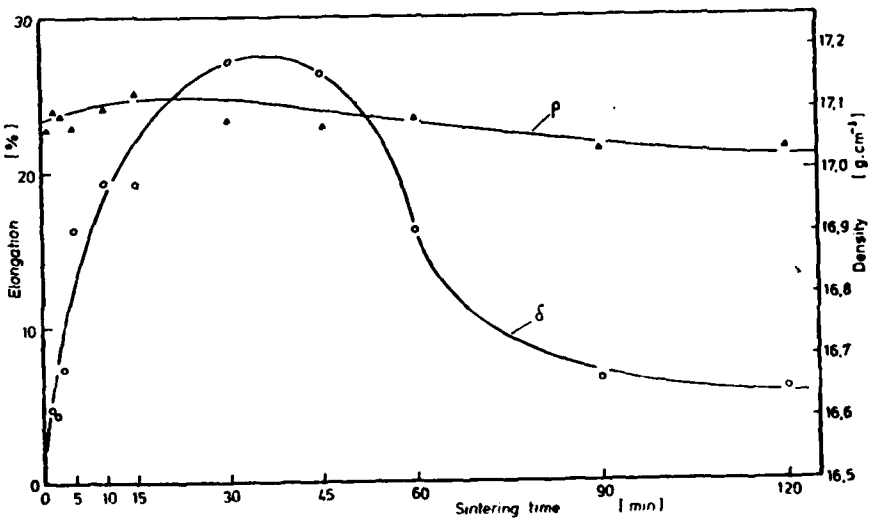

Fig.39/40: Mechanical properties of W heavy metals (90%W - 6,7%Ni - 3,3%Fe) as a function of the sintering time (Sintering temp. 1475°C)

The elongation showed a behaviour similar to that of the tensile strength: the prereduced samples were extremely brittle with unmeasurable low elongation, but after only 1-2 min of liquid phase sintering the samples showed a measurable ductility. The elongation increases much slower with longer sintering times than the tensile strength does, the maximum values being attained at 30-45 min. The elongation also drops sharply after 60 min to a rather low level; apparently the pores formed at the time act as crack initiators and cause the material to fail even at very low degrees of deformation.

The scatter of the individual values of σ_B and δ also indicates the quality of the heavy metals. With the tensile strength, an interesting trend was observed: the higher the value, the lower the absolute scatter. The absolute scatter of the elongation values, however, remains largely constant over the entire range of sintering time. Broad scatter of the tensile strength values would thus indicate some defect in the sintering process, as the tensile strength is not as sensitive to the external parameters as is the elongation.

SEM investigations of the fracture surface revealed a fundamental change both in structure of the heavy metal and in fracture behaviour: The samples which were merely pre-reduced or sintered for very short times (Fig. 41,42,43) exhibited angular W grains with entire surfaces formed by sintering necks or pore surfaces. The binder is concentrated in a few spots separated by large areas of pure W and numerous pores mostly at the junctions of several grains are visible. It is also evident, however, that even during prereduction rapid grain growth occurs: Comparing Fig.41 (usual prereduction) and Fig.42 (prereduction extended for 1 h), both the different grain sizes and grain shapes are evident. In Fig.41 the grains are still separated by many pores, and their shape is partially polyhedral, partially irregular; but after treatment at 1400°C, the grains have grown together and are almost entirely

polyhedral to fill up all possible pores (an observation which is also confirmed by the remarkable increase in density, see Tab.2). Apparently the tendency of the fine W grains to sinter together is very marked during solid state sintering also; a grain size similar to that in Fig.42 is obtained after only 5-10 minutes of liquid phase sintering. Maybe this pre-treatment could offer an advantage by removing the very fine W grains responsible for the extremely rapid grain growth in the first moments of sintering.

During the sintering process, the binder becomes more evenly distributed; after only 3 min. the binder concentrations have disappeared (Fig.44). Simultaneously, the W grains become more spherical in shape, and the percentage of the W surface covered by sintering necks decreases significantly. After 5-10 min., the typical microstructure of heavy metals has formed, and accordingly high elongations are obtained. Some transgranular fractures can be observed even after 3 min. sintering time, but this type of fractures becomes predominant. at 30 min. At shorter sintering times the fracture tends to run through the binder and across the sintering necks. The highly ductile samples (Fig.46, 47) exhibit the typical features of a satisfactory heavy metal: mainly transgranular fracture, considerable binder deformation and only rather few and small sintering necks in the fracture surface. At longer sintering times, pore formation begins to cause serious problems (Fig.48). Although the fracture surface apart from the pores appears to be sound (Fig.49) with numerous transgranular fractures, the larger pores formed at that stage sufficiently weaken the microstructure and cause it to fail prematurely.

Churn and Yoon (16) offer two explanations for this pore formation : either coalescence of small pores or generation of H_2O by reduction of small amounts of oxides. In our opinion the two processes work together and cannot be separated. It had been observed earlier that heavy metals with high oxygen contents

result in extremely porous samples when sintered without pre-reduction (3), apparently due to the generation of H_2O in the samples during liquid phase sintering. But even in carefully pre-reduced samples some oxygen remains, at least in oxides of Na, Li etc. (elements which incidentally, also lead to pore formation, see 1,3) as oxygen trapped in the W grains and set free during the solution/reprecipitation process. Due to its rather high solubility in the Ni-Fe binder, oxygen can be transported in the binder but inadvertently reacts with hydrogen,which is also dissolved in the binder to form H_2O. The H_2O is much less soluble and tends to form bubbles. At first these bubbles are small and most of them will disappear again. During the sintering process, however, Ostwald ripening of the pores occurs, and soon larger,stable pores are formed. Such pore growth processes are well known from annealing of Al in humid atmosphere, where hydrogen blisters grow in a quite similar manner (17, 18). As indicated by the dihedral angles between binder and W grains, the pores are further stabilized by deterioration of wetting, as, due to the oxygen equilibrium between pore atmosphere and W surface, small amounts of oxides are formed on the W grains and in turn inhibit wetting of the grains by the binder, thus causing the binder to retreat from this area. In Fig.48 the high dihedral angles are clearly visible, as are the sintering necks, which indicate that the pores are not completely empty but simply areas without binder and filled only with W grains. The spherical shape of the W grains indicates that there must have been binder in this area, as the usual grain growth processes have taken place and only afterwards has the binder been driven away. Fortunately such pore formation is characteristic of sintering times not recommendable for technical applications for other reasons, as well such as grain coarsening.

3.3 Metallographic investigations

To evaluate the microstructure of the samples, metallographic sections of the differently sintered samples were prepared and etched in $CuSO_4/NH_3$ solutions. Photos taken from these sections are shown in Fig.50-55. As clearly visible, grain growth starts very rapidly at the beginning of liquid phase sintering; along with it the typical microstructure of heavy metals is formed. After 1 min. the W grains are still angular and are mostly sintered together, and the binder is concentrated in a few places, as already shown by the respective SEM photos. After 3 min., the grains have grown and rounded considerably; they are still sintered together in many places, but the binder is already more evenly distributed and begins to surround all W grains. After 10 min., further grain growth has occurred but the microstructure is still not homogeneous and numerous large sintering necks are present. These are probably responsible for the still unsatisfactory elongation because of the separation under stress and formation of microcracks. After 30 min. sintering time the microstructure is finally rather homogeneous; the sintering necks are generally small, and most W grains are almost completely surrounded by binder. At 60 min. considerable grain coarsening is evident; while at 30 min. many grains are <20 µm in diameter, here most grains are ~30 µm, although there are still some small ones. Even after 120 min. the small grains have not completely disappeared, but the grains >50 µm predominate, and there are very long, pronounced sintering necks because of the extreme grain shape accommodation.

The average grains sizes were determined by counting and measuring the individual grains on the photos. In Fig.56 the resulting apparent average grains size is given as a function of the sintering time. The rapid grain growth at the beginning of the liquid phase sintering process is clearly discernible,

but then the rate of growth follows an almost straight line. A comparison of this with observations in the literature (12) concerning the rate of grain growth and the final grain size indicates that even a time of 120 min. is still rather short relative to the entire process. Earlier investigations (2) have shown that after 15 hrs. of sintering a grain size of >100 µm is attained. Since the relative differences between real (3-dimensional) and apparent (2-dimensional) grain size should always be the same, the real diagram would be quite similar, with only slightly increased absolute values.

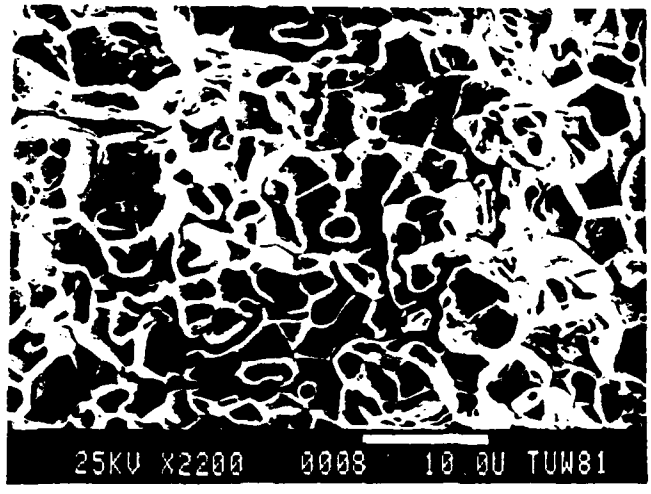

Fig.41
Fracture surface of pre-reduced heavy metal (90%W; pre-reduction a) in Fig.38)

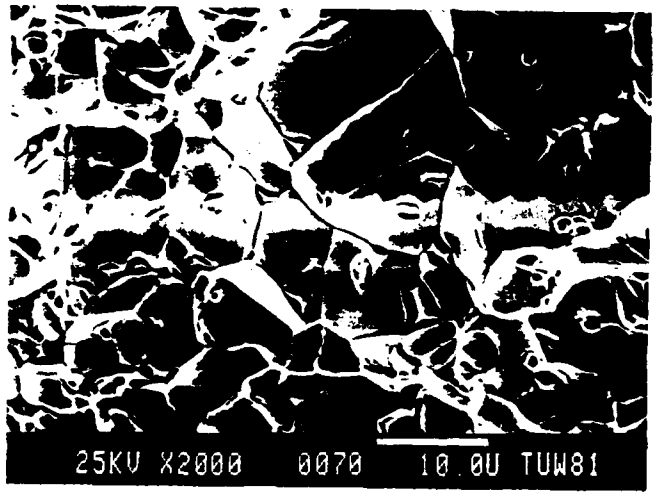

Fig.42
Pre-reduction extended for 1 hr at 1400°C (Pre-red. b) in Fig.38)

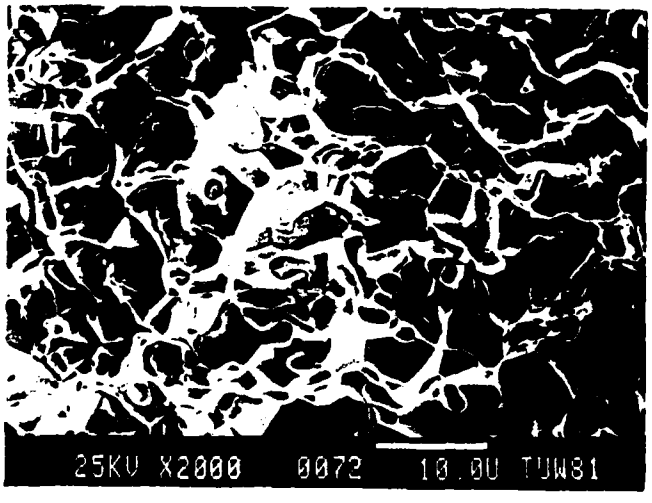

Fig.43
Heavy metal liquid-phase sintered 1 min at 1475°C

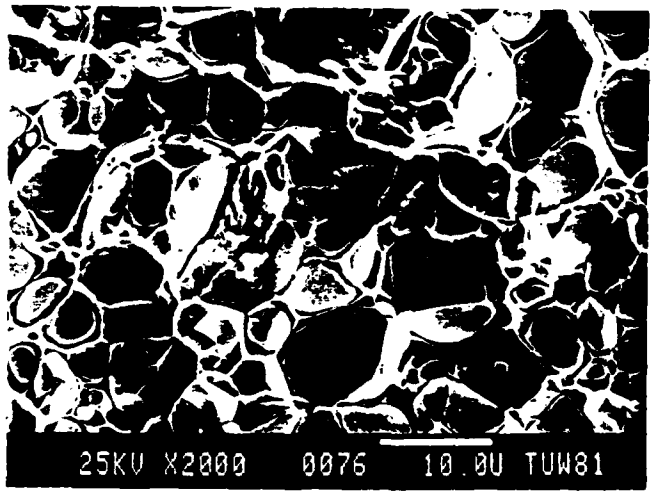

Fig.44
W heavy metal (90%W) liquid phase sintered 3 min at 1475°C. Marked rounding of the W grains

Fig.45
Sintered 5 min at 1475°C. 2000x

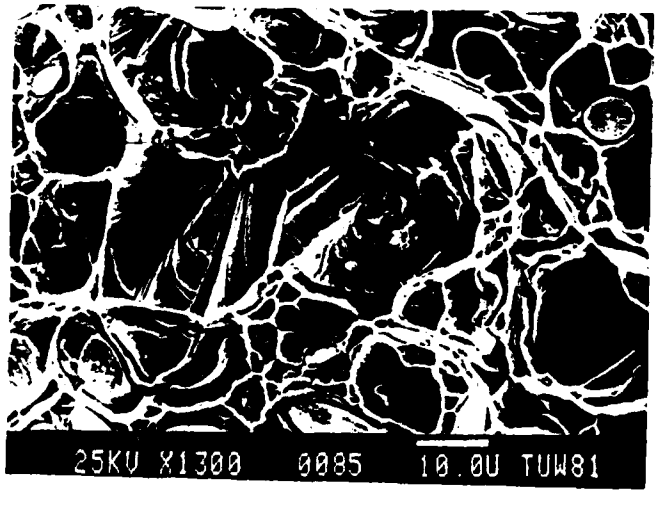

Fig.46
Sintered 30 min at 1475°C.

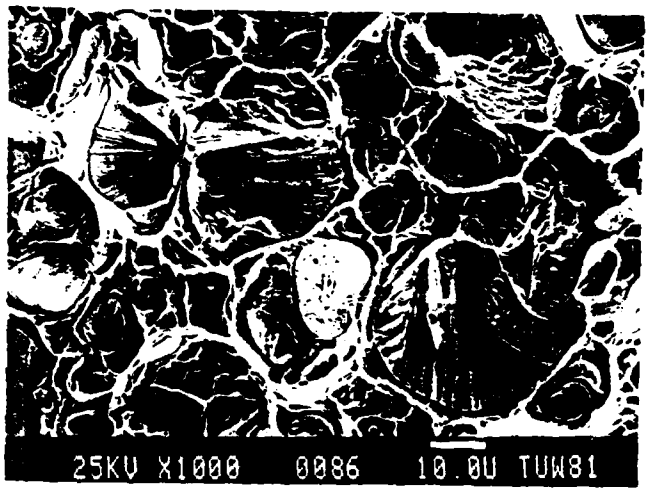

Fig.47
W heavy metal (90%W) liquid phase sintered 45 min at 1475°C

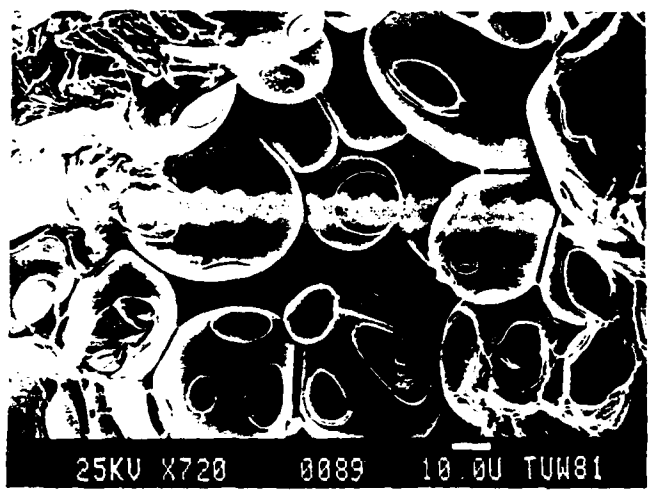

Fig.48
Sintered 90 min at 1475°C. Pore

Fig.49
Same sample as on Fig.48; apparently sound structure except of the pores

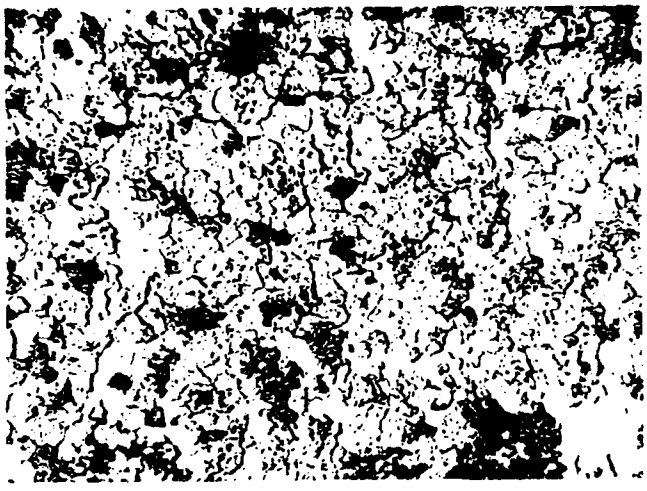

Fig.50
W heavy metal (90%W) sintered 1 min at 1475°C. Etched 2 min in $CuSO_4/NH_3$.
500x

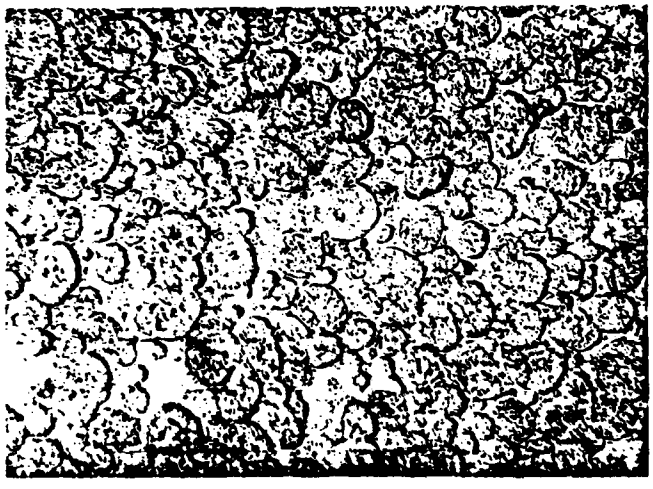

Fig.51
Sintered 3 min at 1475°C.
500x

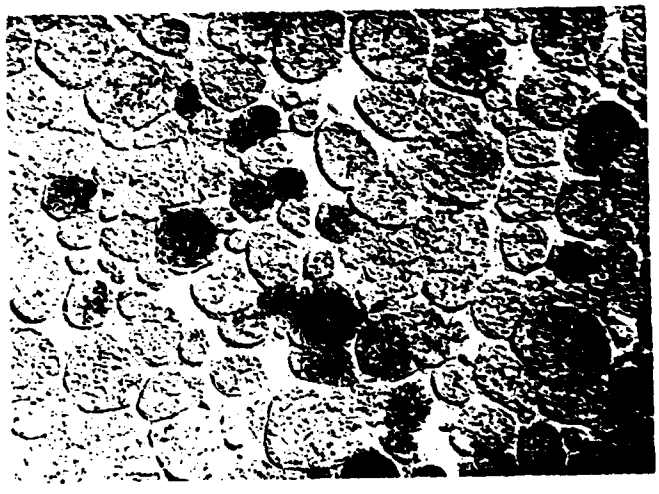

Fig.52
Sintered 10 min at 1475°C.
500x

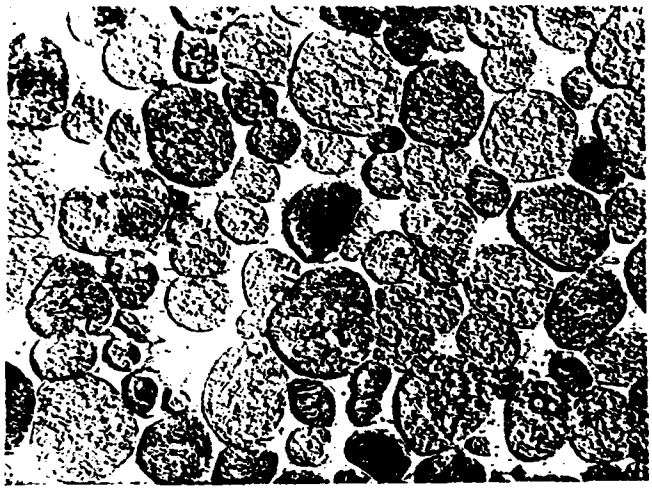

Fig.53
W heavy metal (90%W) sintered 30 min at 1475°C.
500x

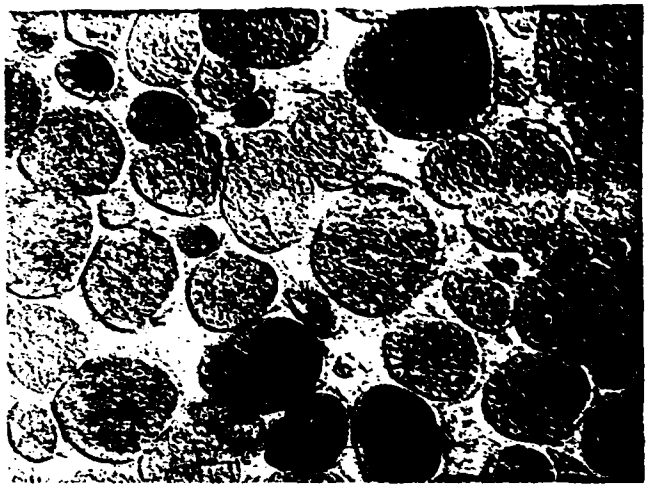

Fig.54
Sintered 60 min at 1475°C.
500x

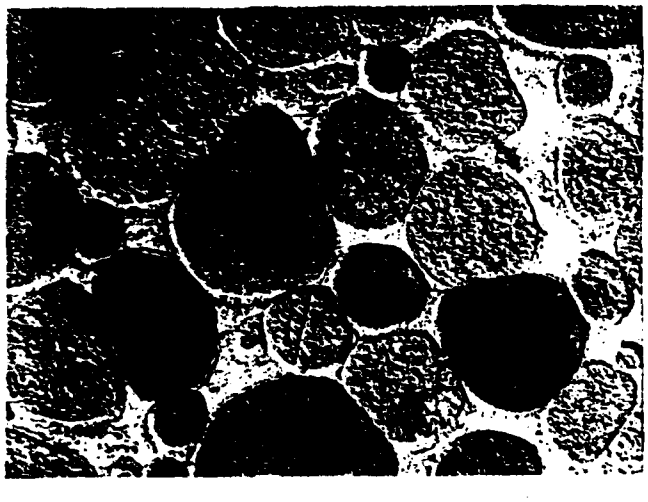

Fig.55
Sintered 120 min at 1475°C.
500x

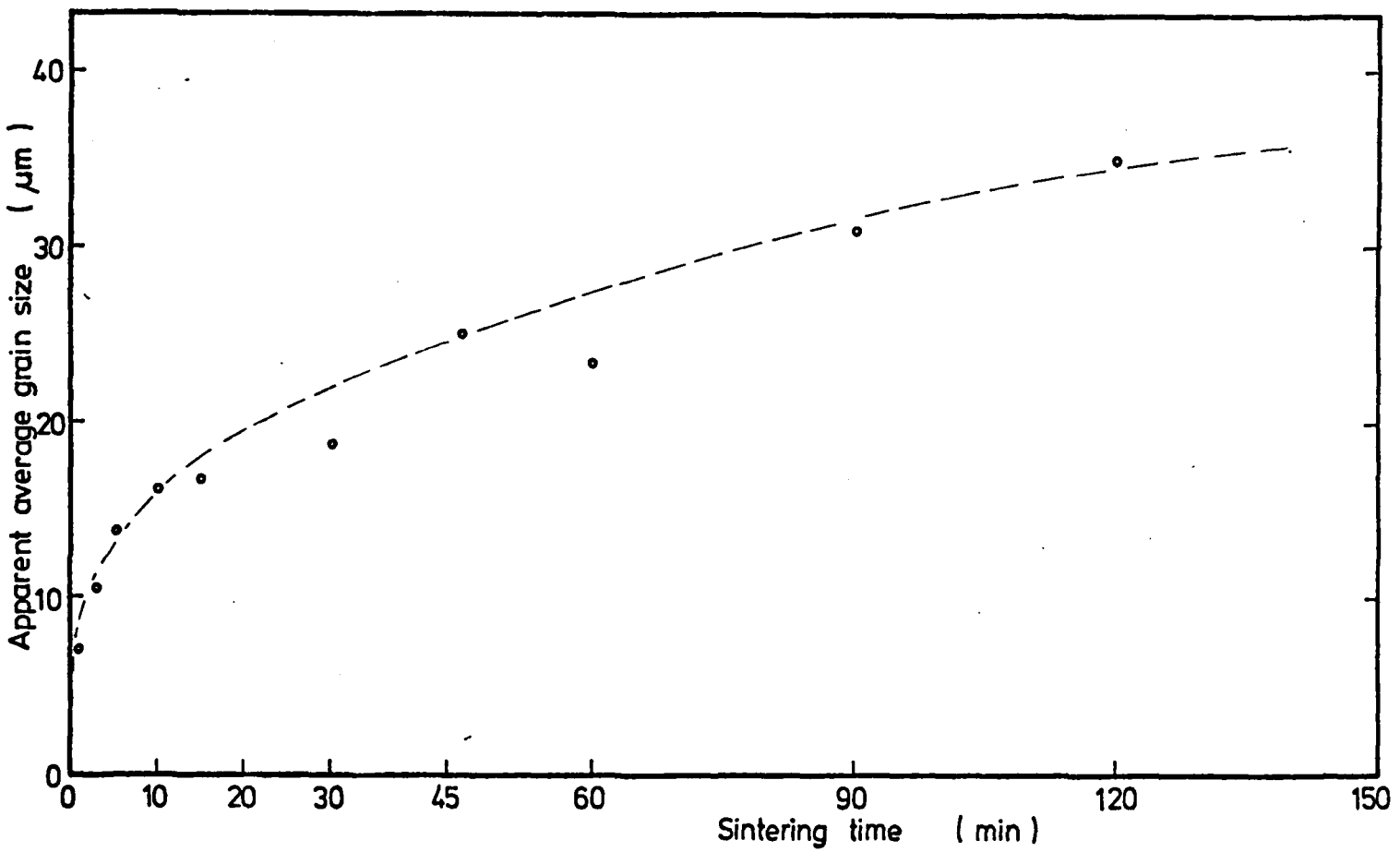

Fig.56: Grain growth of heavy metals (90%W - 6,7%Ni - 3,3%Fe) during liquid phase sintering (2-dimensional grain size measured on metallographic sections)

4. Heavy metals prepared from doped W powders

Heavy metals containing 90 and 96% W were prepared from the doped W powders described in Chapter 2. As had been shown by earlier experiments (1,3) due to the higher W content, the effect of the doping elements could be expected to be more pronounced in the samples containing 96% W. As stated above, the elements selected for doping were those most probable to be encountered in commercial W powders, and thus most probable to cause difficulties when shifting from one W powder to another. The final goal was, of course, to identify those elements whose presence must be investigated and analyzed before a powder is to be used for heavy metal sintering.

4.1 90% W content

The samples containing 90% W were prepared as described in chapter 3; the standard composition of 90% W - 6,7% Ni -3,3% Fe was maintained, and after addition of 1% camphor as pressing lubricant the powders were wet mixed, granulated and compacted; the green compacts were sintered following the cycle shown in Fig.38, the sintering being performed uniformly at $1475 \pm 5^{o}C$ for 30 min. As described also in earlier reports (1,3) together with each batch of 4-5 doped samples an equal number of bars prepared from the standard powder W 640/81 was sintered for comparison purposes to indicate any effects of small changes in the sintering parameters. They were arranged in the sintering boat following the pattern shown in Fig.57

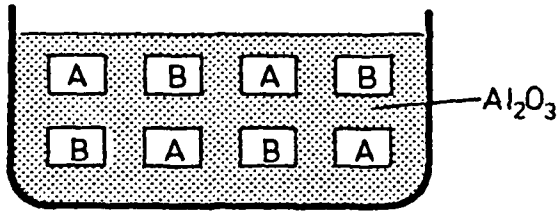

Fig.57: Arrangement of doped and undoped test bars in the sintering boat

The large number of parallel samples of each powder - at least 10 - enabled statistical evaluation of the results using the Weibull statistics (19,20) which allows calculation of the probability of fracture at a given stress.

The theoretical background, as also described in (1) is the following:

The probability of fracture (P) is influenced by the sample volume (V), tensile strength (σ) and a parameter indicating the homogeneity of the material (m), according to the equation

$$P = 1 - 1/\exp. \frac{V}{V_o} \cdot \left(\frac{\sigma}{\sigma_o}\right)^m \quad (V_o, \sigma_o \text{ refer to standard sample})$$

The equation is then transformed and σ_{50} inserted

$$\lg\lg \frac{1}{1-P} - \lg\lg 2 = m \cdot (\lg\sigma - \lg\sigma_{50})$$

For a given number N of samples, the P values depend only on the sample number n (from 1 to N). The graphic evaluation is carried out by taking the left side of the equation for the x-values and the right for y-values.

$$x = \lg\lg \frac{1}{1-P} \qquad \text{with} \quad P_n = \frac{n}{N+1}$$

$$x = \lg\lg \frac{N+1}{N+1-n}$$

$$y = \lg\sigma$$

$$s_w = 1/m$$

This is the equation of a straight line

$$y - y_{50} = s_w \cdot (x-x_{50})$$

The slope of this straight line indicates the scatter of the individual values; the broader the scatter, the more pronounced the slope and the greater the probability of fracture at stresses considerably below the average tensile strength.

The mechanical properties of heavy metals prepared from those doped W powders not covered by (3), i.e. the powders E48 - E115 are listed in the following tables and diagrams.

Powder E 48 (200 ppm Na)

Table 3: Mechanical properties of the samples prepared from E 48 and of the reference sample from W 640/81

E 48			W 640		
ρ (g/cm^3)	σ_B (MPa)	δ (%)	ρ (g/cm^3)	σ_B (MPa)	δ (%)
16,8635	894	6,0	17,0933	946	25,0
16,9559	796	10,0	17,0850	956	20,4
16,6594	755	8,8	17,0779	946	21,6
16,5630	772	12,0	17,0320	964	24,0
16,7392	778	6,0			
17,0900	853	10,4 x)	17,0660	956	22,4 x)
17,0757	709	8,0 x)	17,0283	911	20,0 x)
17,1235	738	5,2 x)	17,0480	928	25,6 x)
17,1128	764	5,2 x)	17,0375	918	16,0 x)
17,1118	787	6,0 x)			
17,1390	726	4,8 x)			

x) sintered at 1510°C

Mean values ± standard deviations

E 48	16,948 ± 0,210	775 ± 46	7,5 ± 2,5
W 640	17,058 ± 0,025	939 ± 18	21,9 ± 3,1

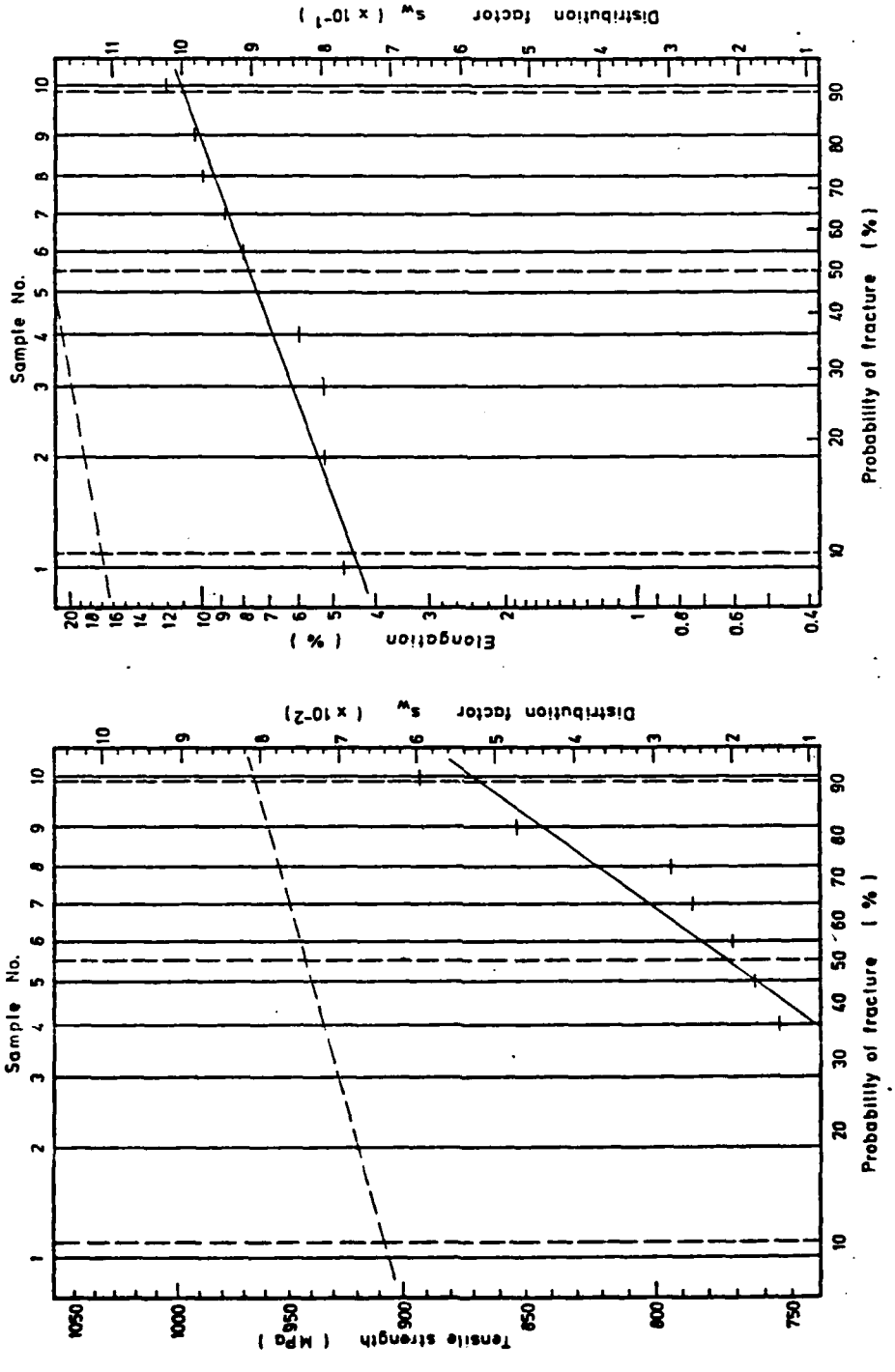

Fig.58: Weibull-diagrams for E48W (——) and W640/81 (– – –)

Powder E 51

Table 4: Mechanical properties of the samples prepared from E 51 and of the references sample from W 640/81

E 51			W 640		
ϱ	σ	δ	ϱ	σ	δ
15,3712	602	3,0	17,0864	960	20,0
15,4735	559	3,2	17,0514	945	18,4
15,7986	612	4,0	17,0494	953	27,4
15,7558	663	4,4	17,1148	941	22,8
15,7474	564	2,8			
15,6246	615	4,0	17,0510	955	23,6
15,9797	599	3,2	17,0532	960	24,0
15,8924	596	4,0	17,0621	946	22,6
15,9900	555	2,4	17,0739	979	24,0
15,4951	547	3,0			

Mean values $\pm$ standard deviations

E 51	15,713 $\pm$ 0,215	591 $\pm$ 36	3,4 $\pm$ 0,7
W 640	17,068 $\pm$ 0,023	954 $\pm$ 12	22,8 $\pm$ 2,7

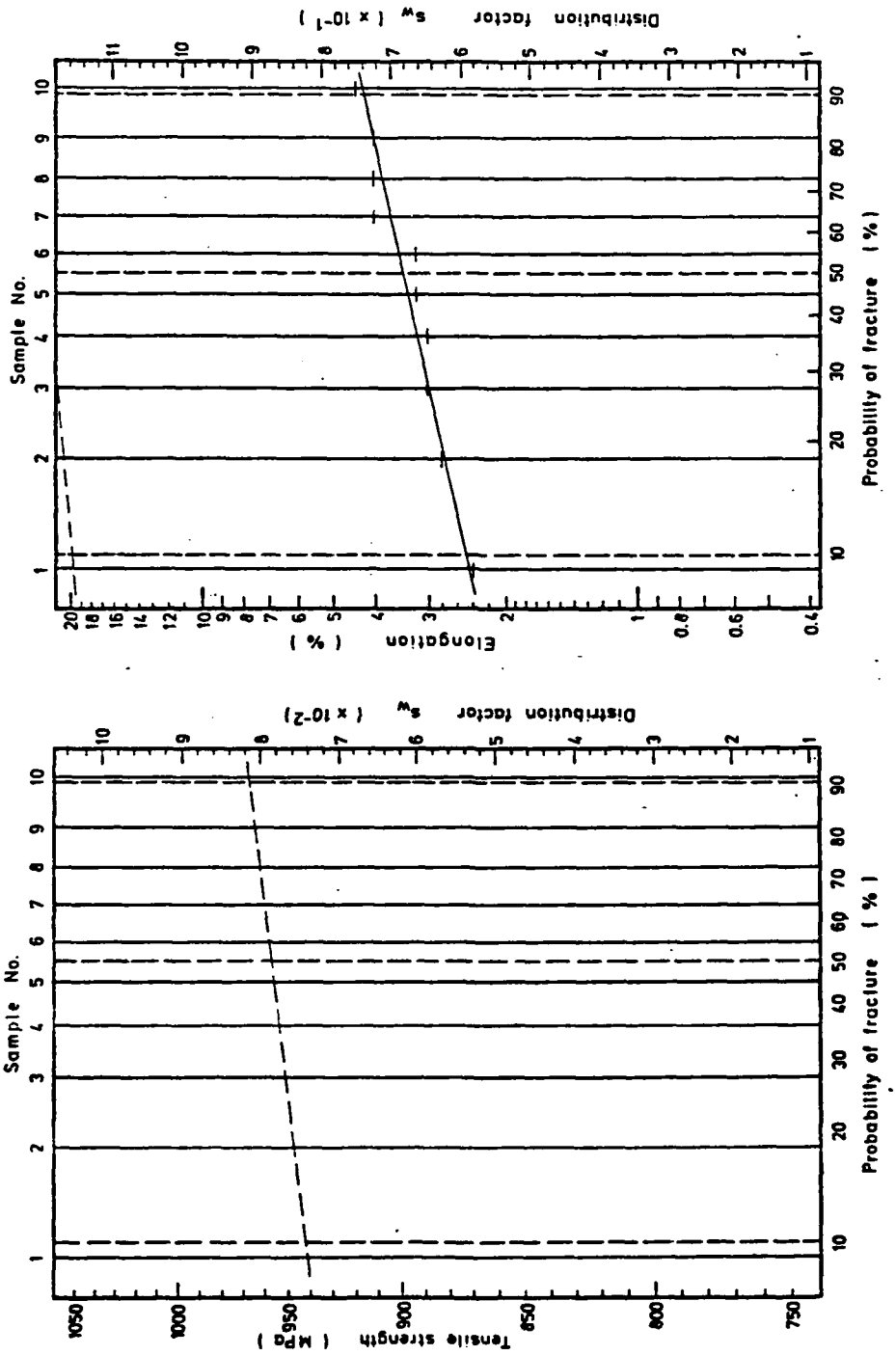

Fig.59: Weibull-diagrams for E51W (——) and W640/81 (- - -)

Powder E 56

Table 5: Mechanical properties of the samples prepared from E 56 and of the reference sample from W 640/81

E 56			W 640/81		
ρ (g/cm^3)	σ_B (MPa)	δ (%)	ρ (g/cm^3)	σ_B (MPa)	δ (%)
16,9905	933	16,4	17,0758	941	24,0
16,9906	907	14,8	17,0753	963	22,8
17,0012	947	22,8	17,0319	975	25,0
16,9756	902	10,8	17,0340	987	22,6
17,0241	923	17,2	17,0428	966	28,0
17,0201	936	22,4	17,0506	959	25,0
17,0077	950	20,3	17,0749	960	20,4
17,0004	864	18,4	17,0859	965	26,0
17,0083	909	18,0	17,0942	946	23,2
17,0044	944	20,8			
17,0358	908	21,0			

Mean values $\pm$ standard deviations

E 56	17,0053 $\pm$ 0,017	920 $\pm$ 25	18,4 $\pm$ 3,6
E 640	17,0628 $\pm$ 0,023	962 $\pm$ 14	24,1 $\pm$ 2,2

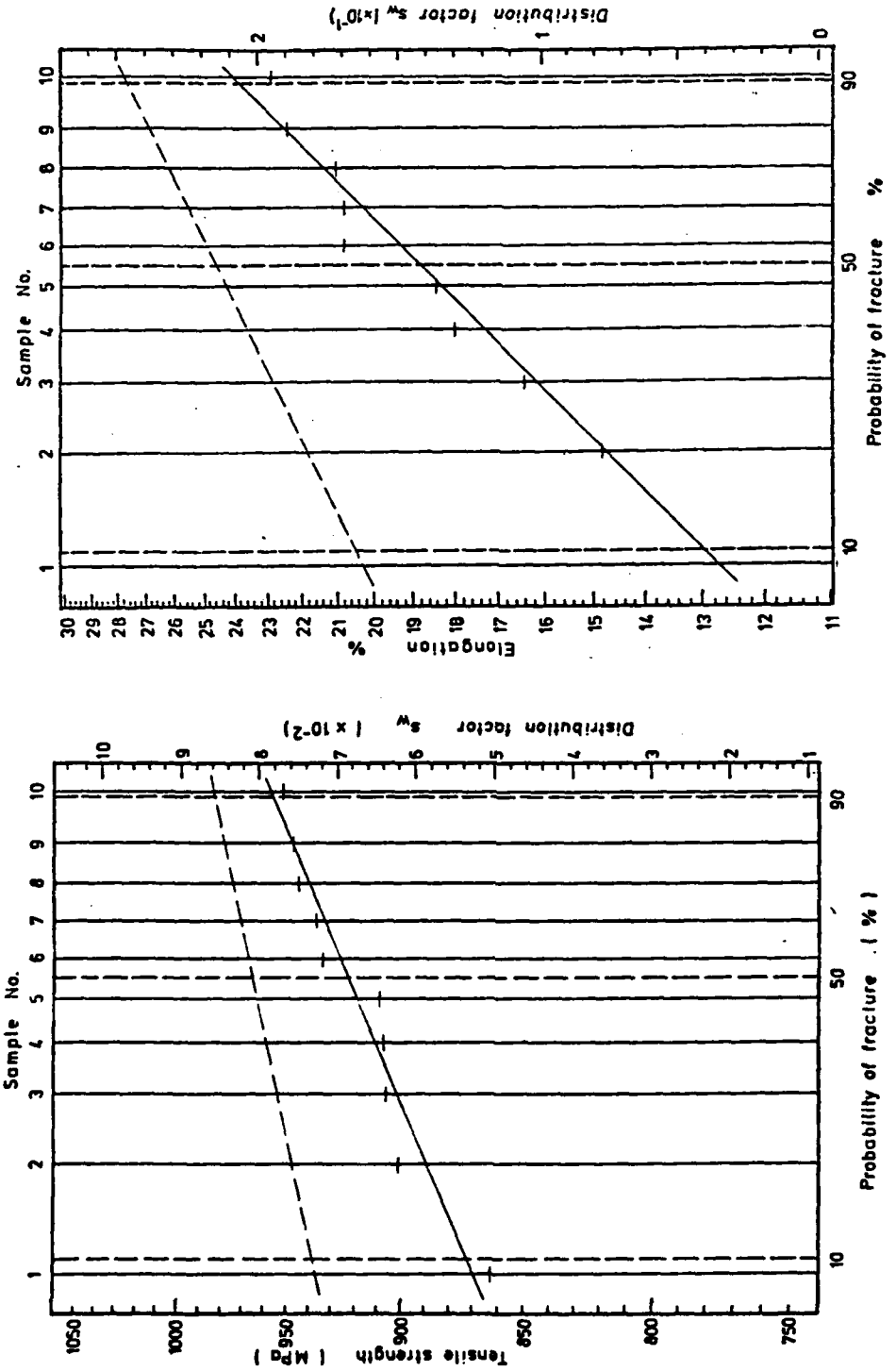

Fig.60: Weibull-diagrams for E56W (——) and W640/81 (- - -)

Powder E 61

Table 6: Mechanical properties of the samples prepared from E 61 and of the reference sample from W 640/81

E 61			W 640/81		
ϱ	σ	δ	ϱ	σ	δ
16,9651	947	16,8	17,0749	960	20,4
16,9846	845	8,4	17,0859	956	26,0
16,9971	931	14,4	17,0942	946	23,2
17,0088	898	10,6	17,0319	975	25,0
17,0067	805	5,2	17,0340	987	22,6
17,0157	936	18,0	17,0428	966	28,0
17,0204	930	14,8	17,0506	959	25,0
16,4855	911	12,0	17,0131	957	20,8
16,4651	854	8,8	17,0728	953	23,0
16,7564	905	12,0	17,0486	963	22,8
E 61	16,870 $\pm$ 0,222		896 $\pm$ 47		12,1 $\pm$ 4,0
W 640	17,055 $\pm$ 0,026		963 $\pm$ 11		23,7 $\pm$ 2,3

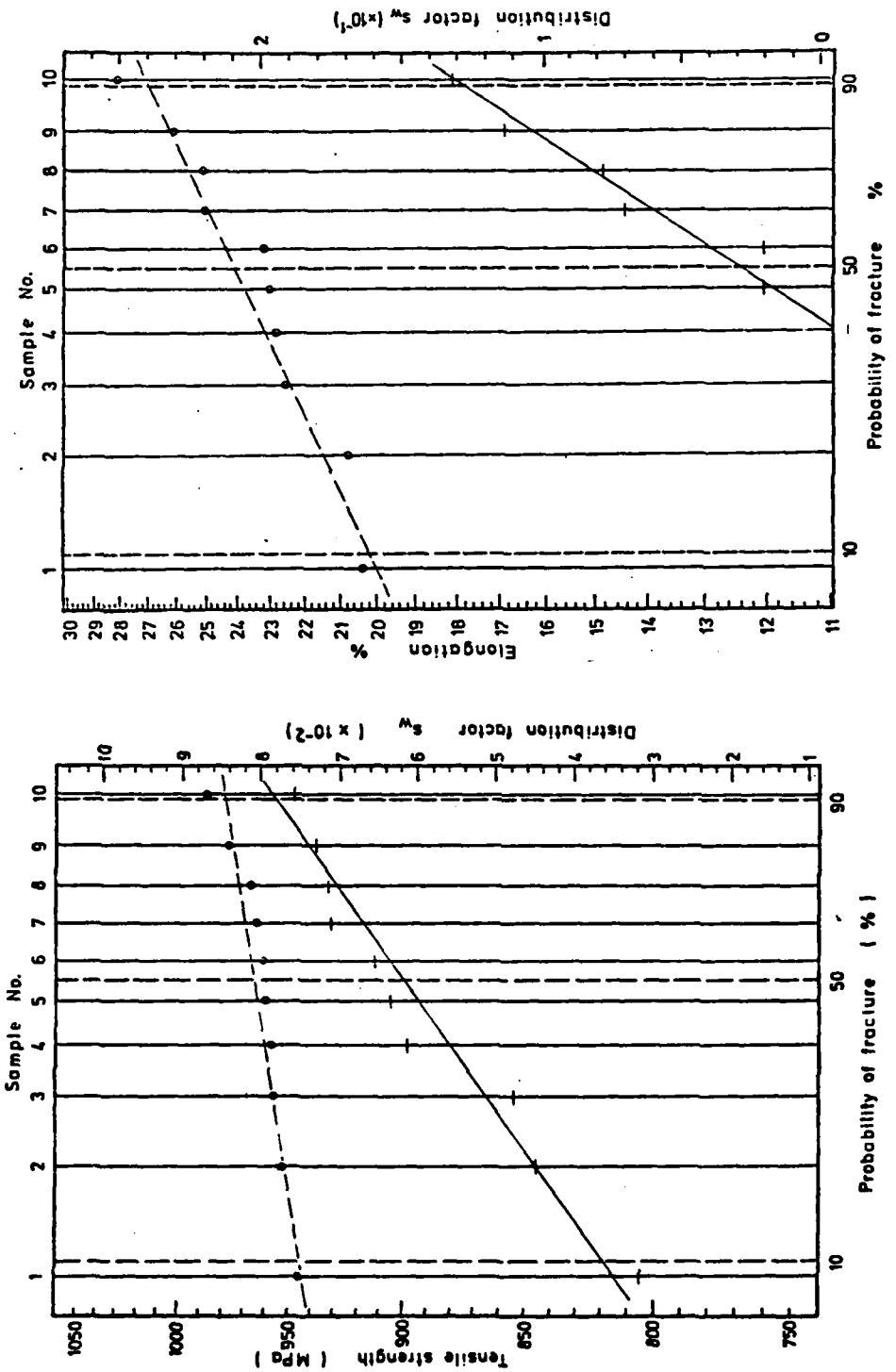

Fig.61: Weibull-diagrams for E61W (——) and W640/81 (- - -)

Powder E 63

Table 7: Mechanical properties of the samples prepared from E 63 and of the reference sample from W 640/81

E 63			W 640/81		
ϱ	σ	δ	ϱ	σ	δ
17,1004	969	19,2	17,0410	949	18,8
17,0986	925	15,2	17,0324	939	25,4
17,1029	900	11,8	17,0515	907	16,6
17,0476	925	13,4	17,0795	919	19,2
17,0245	919	15,4	17,0270	939	21,4
17,0310	928	13,4	17,0125	949	19,6
17,0194	929	15,6	17,0229	930	22,0
17,0005	924	16,0	17,0314	918	20,4
17,0172	926	18,0	17,0231	923	19,0
17,1025	952	16,0	17,0602	950	20,8
17,0929	963	16,8	17,0553	963	23,2
17,0936	927	12,8	17,0444	942	19,8

Mean values ± standard deviations

E 63	17,061 ± 0,041	932 ± 19	15,3 ± 2,2
W 640	17,040 ± 0,019	935 ± 16	20,5 ± 2,3

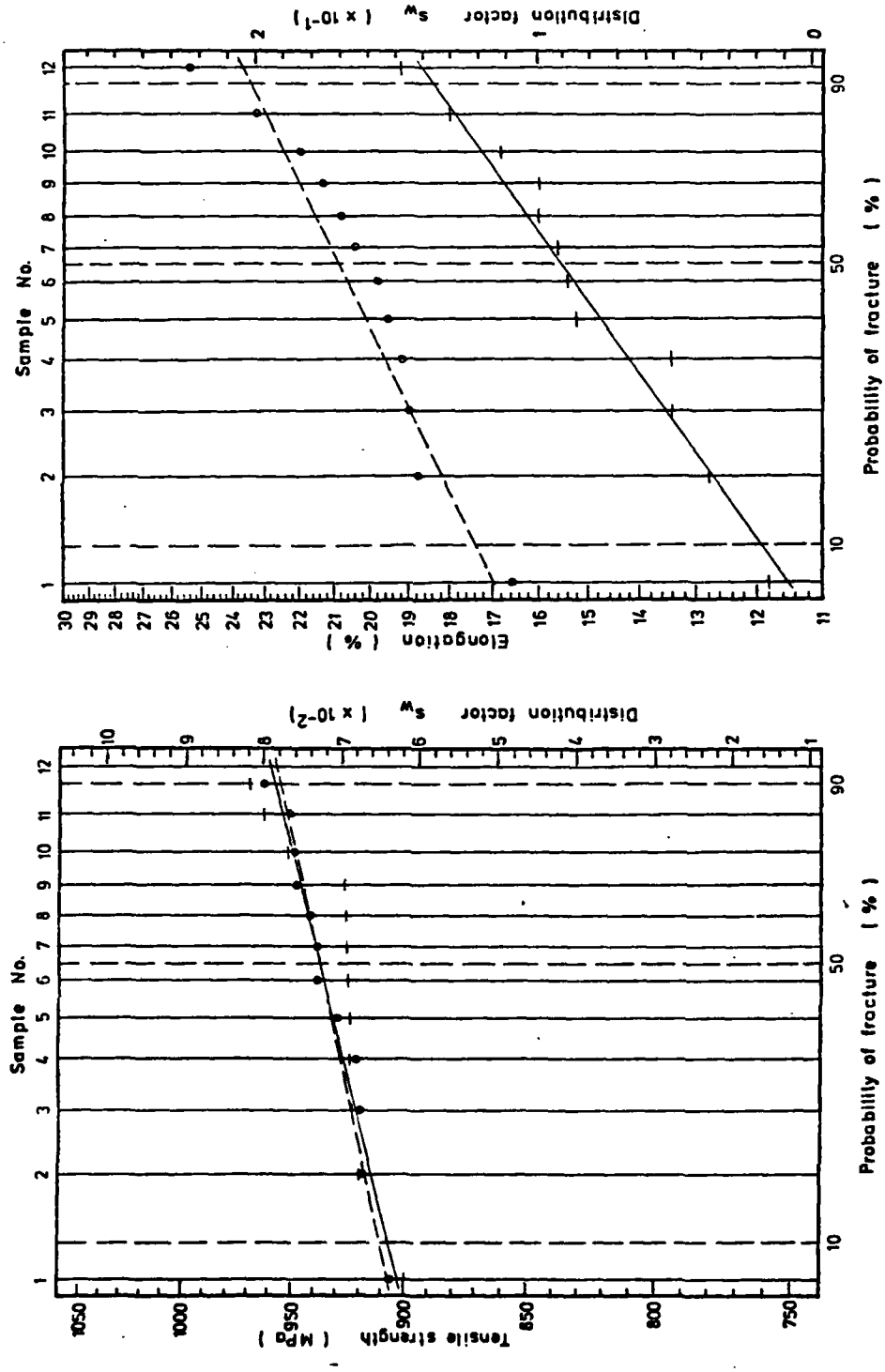

Fig.62: Weibull-diagrams for E63W (——) and W640/81 (- - -)

Powder E 67

Table 8: Mechanical properties of the samples prepared from E 67 and of the reference sample from W 640/81

E 67			W 640/81		
ϱ	σ	δ	ϱ	σ	δ
17,0243	951	14,4	17,0131	957	20,8
17,0679	920	19,2	17,0118	917	20,8
17,0610	961	23,2	17,0131	938	24,0
17,0618	975	18,0	17,0905	939	24,6
17,1072	958	20,0	17,0903	947	24,6
17,0634	901	12,8	17,0986	952	25,2
17,0244	932	19,4	17,0765	962	23,6
17,0646	969	23,2	17,0357	947	21,0
16,9990	905	18,4	17,0614	945	20,0
17,0966	914	10,8	17,0384	955	20,6

Mean values ± standard deviations

E 71	17,057 ± 0,033	938 ± 27	17,9 ± 4,1
W 640	17,053 ± 0,035	946 ± 13	22,1 ± 2,0

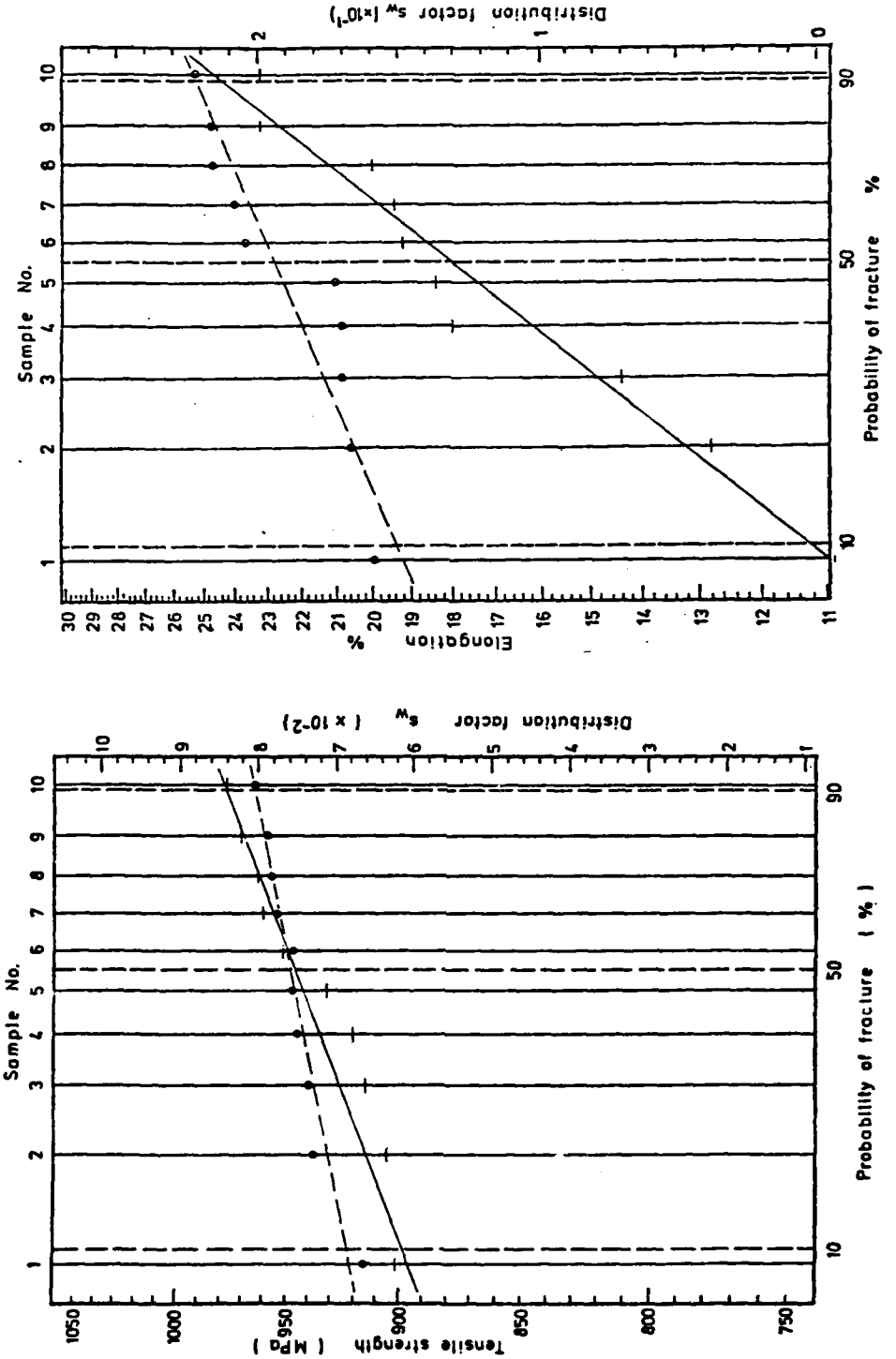

Fig.63: Weibull-diagrams for E67W (——) and W640/81 (- - -)

Powder E 71

Table 9: Mechanical properties of the samples prepared from E 71 and of the reference sample from W 640/81

E 71			W 640/81		
ρ(g/cm^3)	σ_b(MPa)	δ(%)	ρ(g/cm^3)	σ_b(MPa)	δ(%)
17,0741	964	23,2	17,0765	962	23,6
17,0408	932	19,2	17,0440	945	21,0
17,0179	949	23,2	17,0250	953	26,8
17,0323	971	27,6	17,0400	928	(16,8)
17,0302	954	27,6	17,0212	951	23,6
One sintering batch omitted because of faulty temperature control					
17,0391	954	24,2	17,0413	949	23,8

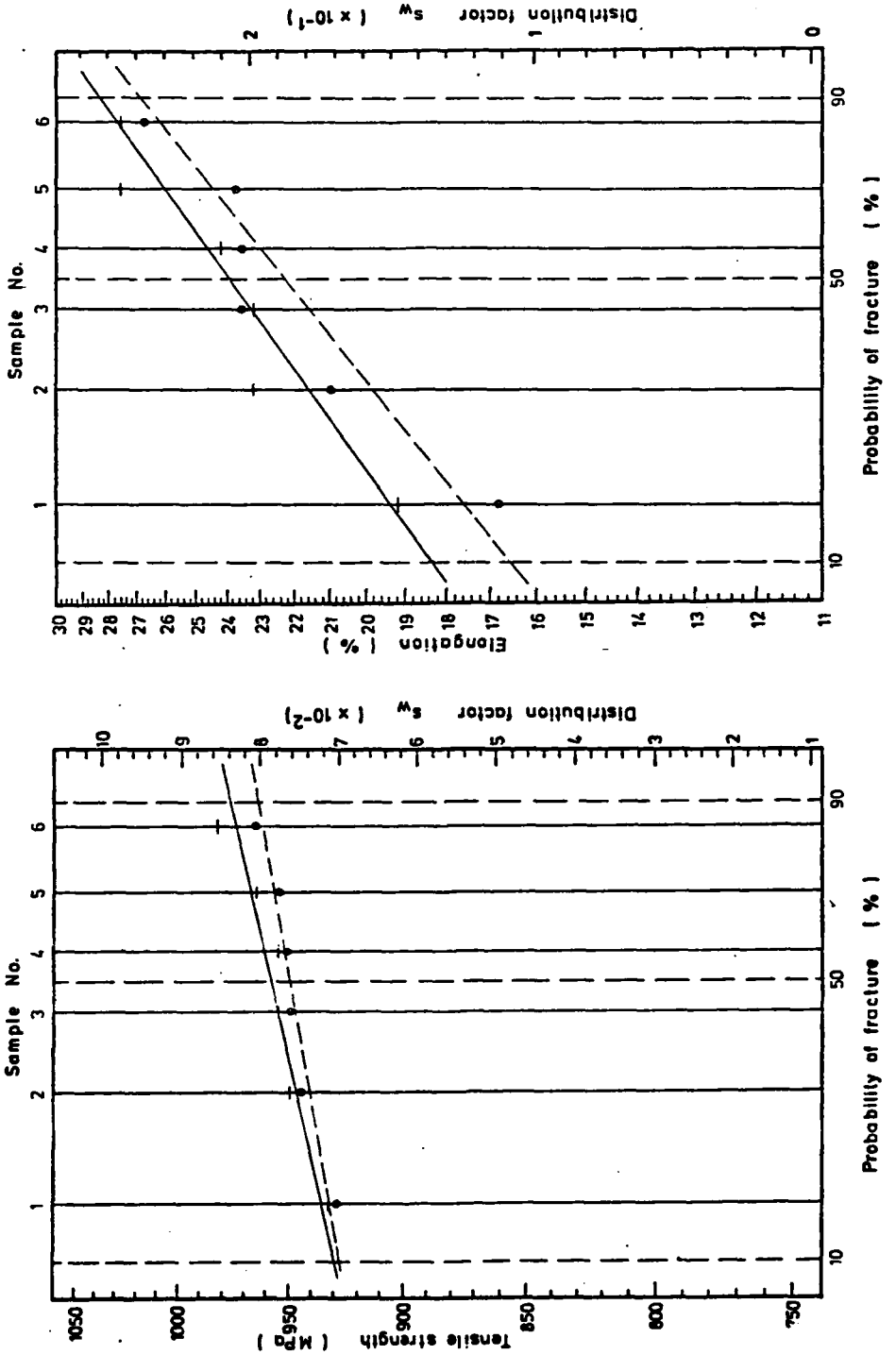

Fig.64: Weibull-diagrams for E71W (——) and W640/81 (- - -)

Powder E 79

Table 10: Mechanical properties of the samples prepared from E 79 and of the reference sample from W 640/81

E 79			W 640/81		
ς	σ	δ	ς	σ	δ
17,0915	814	5,4	17,044	961	22,0
17,0884	860	8,8	17,0615	924	20,0
17,1125	964	17,8	17,0467	926	16,6
17,1129	914	12,0	17,0771	944	20,8
17,090	846	7,6	17,0827	956	22,0
17,083	872	8,4	17,040	947	22,6
17,097	944	12,4	17,067	939	19,2
17,099	829	6,4	17,024	942	16,8
17,099	894	13,6	17,049	960	22,8
17,081	965	22,0	17,044	947	21,6

Mean values ± standard deviations

E 79	17,095 ± 0,011	890 ± 55	11,4 ± 5,3
W 640	17,053 ± 0,018	945 ± 13	20,4 ± 2,3

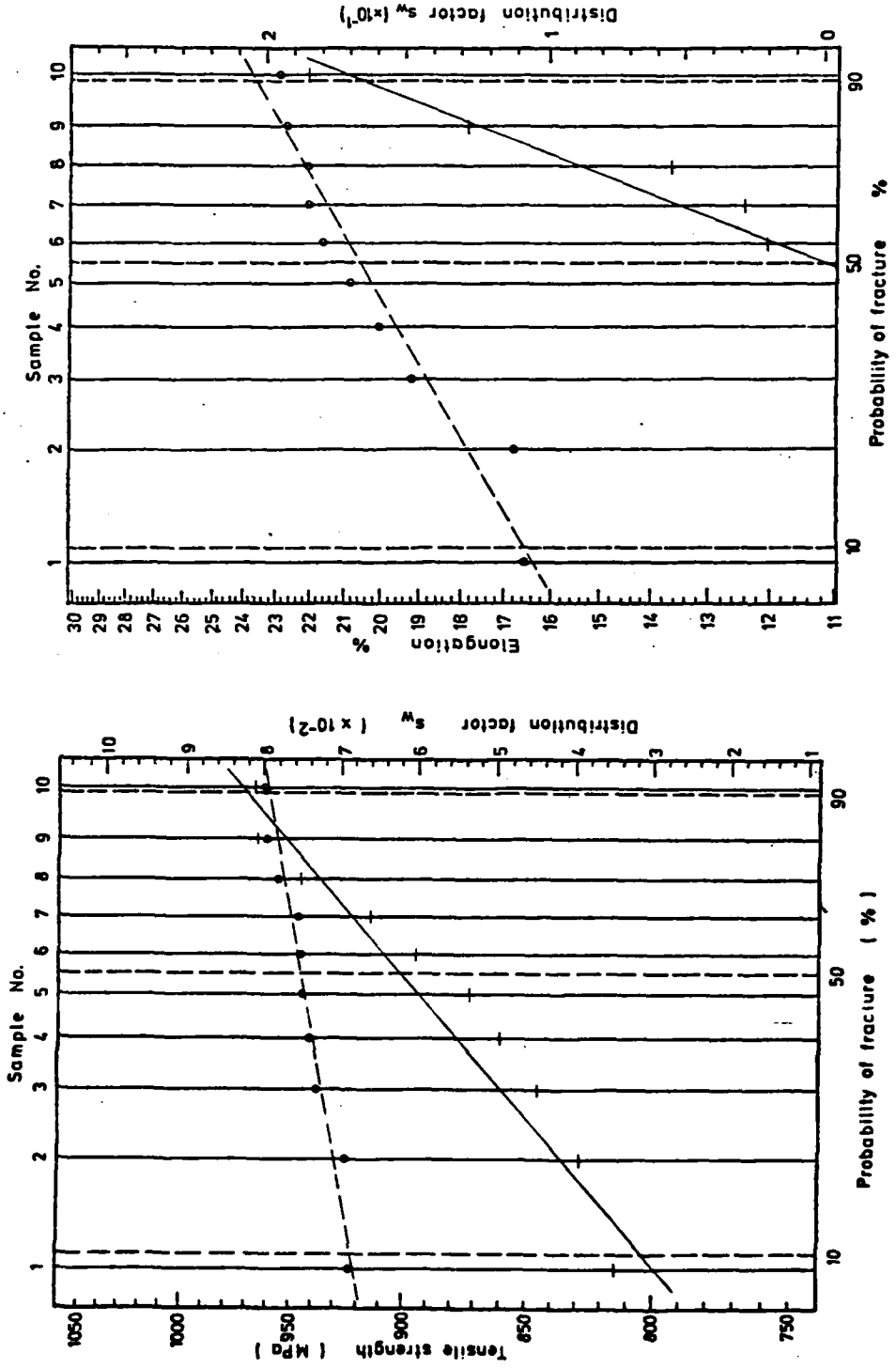

Fig.65: Weibull-diagrams for E79W (——) and W640/81 (- - -)

Powder E 83

Table 11: Mechanical properties of the samples prepared from E 83 and of the reference sample from W 640/81

E 83			W 640/81		
ϱ	σ	δ	ϱ	σ	δ
17,037	1024	22,6	17,062	998	27,4
17,088	995	13,6	17,086	1000	28,2
17,095	997	22,8	17,088	976	25,6
17,080	999	26,2	17,046	976	24,0
17,088	984	30,0	17,075	975	27,2
17,067	961	18,4	17,080	994	28,8
17,067	952	22.4	17,080	964	29,2
			17,088	957	32,2
17,049	956	23,4	17,081	959	24,0
17,038	940	25,6	17,074	979	24,0
17,078	987	28,0	17,100	977	26,4
			17,091	997	28,0

Mean values $\pm$ standard deviations

E 83	17,067 $\pm$ 0,020	974 $\pm$ 29	23,3 $\pm$ 4,7
W 640	17,079 $\pm$ 0,014	979 $\pm$ 15	27,1 $\pm$ 2,5

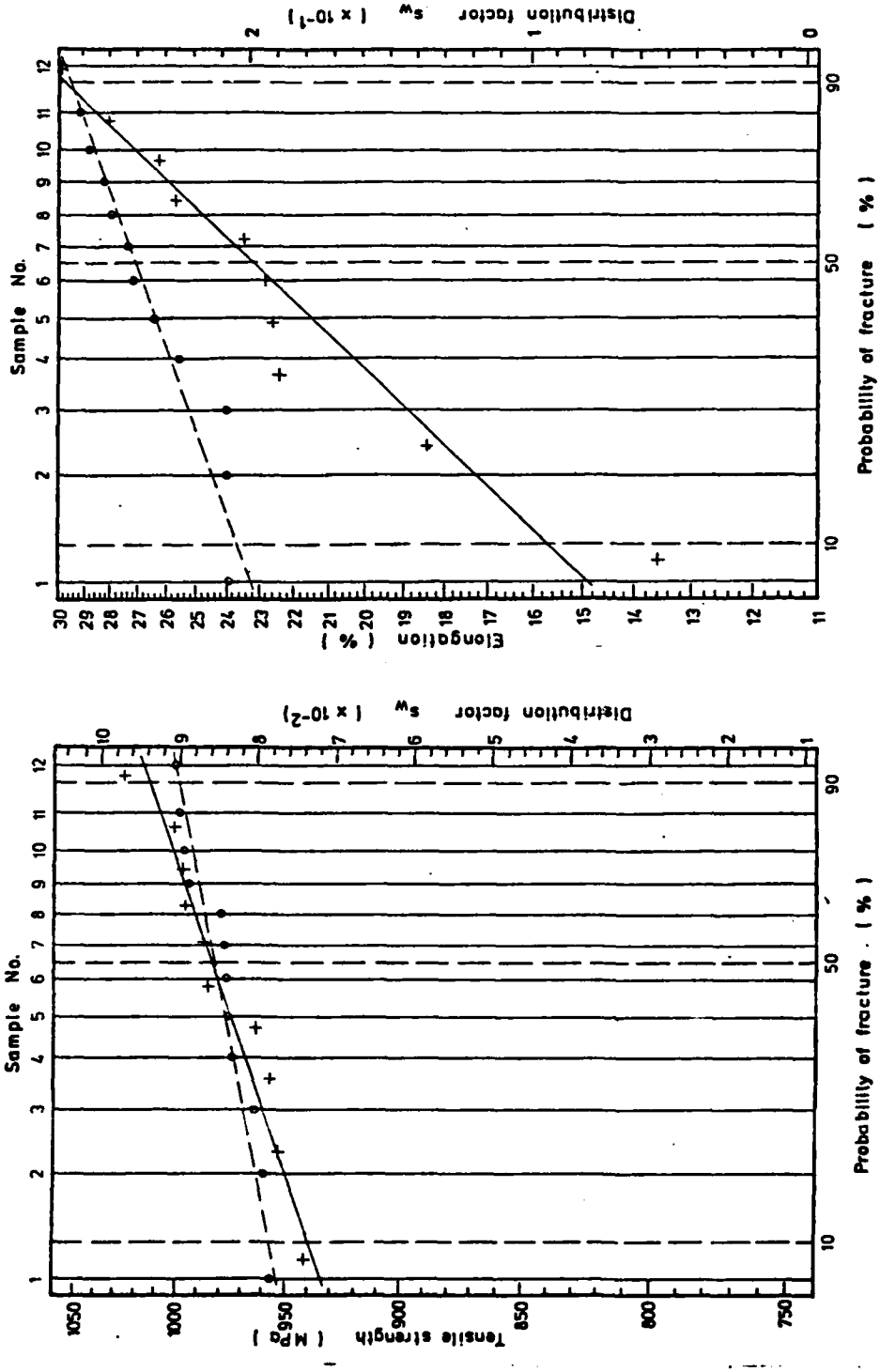

Fig.66: Weibull-diagrams for E03W (——) and W640/81 (- - -)

Powder E 87

Table 12: Mechanical properties of the samples prepared from E 87 and of the reference sample from W 640/81

E 87			W 640/81		
ϱ	σ	δ	ϱ	σ	δ
17,001	957	20,8	17,020	959	27,6
16,994	968	26,5	17,026	969	28,0
17,043	963	24,0	17,030	973	23,6
17,024	953	24,0	17,042	971	29,6
17,050	923	18,8	17,044	961	22,0
17,043	933	23,2	17,051	955	23,6
			17,072	971	22,8
			17,060	937	19,6
17,048	933	8,0	17,039	930	16,0
17,039	930	16,0	17,080	928	14,8
17,072	938	18,8			
17,063	935	24,0			
17,0377	943	20,4	17,0467	955	22,8

Mean values ± standard deviations

E 87	17,037 ± 0,025	943 ± 16	20,4 ± 5,4
W 640	17,046 ± 0,019	955 ± 18	22,8 ± 4,9

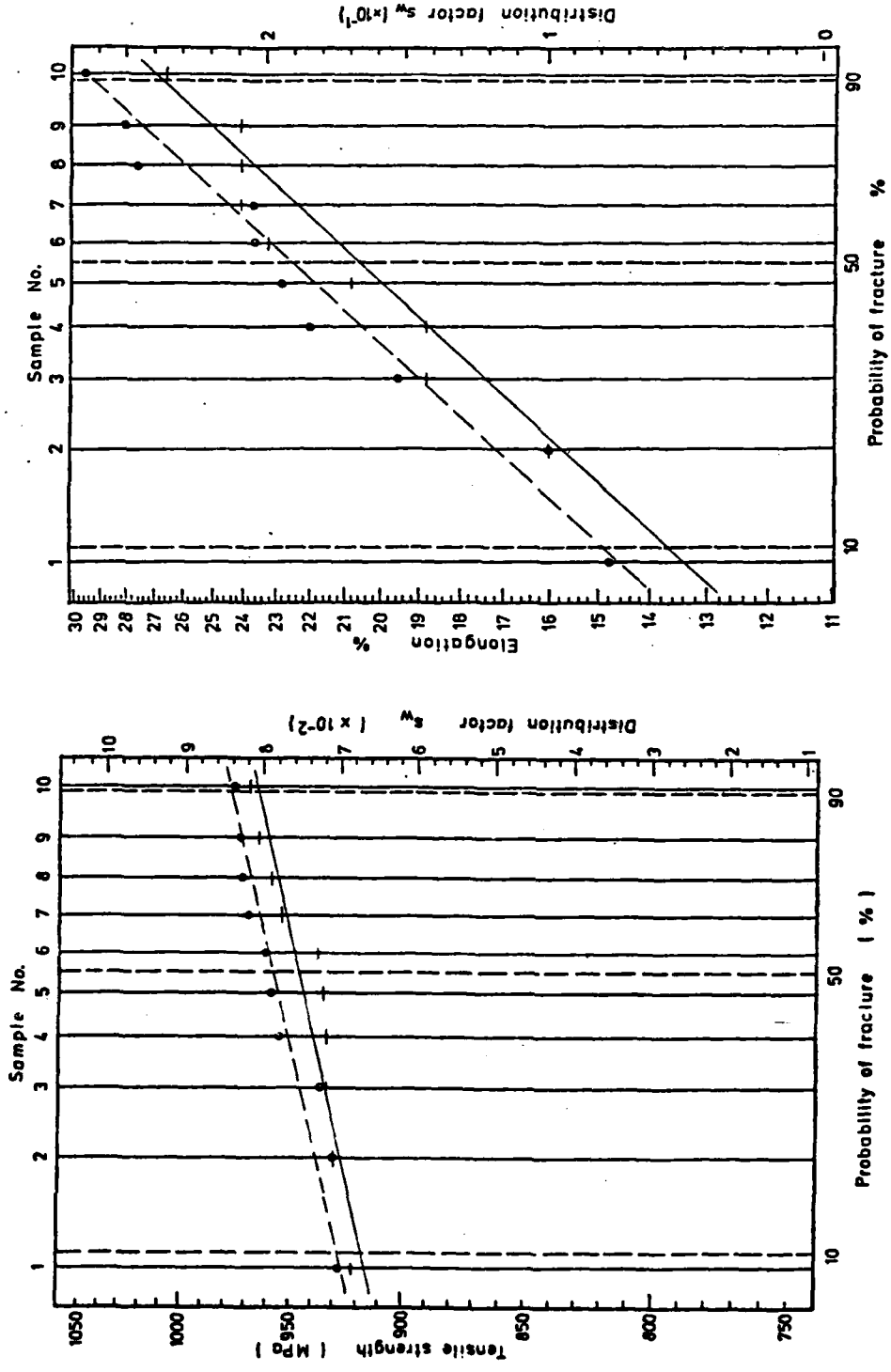

Fig.67: Weibull-diagrams for E87W (——) and W640/81 (- - -)

Powder E 91

Table 13: Mechanical properties of the samples prepared from E 91 and of the reference sample from W 640/81

E 91			W 640/81		
ϱ	σ	δ	ϱ	σ	δ
17,034	836	7,6	17,036	945	26,8
17,045	893	9,6	17,055	941	24,4
17,003	912	17,2	17,032	962	29,6
17,012	942	15,4	17,053	949	28,8
16,921	941	18,8	17,079	942	27,2
16,987	950	24,8	17,072	954	27,6
17,005	968	16,0	17,002	958	28,8
17,017	977	16,0	17,034	940	27,2
17,0030	927	15,7	17,0454	949	27,6
16,7200	794	9,2	17,0640	950	29,0
16,9035	855	11,6	17,0769	938	22,8
17,0429	891	11,6	17,0904	964	24,0
17,0848	911	14,6	17,0744	956	22,4
17,0865	969	12,8	17,0591	964	28,0
17,0741	938	10,0			

Mean values $\pm$ standard deviations

E 91	16,996 $\pm$ 0,092	913 $\pm$ 52	14,1 $\pm$ 4,4
W 640	17,055 $\pm$ 0,024	950 $\pm$ 9	26,7 $\pm$ 2,4

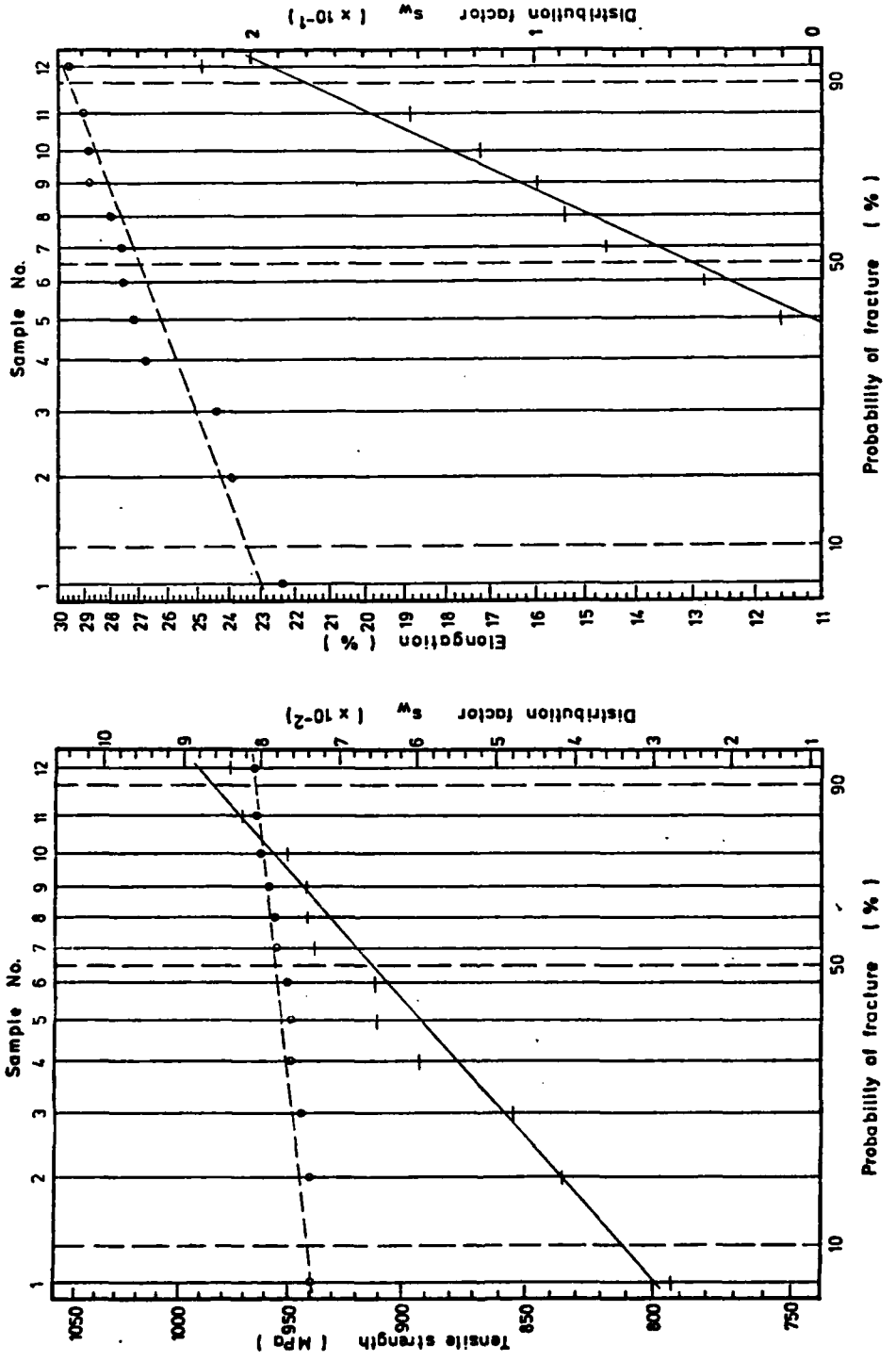

Fig.68: Weibull-diagrams for E91W (——) and W640/81 (- - -)

Powder E 95

Table 14: Mechanical properties of the samples prepared from E 95 and of the reference sample from W 640/81

E 95			W 640/81		
ϱ	σ	δ	ϱ	σ	δ
17,0797	942	15,6	17,0680	945	15,8
17,0807	964	15,2	17,0239	967	19,8
			17,0672	958	18,0
17,0875	956	16,6	17,0583	961	22,2
17,1048	976	21,8	17,0654	967	22,2
17,0841	950	14,2			
17,1018	1023	19,2	17,0262	973	21,6
17,0747	952	12,6	17,0673	990	21,6
			17,0843	965	18,2
17,1141	990	23,2	17,1166	992	21,6
17,1061	945	13,0	17,1054	994	18,4
17,0985	1001	20,2	17,0723	961	19,4
17,1221	1014	20,2	17,1190	960	16,8
17,1253	963	28,2	17,1190	976	25,2
17,1224	963	15,6	17,0973	994	25,6
			17,1024	1014	19,6
17,0829	997	18,2	17,0998	987	26,6
17,0977	1001	18,8	17,0639	878	9,4
			17,0613	976	18,8
			17,0694	988	22,4
			17,0772	989	23,6

Mean values $\pm$ standard deviations

E 95	17,0989 $\pm$ 0,0169	976 $\pm$ 26	17,5 $\pm$ 3,2
W 640	17,0851 $\pm$ 0,0412	979 $\pm$ 19	20,3 $\pm$ 3,8

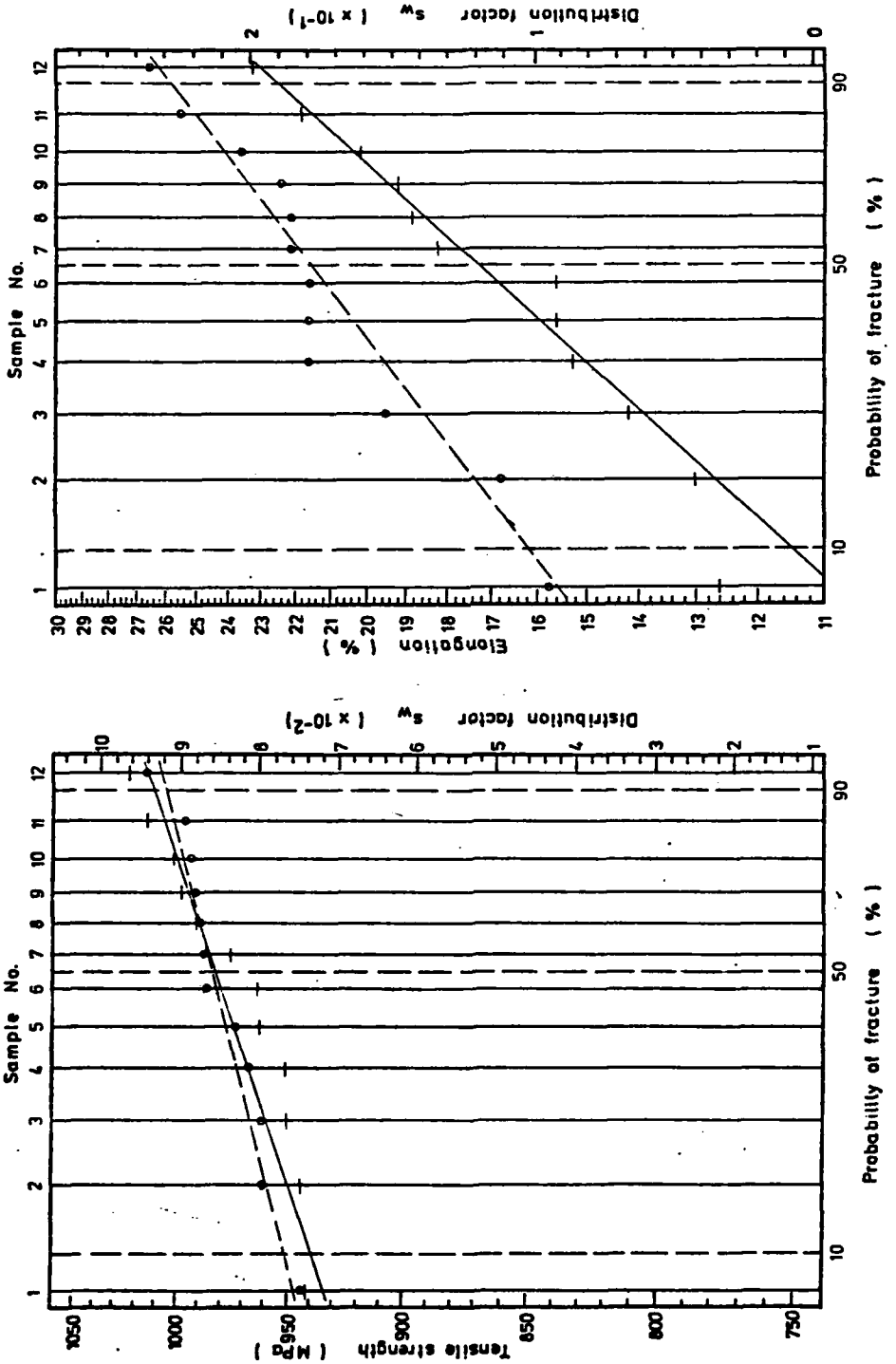

Fig.69: Weibull-diagrams for E95W (——) and W640/81 (- - -)

Powder E 99

Table 15: Mechanical properties of the samples prepared from E 99 and of the reference sample from W 640/81

E 99			W 640/81		
ϱ	σ	δ	ϱ	σ	δ
17,0860	956	26,8	17,0640	950	29,0
17,0945	960	21,2	17,0739	938	22,8
17,0668	939	21,6	17,0251	933	22,8
17,0609	942	18,8	17,0418	926	22,0
17,0980	937	21,0			
17,0972	960	28,0	17,0795	947	23,6
17,0232	909	12,0	17,0602	931	26,0
17,0360	949	21,8	17,0178	948	22,2
17,0656	918	13,4	17,0322	944	20,0
17,0614	948	22,8	17,0257	943	22,2
17,0520	948	17,2	17,0384	932	20,0
17,0657	944	16,6	17,0742	952	21,2
17,0819	970	23,4	17,0544	943	23,2

Mean values $\pm$ standard deviations

E 99	17,0684 $\pm$ 0,023	944 $\pm$ 17	20,3 $\pm$ 4,7
W 640	17,049 $\pm$ 0,021	940 $\pm$ 8	22,9 $\pm$ 2,5

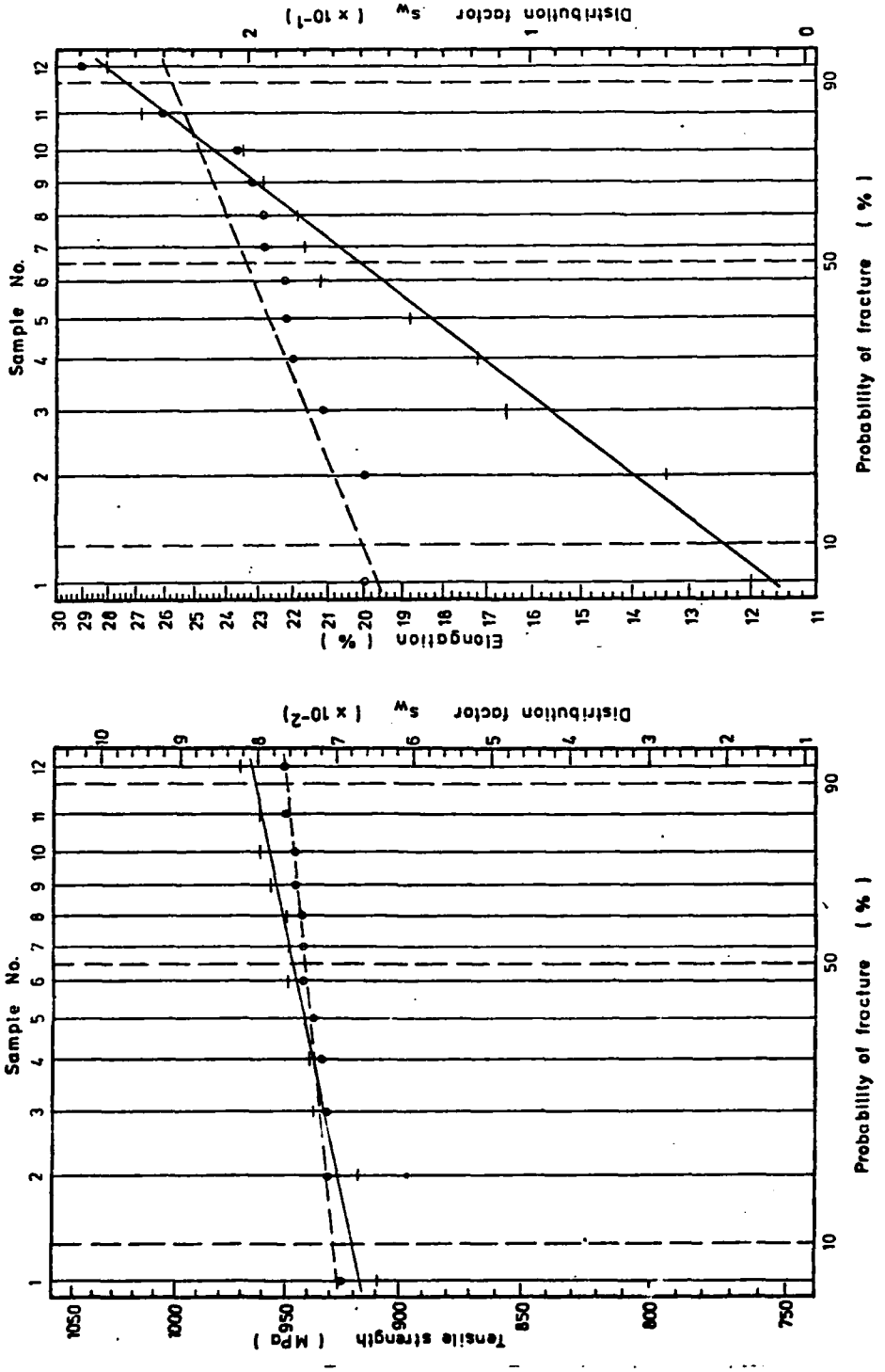

Fig.70: Weibull-diagrams for E99W (——) and W640/81 (- - -)

Powder E 103

Table 16: Mechanical properties of the samples prepared from E 103 and of the reference sample from W 640/81

E 103			640/81		
ρ (g/cm^3)	σ_B (MPa)	δ (%)	ρ (g/cm^3)	σ_B (MPa)	δ (%)
17,0711	856	9,2	17,0642	914	18,0
17,0658	860	8,8	17,0454	906	19,6
17,0462	879	12,0	17,0358	917	16,0
17,0594	883	12,0	17,0766	972	23,0
17,0349	895	16,0	17,0239	967	19,8
17,0807	956	21,0	17,0583	961	22.2
17,0662	941	17,6	17,0262	973	21,6
17,0879	918	14,8	17,1166	992	21,6
17,0858	897	12,0	17,0723	961	19,4
17,0930	960	20,8	17,0694	988	22,4
17,0654	871	10,8	17,0772	989	23,6
17,1061	928	16,8			

Mean values $\pm$ standard deviations

E 103	17,072 $\pm$ 0,020	904 $\pm$ 36	14,3 $\pm$ 4,2
W 640	17,061 $\pm$ 0,027	958 $\pm$ 31	21,5 $\pm$ 3,6

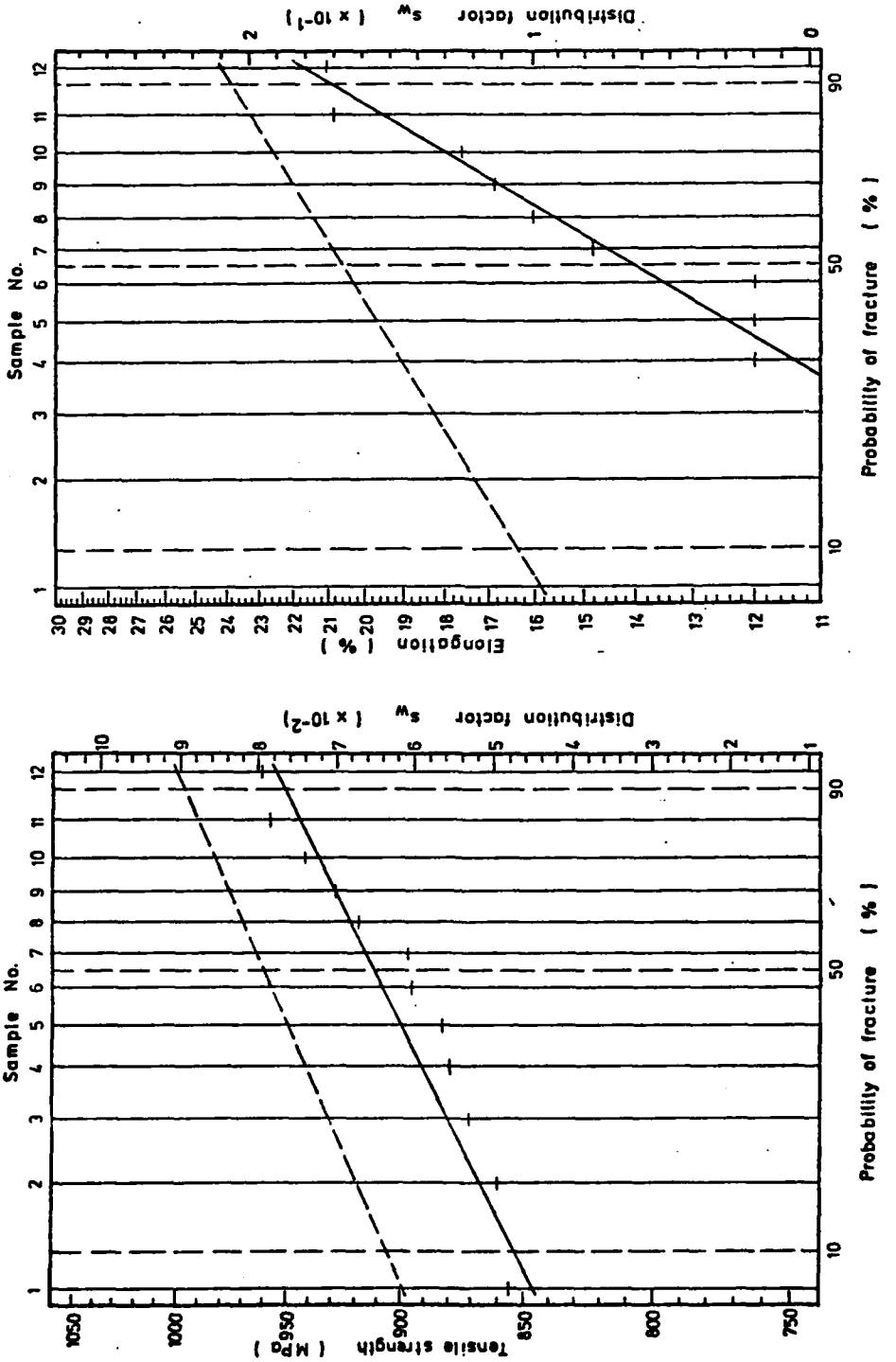

Fig.71: Weibull-diagrams for E103W (——) and W640/81 (- - -)

E 107

Table 17: Mechanical properties of the samples prepared from E 107 and of the reference sample from W 640/81

E 107			W 640/81		
ϱ	σ	δ	ϱ	σ	δ
17,1054	913	12,0	17,1082	987	24,0
17,0563	970	20,0	17,0833	1000	27,6
17,0851	970	17,6	17,0772	976	22,8
17,0946	945	17,2			
17,0924	930	14,4	17,0892	951	19,2
17,0946	950	16,2	17,0850	956	20,4
17,0697	960	20,0	17,0778	946	24,0
17,0750	855	6,8	17,0660	911	20,2
17,0920	899	11,6	17,0683	952	22,4
17,1014	916	14,6	17,0553	963	20,8
17,0984	780	4,8	17,0975	942	19,8

Mean values $\pm$ standard deviations

E 107	17,088 $\pm$ 0,015	917 $\pm$ 57	14,1 $\pm$ 4,9
W 640	17,081 $\pm$ 0,015	959 $\pm$ 25	22.1 $\pm$ 2,6

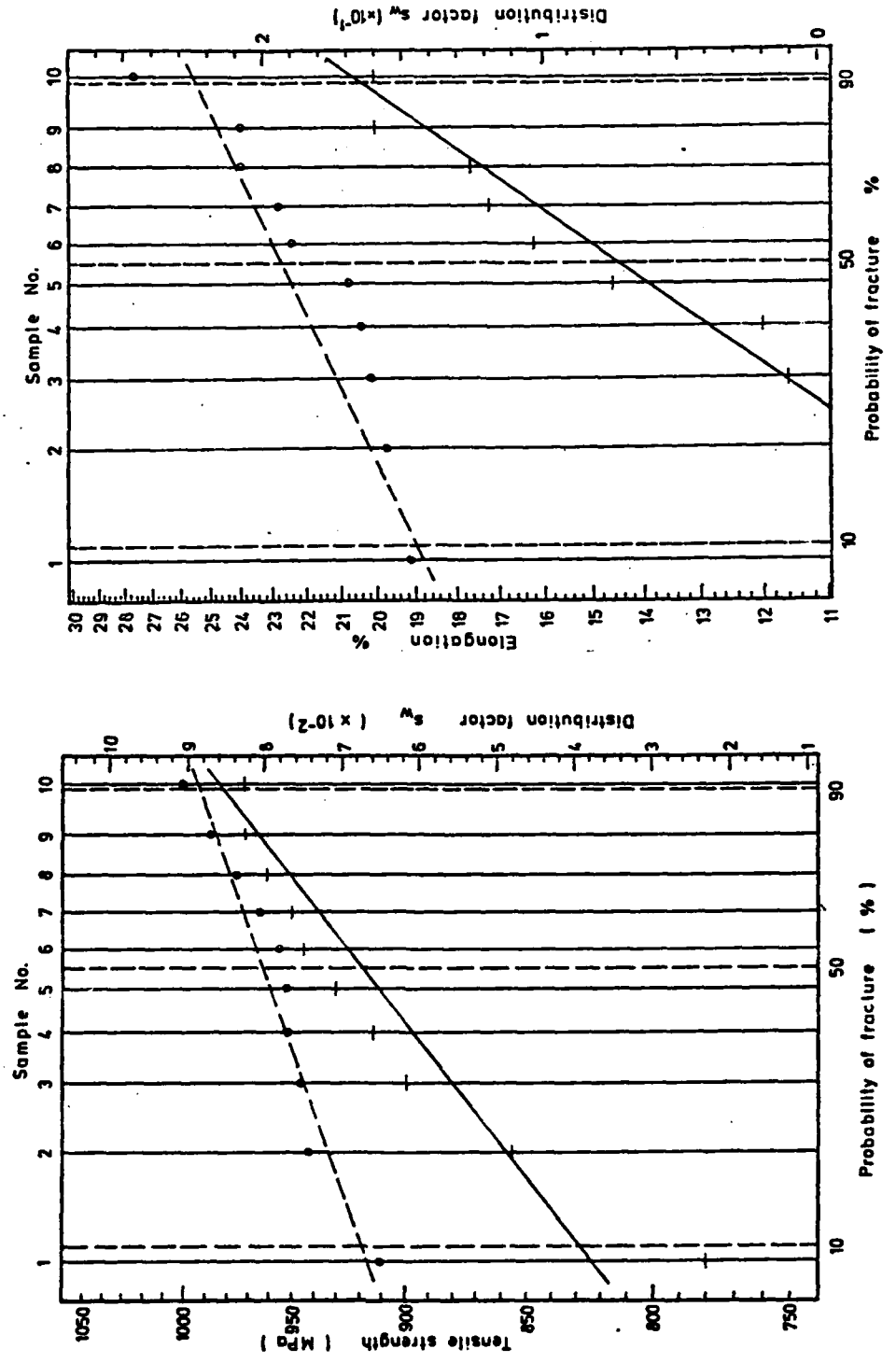

Fig.72: Weibull-diagrams for E107W (——) and W640/81 (- - -)

Powder E 111

Table 18: Mechanical properties of the samples prepared from E 111 and of the reference sample from W 640/81

E 111			W 640/81		
ρ	σ	δ	ρ	σ	δ
15,5661	753	14,4	17,0680	945	15,8
15,4417	757	12,0	17,0239	967	19,8
			17,0672	958	18,0
17,4555	867	14,6	17,0583	961	22,2
16,5128	856	17,4	17,0654	967	22,2
16,4943	857	13,6			
16,3354	855	12,4	17,0262	973	21,6
16,3362	860	12,2	17,0873	990	21,6
			17,0843	965	18,2
16,9206	958	17,2	17,1166	992	21,5
16,9733	965	10,2	17,1054	994	18,4
			17,0723	961	19,4
16,7759	957	26,6	17,0998	987	26,6
16,3555	936	13,8	17,0639	878	9,4
16,5980	942	14,0	17,0613	976	18,8
			17,0694	988	22,4
			17,0772	989	23,6

Mean values $\pm$ standard deviations

E 111	16,3971 $\pm$ 0,4699	880 $\pm$ 74	14,0 $\pm$ 2,2
W 640	17,0704 $\pm$ 0,0244	974 $\pm$ 15	20,7 $\pm$ 2,7

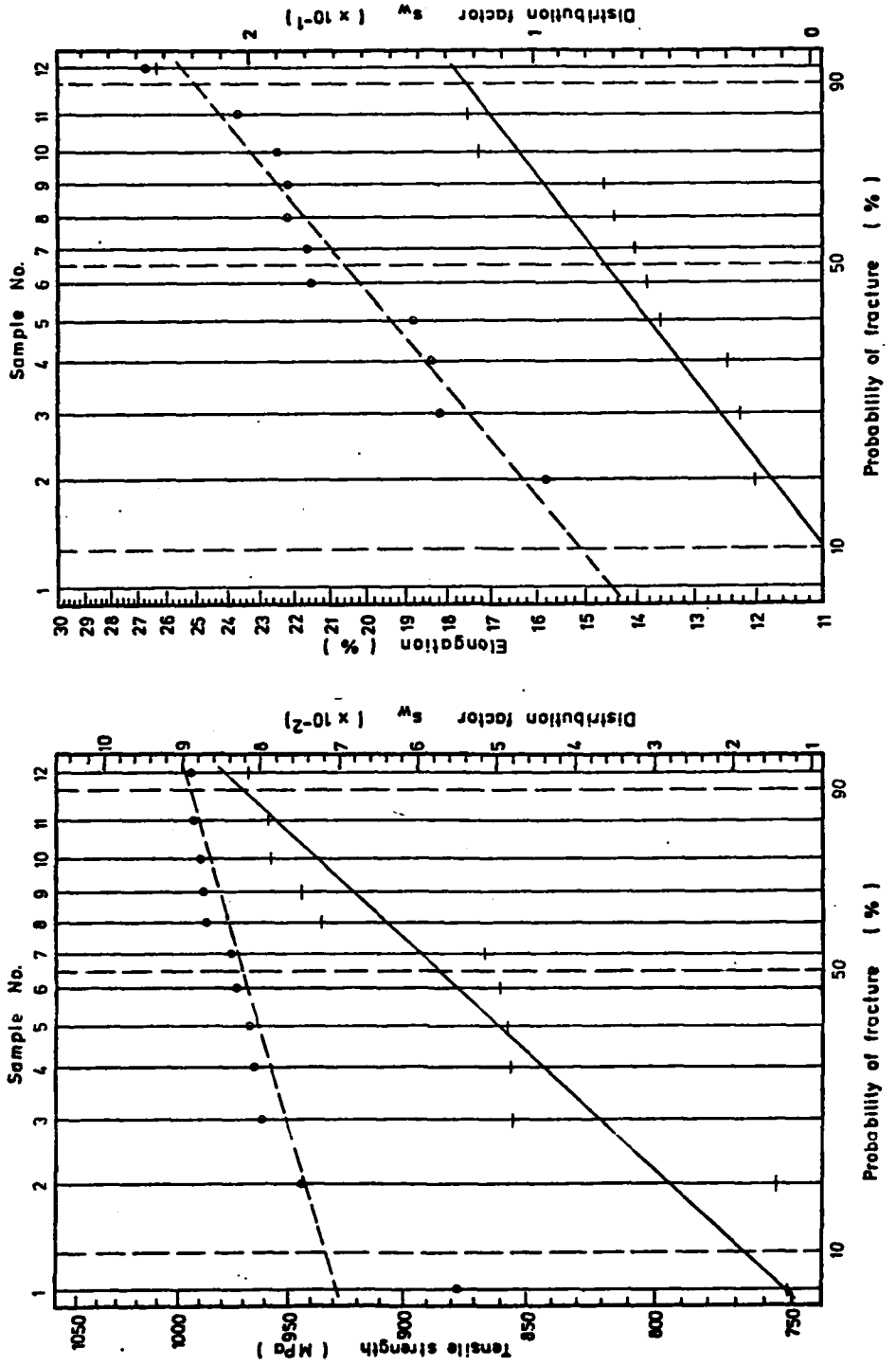

Fig.73: Weibull-diagrams for E111W (——) and W640/81 (- - -)

Powder E 115

Table 19: Mechanical properties of the samples prepared from E 115 and of the reference samples from W 640/81

E 115			W 640/81		
ϱ	σ	δ	ϱ	σ	δ
17,0530	971	17,0	17,0680	945	15,8
17,0900	992	28,0	17,0239	967	19,8
17,0625	978	27,6	17,0672	958	18,0
17,0242	989	15,4	17,0583	961	22,2
17,0710	985	26,0	17,0654	967	22,2
17,1010	977	21,8	17,0262	973	21,6
17,1162	1004	26,6	17,0673	990	21,6
17,0875	944	23,8	17,0843	965	18,2
17,1058	992	27,0	17,1666	992	21,6
17,1254	938	25,6	17,1054	994	18,4
			17,0723	961	19,4
17,1052	992	27,6	17,1190	960	16,8
17,1226	977	26,4	17,1190	975	25,2
17,1184	996	26,8	17,0973	994	25,6
			17,1024	1014	19,6

Mean values $\pm$ standard deviations

E 115	17,0925 $\pm$ 0,0329	984 $\pm$ 15	24,6 $\pm$ 4,1
W 640	17,0795 $\pm$ 0,0306	974 $\pm$ 19	20,4 $\pm$ 2,8

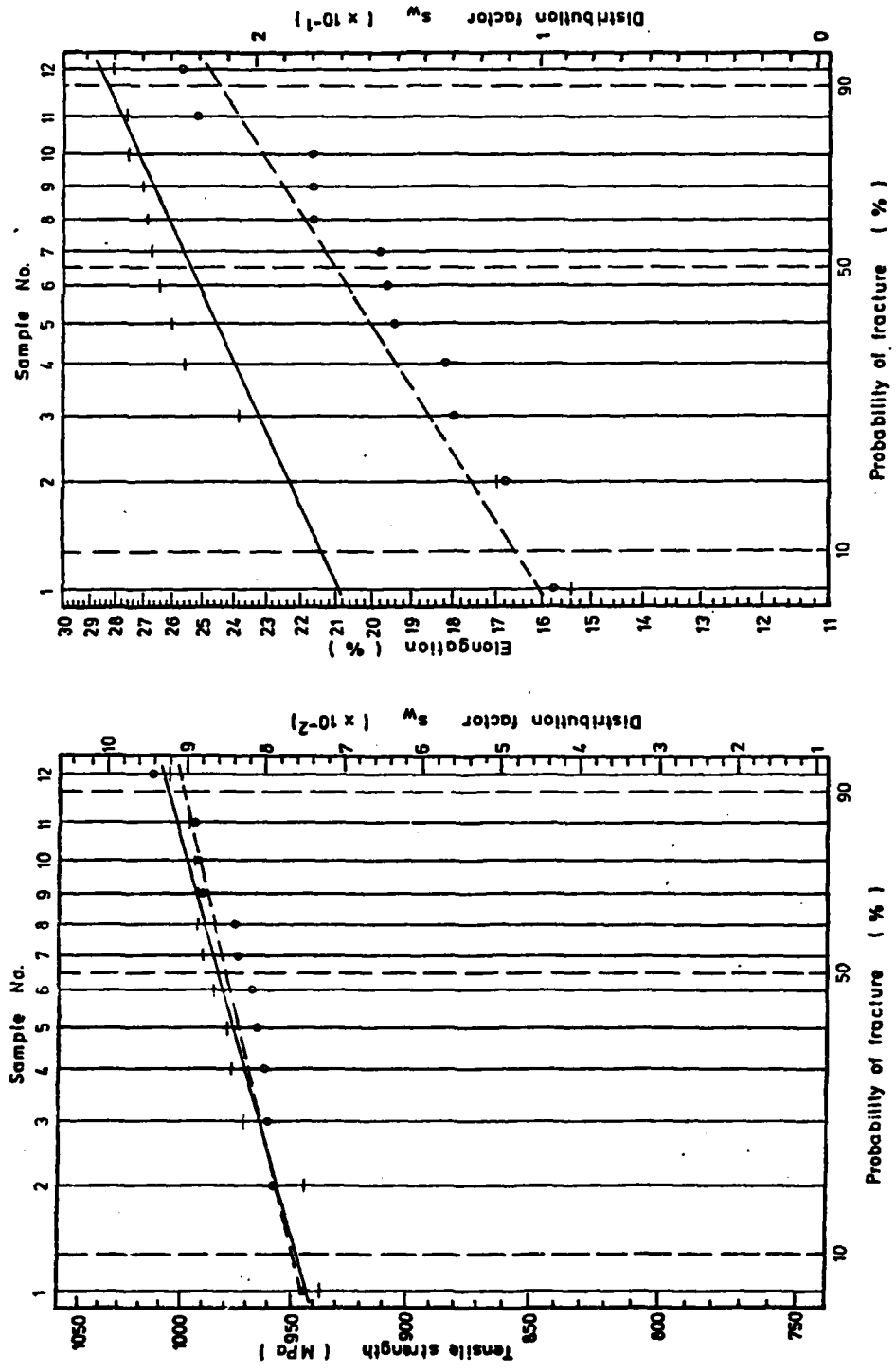

Fig.74: Weibull-diagrams for E115W (——) and W640/81 (- - -)

Regarding the results as a whole, except for those heavy metals roughly equal in quality to those prepared from standard powder, there are two groups of heavy metals with unsatisfactory mechanical properties, esp. elongation: the first group contains those heavy metals with low sintering density due not to pores or blisters but to overall unsatisfactory sintering. Even from their external appearance it can be seen that they are not properly sintered: they do not look metallic but rather dull grey, as if they had not been liquid phase sintered; also they had shrunk very little, much less than the properly sintered samples. Specimens in this group were those heavy metals prepared from E 48(Na) and E 51(Li), the coarser powders with grain sizes >20 um. Both tensile strength and elongation here are correlated to the grain size, E 51(Li), the coarser one, being inferior in both respects. SEM investigations (Fig.76, 77) showed that those samples are only partially sintered and contain large areas where no liquid phase sintering at all had taken place. This is evident from the irregular shape of the W grains as compared to the spherical W grains in the pore on Fig.48, where pore formation had taken place during liquid phase sintering. It must be assumed, therefore, that the starting powder size is of great importance for the heavy metals. Based on the knowledge about the process of liquid phase sintering described in chapter 3 it may be assumed that the capillary driving force that distributes the binder melt homogeneously within the material is too low if the particles are too large in diameter and thus the W skeleton is not uniformly filled with binder. In those places where enough binder is present to fill the pore space, normal liquid phase sintering leads to the usual sound microstructure (Fig.76, right side of the photo) while in the places without binder only solid state sintering occurs, which leads to a structure similar to that of sintered W that may be strong but is necessarily brittle. Generally, with these materials the importance of the correct microstructure even before liquid phase sintering is clearly shown (21,22).

If W grains have not sintered together closely as shown in Fig.41 and 42, even long sintering time at high temperature does not yield fully dense products.

The other group of heavy metals with unsatisfactory properties contains those that have been properly sintered but have formed pores and, in extreme cases, blisters during liquid phase sintering. The latter is the case with E111, containing rare earths. The samples produced from this powder contain small pores, as also observed with heavy metals sintered for a long time, i.e. areas where most of the binder has been driven off (Fig.78). Further, there are verly large pores, with diameters >100 µm (Fig.79), which are really empty spaces apparently formed by considerable internal pressure. Similar pores have been observed with the samples prepared from E36 and E39 (see Fig.50 in (1)). For E111, however, those large pores were not in the center but rather near the surface; thus the internal structure was not weakened so much and the mechanical properties were not quite as bad as might be expected from the porosity.

There are also several other powders resulting in porous heavy metals, although the pores are not as spectacular as those in E111. Instead they are mostly small ones similar to those in Fig.48 and 78. Again the powders doped with Na show a strong tendency to form pores: E61 prepared from "impure blue oxide" which contains considerable amount of Na, and E79, doped with Na and Si, exhibited numerous pores in the fracture surfaces (Fig.80, 81). As typical for this class of heavy metals, the fracture surfaces, except for the pore look rather sound, exhibiting transgranular fracture of the W grains and generally good interphase strength between W grains and binder (Fig.82, 83). In contrast to E79 (Na,Si) the powder E83 (Na,F) resulted in quite satisfactory materials, with elongations well above 20%. It may be assumed that the higher Na content of the former powder is responsible for its different behaviour,

although experiences with the furnace lining indicate that SiO_2 in which form Si is still present after reduction is probably reduced to a considerable degree at sintering temperature and the resulting H_2O causes pore formation.

With K, which was added to W powders in 3 different concentrations, a certain tendency to form pores was observed for those powders doped with 500 and 100 ppm K (Fig.84) while with 50 ppm the resulting bars were even somewhat better than the reference bars prepared from W 640/81. As the analysis sheets for all three powders showed K contents <10 um, the difference in sintering behaviour remains inexplicable unless it is assumed that - unmeasurable - differences in K content below 10 ppm are responsible for this phenomenon.

Slight pore formation was also observed for E91, containing 200 ppm Ba, and E107, doped with Ni, although the pores in these cases are rather small and not conspicuous (Fig.85, 86). They do, however, have a considerable effect on the ductility, esp. regarding the scatter of the individual values. Generally, the characteristic difference between the samples prepared from E48 and E51 and the other porous ones regarding the elongation is the scatter of the individual values: the former exhibit consistently low elongation, as their microstructure is unable to withstand higher degrees of deformation. The latter are characterized by a very broad spread in the elongation values, often with values <10% and >20% being measured in the same sintering batch. As their basic structure is ductile, the probability of fracture at a given degree of deformation depends on the - largely statistical - distribution of the pores within the material.

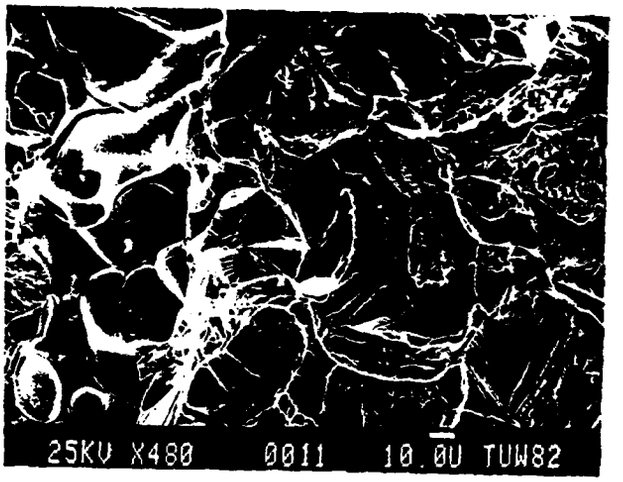

Fig.76
Heavy metal (90%W) prepared from E51W; insufficient densification

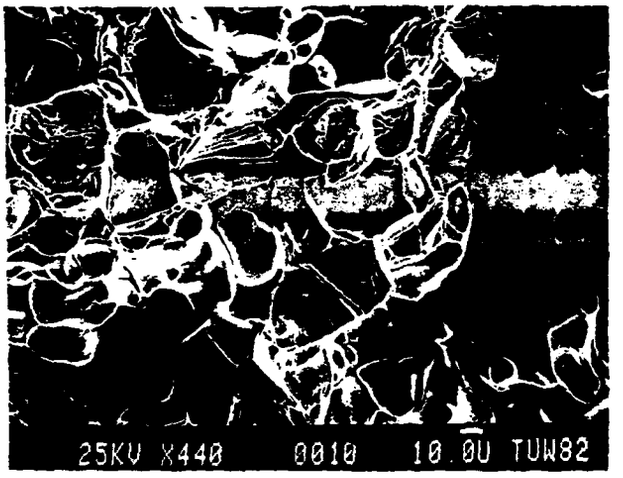

Fig.77
as Fig.76

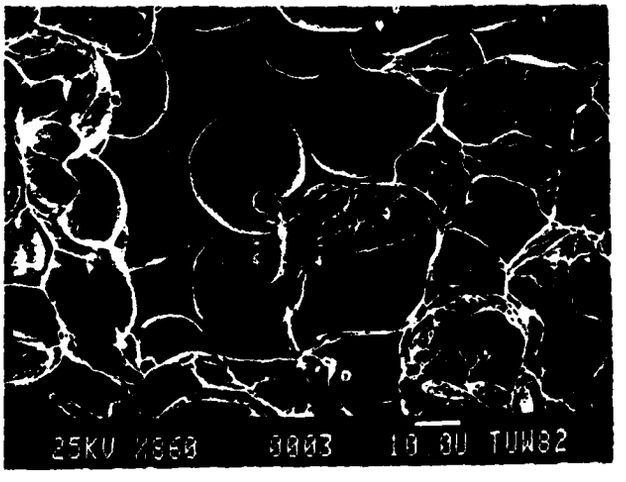

Fig.78
Heavy metal doped with rare earths (E111W); pore formation during sintering

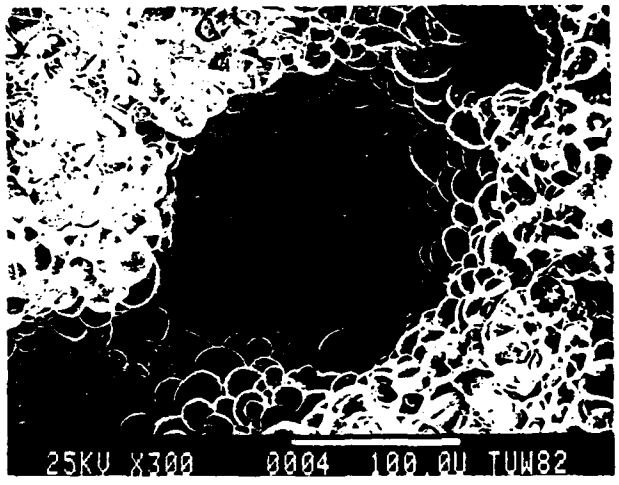

Fig.79
As Fig.78; large pore directly beneath the surface

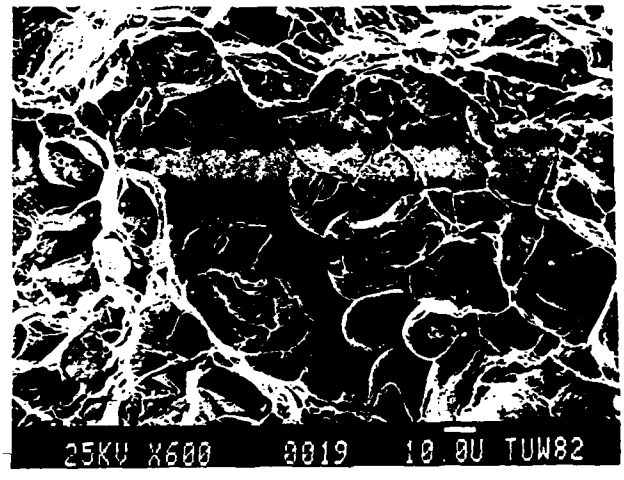

Fig.80
Heavy metal sintered from E61W (containing impurities from blue oxide)

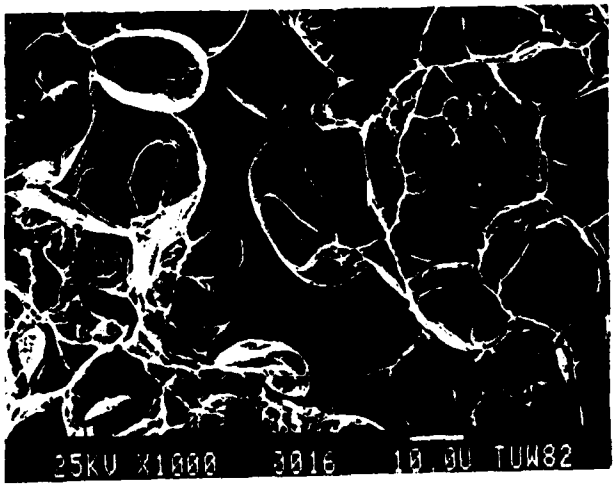

Fig.81
Heavy metal doped with Na, Si (E79W)

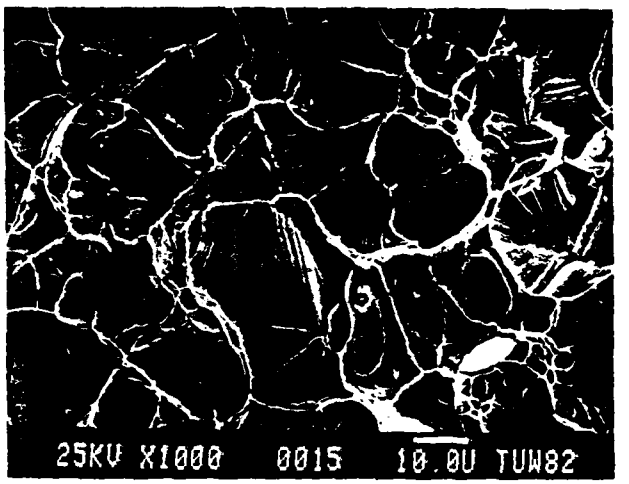

Fig.82
Same surface as on Fig.81; only local porosity

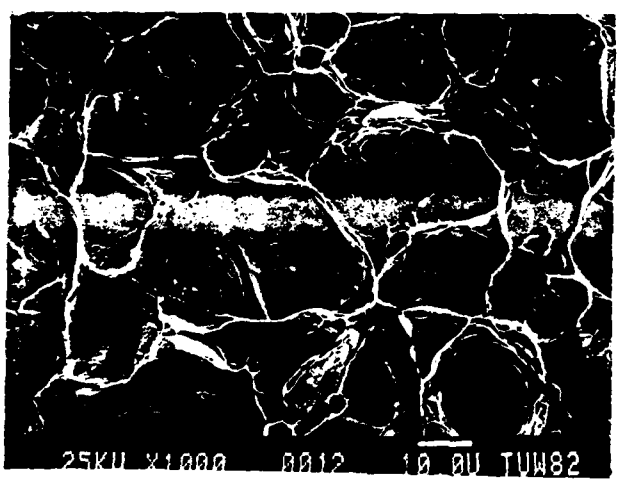

Fig.83
Same surface as on Fig.80; sound dtructure

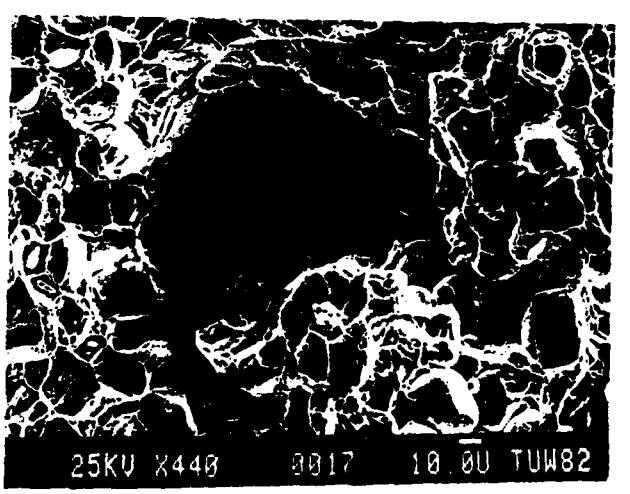

Fig.84
Heavy metal (90%W) prepared from E63W; some isolated pores

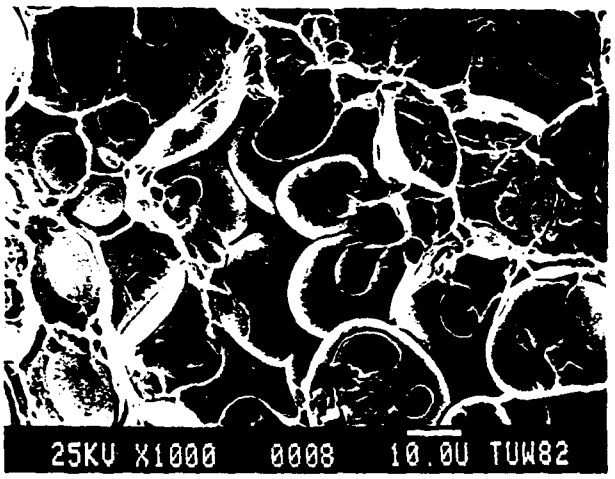

Fig.85
Heavy metal (90%W) prepared from E91W

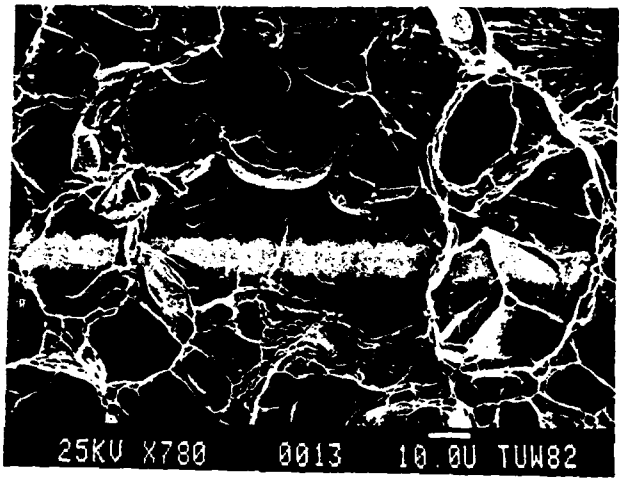

Fig.86
Heavy metal prepared from E107W

4.2 96% W content

The samples with high W content were prepared in quite the same manner as those containing 90% W. Due to the very effective granulation treatment, no problems were encountered during compaction even with this high W content and no pressing faults were observed . Beginning with E 48(Na),however, the sintering cycle was modified . Investigations had shown that,unlike the 90% W samples, the 96% W test bars were still porous after pre-reduction, and it was thought that inter-cooling as shown in Fig.38 might cause re-oxidation which would worsen the properties. Thus the samples were held for 1h at 1400°C and then slowly heated up to sintering temperature. As already described in (1) the optimum sintering temperature for these samples was found to be considerably higher than with the 90% W bars, 1570-1580°C was selected for optimum ductility. The temperature/time diagram for the modified sintering cycle is shown in Fig.87. As described in 4.1. reference samples prepared from W 640/81 were sintered together with the doped samples to set a standard against which the doped powders could be evaluated. The experimental results and Weibull diagrams are shown on the following pages.

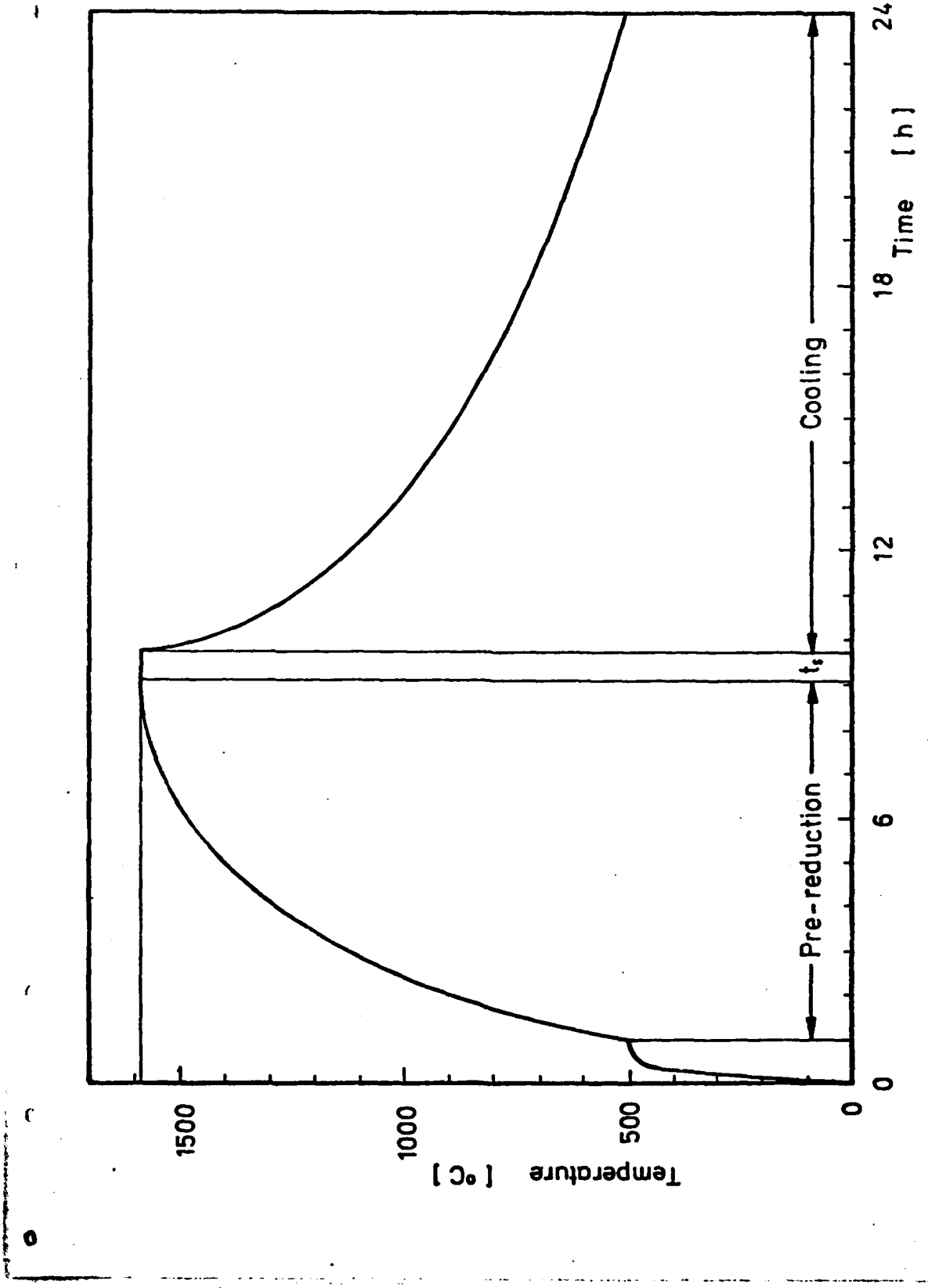

Fig.87: Standard sintering cycle for heavy metals containing 96%W.

Powder E 48

Table 20: Mechanical properties of the samples prepared from E 48 and of the reference samples from W 640/81

E 48			W 640/81		
ρ (g/cm^3)	σ_B (MPa)	δ (%)	ρ (g/cm^3)	σ_B (MPa)	δ (%)
16,7525	535	2,4	18,3325	973	16,0
16,8901	500	0	18,3093	973	19,0
			18,3262	973	18,5
			18,3001	972	19,2
16,9636	610	4,8	18,322	975	19,2
16,9416	576	4,0	18,3198	965	20,6
			18,3333	979	15,2
16,5979	452	0	18,3295	958	20,4
16,7850	544	2,0	18,3325	967	19,6
			18,3150	959	17,6

Mean values $\pm$ standard deviations

E 48	16,8218 $\pm$ 0,1381	536 $\pm$ 56	2,2 $\pm$ 2,0
W 640	18,3220 $\pm$ 0,0111	969 $\pm$ 7	18,5 $\pm$ 1,8

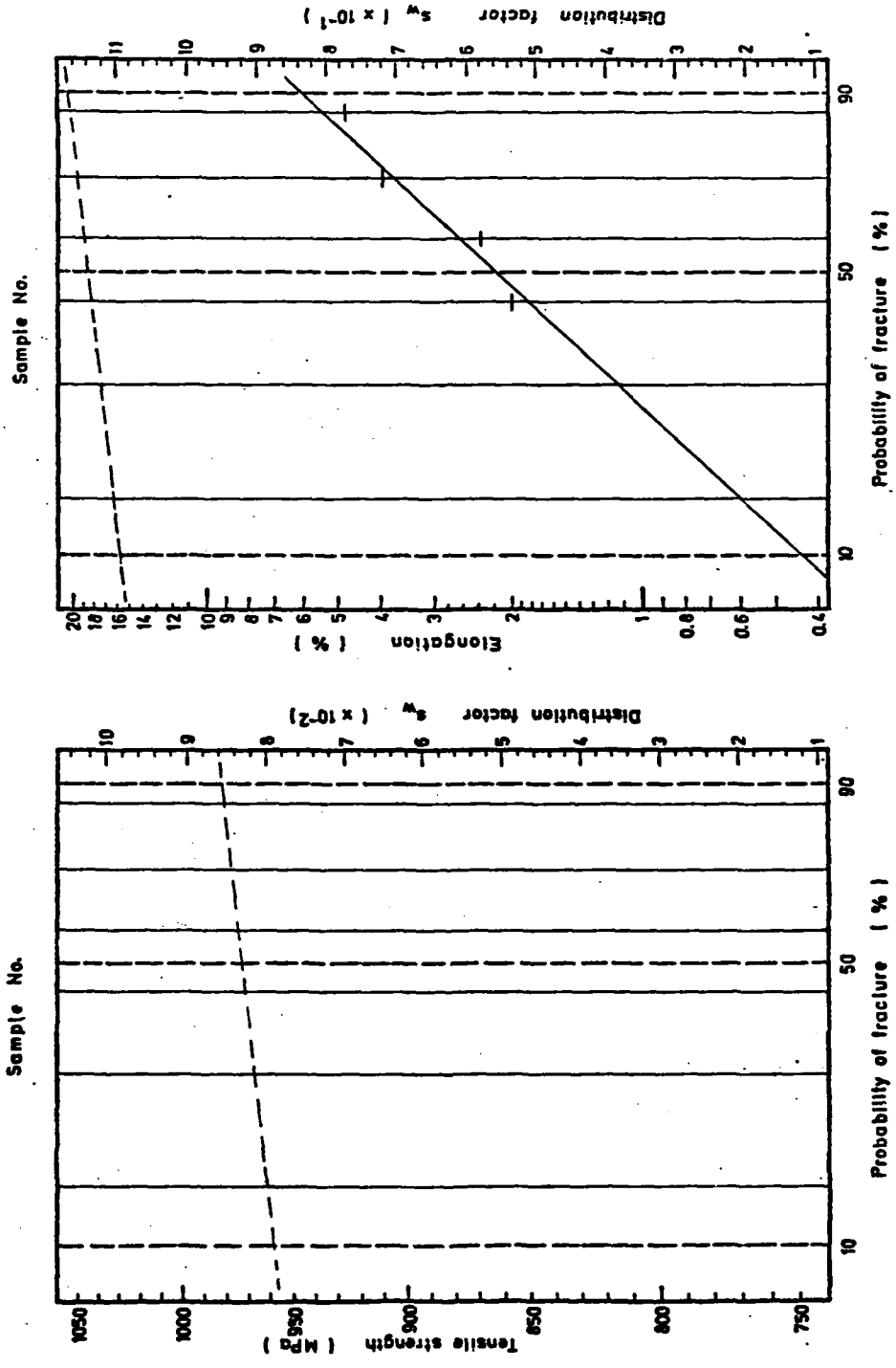

Fig. 88: Weibull-diagrams for E48W (——) and W640/81 (- -- -)

Powder E 51

Table 21: Mechanical properties of the samples prepared from E 51 and of the reference samples from W 640/81

E 51			W 640/81		
ϱ	σ	δ	ϱ	σ	δ
16,8551	449	<1	18,2722	989	16,0
16,8400	469	<1	18,2550	989	17,6
16,8693	467	<1	18,2728	979	19,2
			18,2684	984	16,4
16,5932	456	<1	18,2837	993	15,2
		<1	18,2774	981	14,0
		<1	18,2810	988	15,2

Mean values ± standard deviations

E 51	16,7894 ± 0,1313	460 ± 9	<1%
W 640	18,2729 ± 0,0095	986 ± 5	16,2 ± 1,7

Powder E 56

Table 22: Mechanical properties of the samples prepared from E 56 and of the reference sample from W 640/81

E 56			W 640/81		
ρ	σ	δ	ρ	σ	δ
18,1157	857	8,4	18.3151	945	12,0
18,0280	860	8,4	18,3049	925	12,0
			18,3172	950	9,8
17,9758	859	5,6	18,3543	972	13,6
18,2278	855	7,4	18,3458	972	11,2
			18,3337	1004	20,2
			18,3400	994	19,6
18,2368	865	7,6	18,3268	998	14,6
18,2403	818	5,2	18,3160	998	10,0
			18,3215	1014	15,0
			18,3049	1014	18,8
18,2940	865	7,2	18,3225	979	18,8
18,2934	855	7,0	18,3510	981	15,2
			18,3205	980	19,0
			18,2987	976	19,6

Mean values $\pm$ standard deviations

E 56	18,1765 $\pm$ 0,1218	855 $\pm$ 16	7,1 $\pm$ 1,2
W 640	18,3249 $\pm$ 0,0170	981 $\pm$ 28	15,3 $\pm$ 3,8

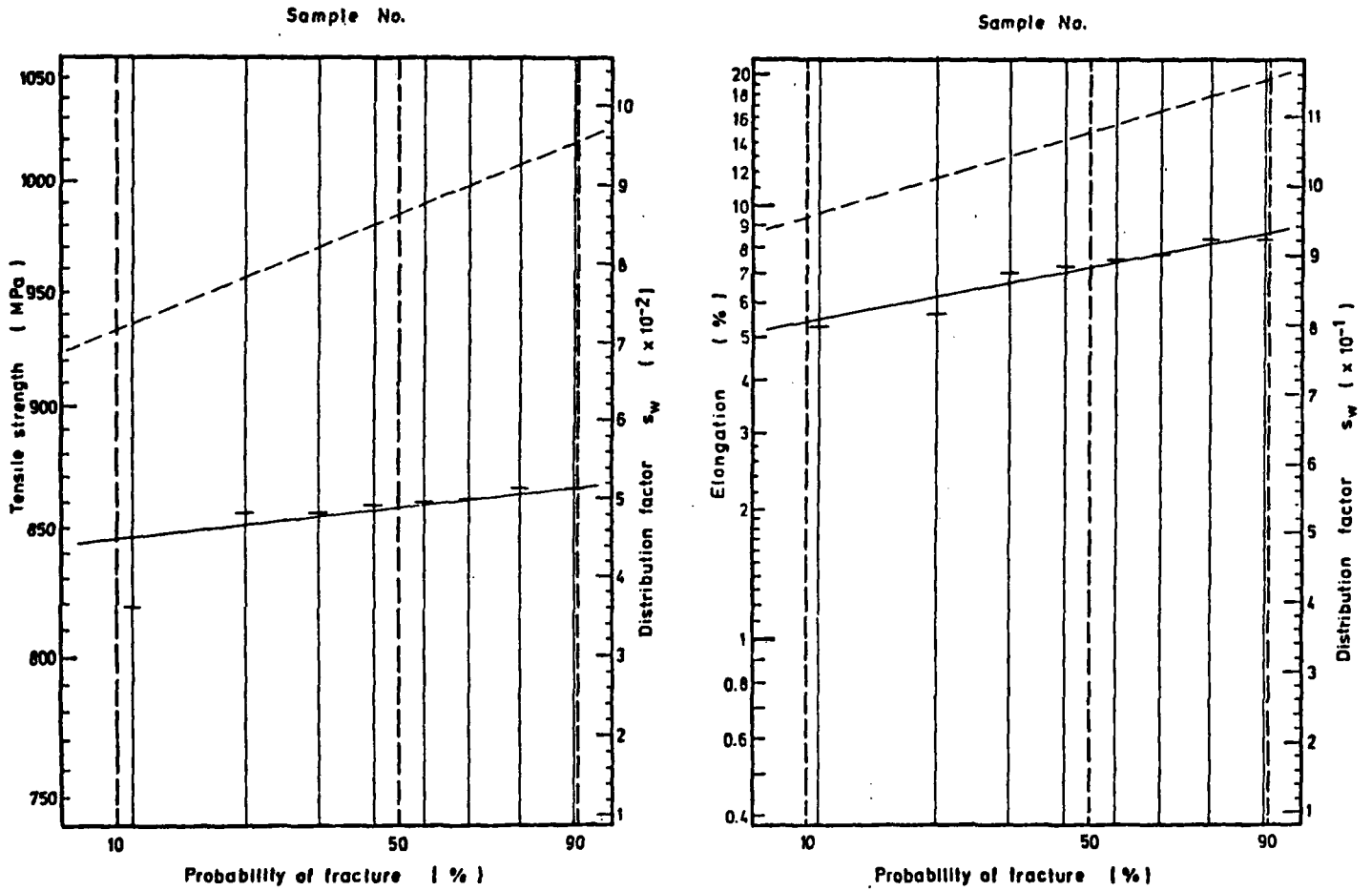

Fig.89 Weibull diagrams for E56W (——) and W640/81 (- ·· -)

Powder E 61

Table 23: Mechanical properties of the samples prepared from E 61 and of the reference sample from W 640/81

E 61			W 640/81		
ρ	σ	δ	ρ	σ	δ
16,8690	661	4,8	18,3325	973	16,0
17,0650	696	4,4	18,3093	973	19,0
			18,3262	973	18,6
			18,3001	972	19,2
17,1695	683	5,6	18,322	975	19,2
17,0846	687	5,8	18,3198	965	20,6
			18,3333	975	15,2
17,0549	660	6,8	18,3295	958	20,4
17,1214	693	6,8	18,3325	967	19,6
			18,3150	959	17,6

Mean values $\pm$ standard deviations

E 61	17,0607 $\pm$ 0,1029	680 $\pm$ 16	5,7 $\pm$ 1,0
W 640	18,3220 $\pm$ 0,0111	969 $\pm$ 7	18,5 $\pm$ 1,8

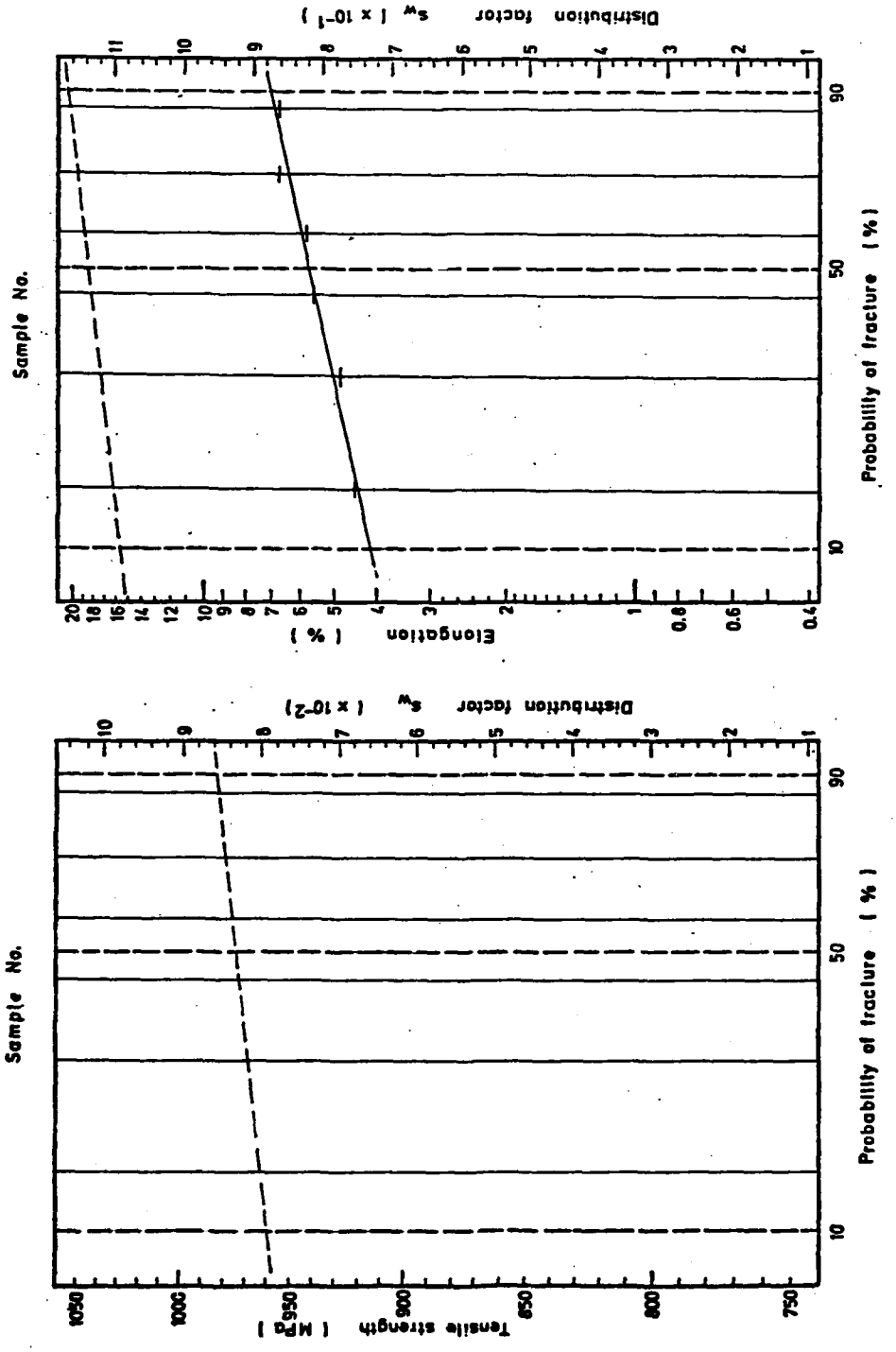

Fig.90: Weibull-diagrams for E61W (——) and W640/81 (- - -)

Powder E 63

Table 24: Mechanical properties of the samples prepared from E 63 and of the reference sample from W 640/81

E 63			W 640/81		
ρ	σ	δ	ρ	σ	δ
18,3437	963	14,8	18,3092	963	16,0
18,3283	967	16,8	18,3211	957	19,6
			18,3198	959	21,6
18,3266	963	20,0	18,3412	997	18,0
18,3336	937	16,8	18,3162	973	17,6
18,3141	969	16,2			
18,3537	1000	17,6	18,3312	986	17,4
18,3704	1000	18,8	18,3175	966	20,8
18,3302	990	17,2			

Mean values ± standard deviations

E 63	18,3376 ± 0,0177	974 ± 22	17,3 ± 1,6
W 640	18,3222 ± 0,0108	972 ± 15	18,7 ± 2,0

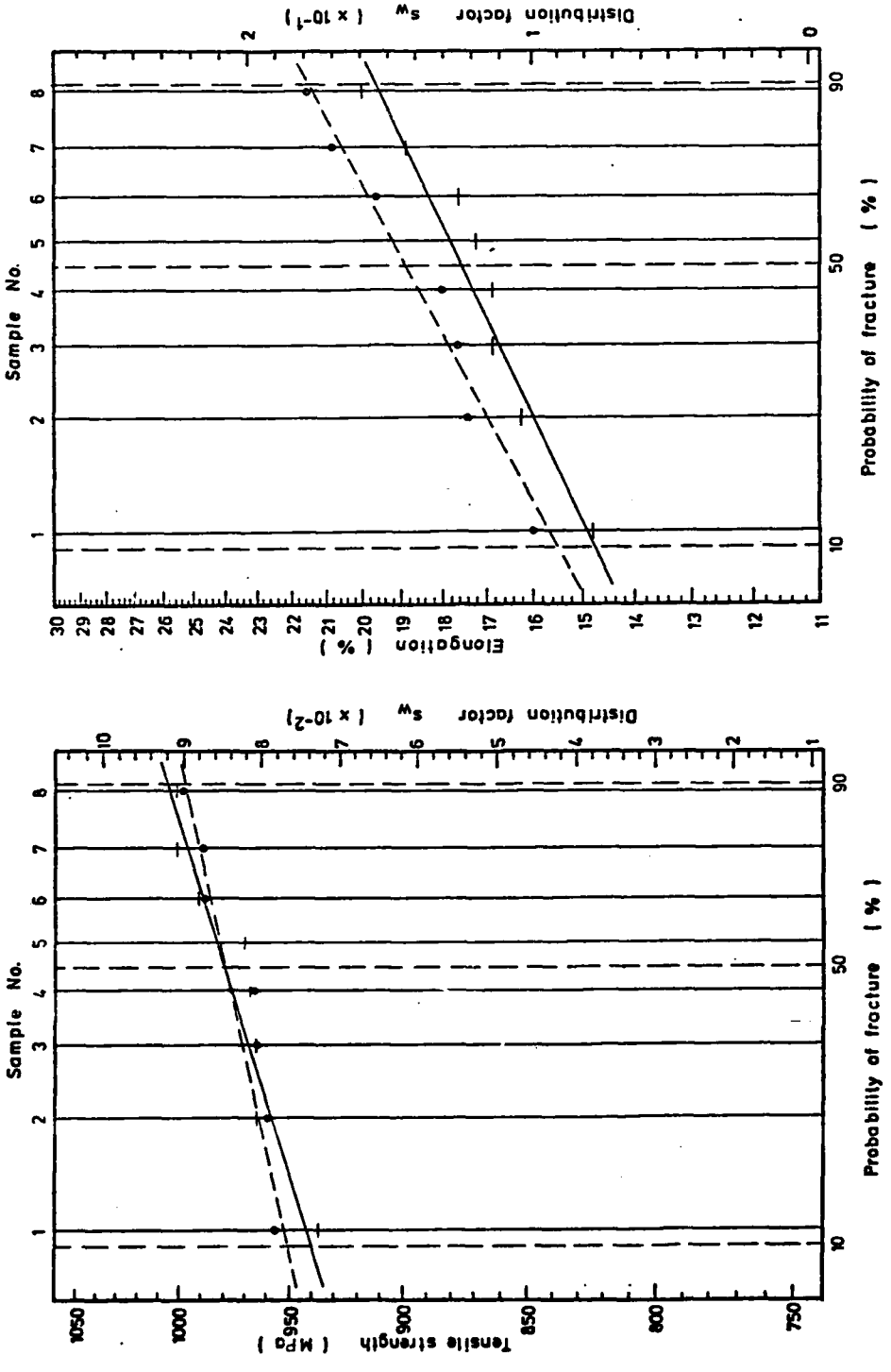

Fig.91: Weibull-diagrams for E63W (——) and W640/81 (- - -)

Powder E 67

Table 25: Mechanical properties of the samples prepared from E 67 and of the reference sample from E 640/81

E 67			W 640/81		
ρ	σ	δ	ρ	σ	δ
18,3545	951	16,0	18,3082	963	16,0
18,3294	965	18,0	18,3211	957	19,6
			18,3198	959	21,6
18,3388	987	20,0	18,3412	997	18,0
18,3119	952	12,6	18,3162	973	17,6
18,3519	967	14,0			
18,3309	982	17,6	18,3312	986	17,4
18,3316	990	19,0	18,3175	966	20,8

Mean values $\pm$ standard deviations

E 67	18,3356 $\pm$ 0,0146	971 $\pm$ 16	16,7 $\pm$ 2,7
W 640	18,3222 $\pm$ 0,0108	972 $\pm$ 15	18,7 $\pm$ 2,0

AD-A129 652 THE INFLUENCE OF IMPURITIES IN TUNGSTEN AND MATRIX COMPOSITION ON THE TUN..(U) TECHNISCHE UNIV VIENNA (AUSTRIA) INST FUER CHEMISCHE TECHNOLO.. B LUX ET AL.

2/2

UNCLASSIFIED OCT 82 DAJA37-80-C-0008 F/G 11/6 NL

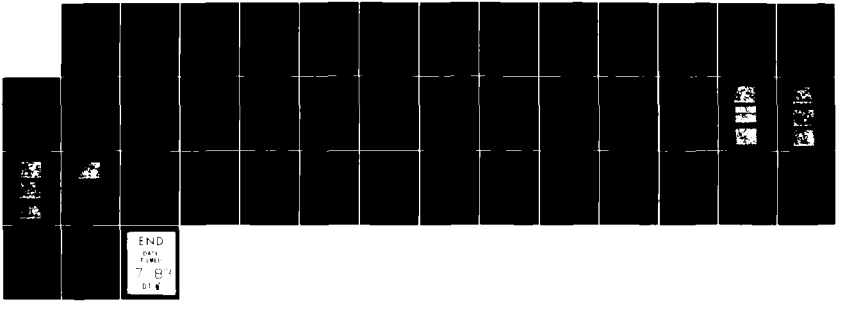

END
DATE FILMED
7 83
DTIC

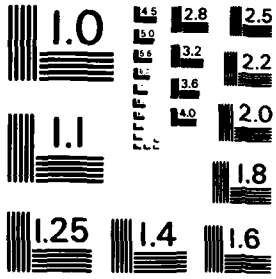

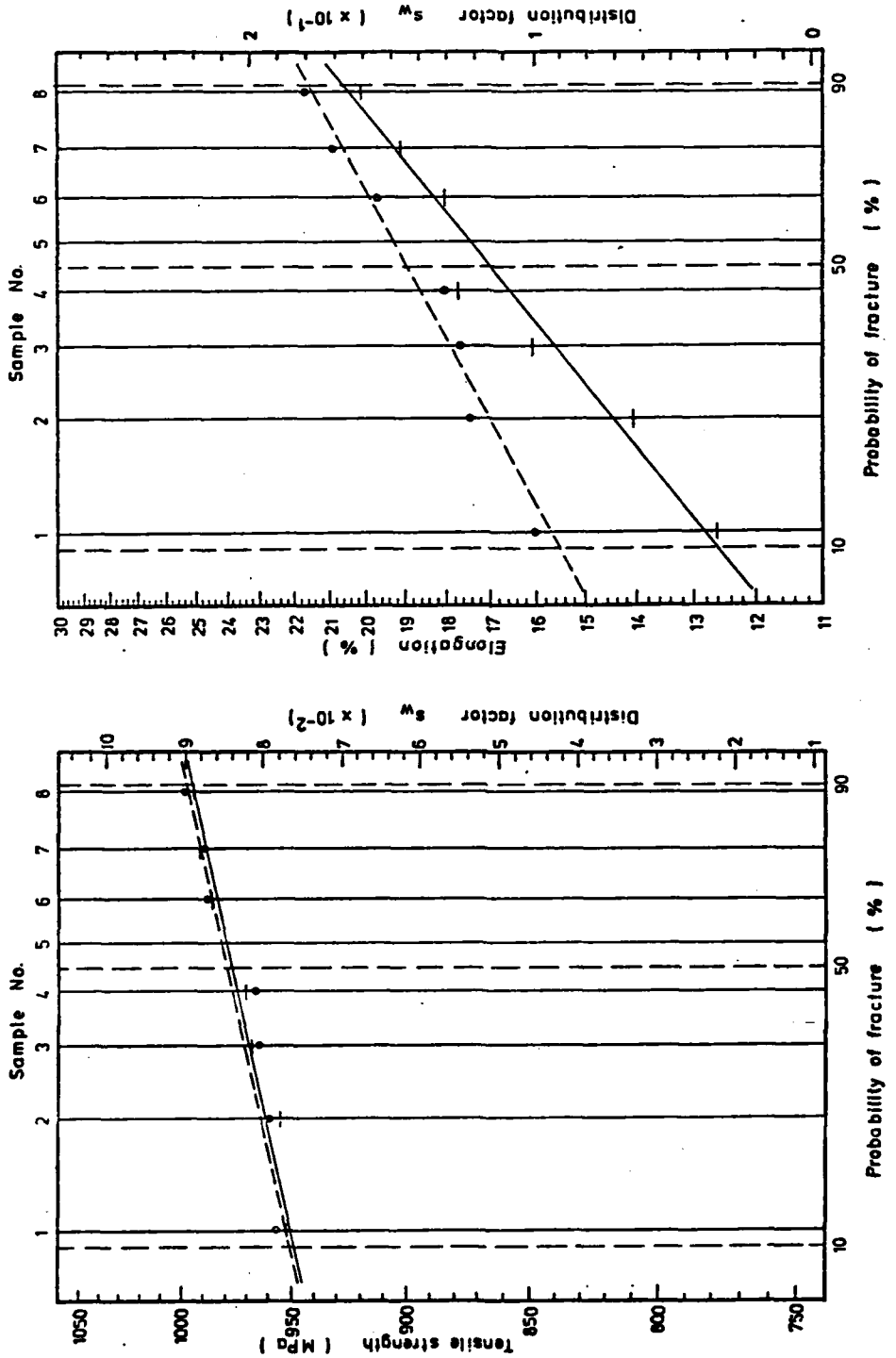

Fig.92: Weibull-diagrams for E67W (——) and W640/81 (- - -)

Powder E 71

Table 26: Mechanical properties of the samples prepared from E 71 and of the reference sample from E 640/81

E 71			W 640/81		
ϱ	σ	δ	ϱ	σ	δ
18,3595	974	19,2	18,3082	963	16,0
18,3414	984	18,0	18,3211	957	19,6
18,3352	816	6,0	18,3198	959	21,5
18,3197	979	20,0	18,3412	997	18,0
18,2330	985	18,2	18,3162	973	17,6
18,3445	995	16,0	18,3312	986	17,4
18,3289	997	21,6	18,3175	965	20,8
18,3167	973	13,6			

Mean values ± standard deviations

E 71	18,3335 ± 0,0147	986 ± 9	18,8 ± 1,9
W 640	18,3222 ± 0,0108	972 ± 15	18,7 ± 2,0

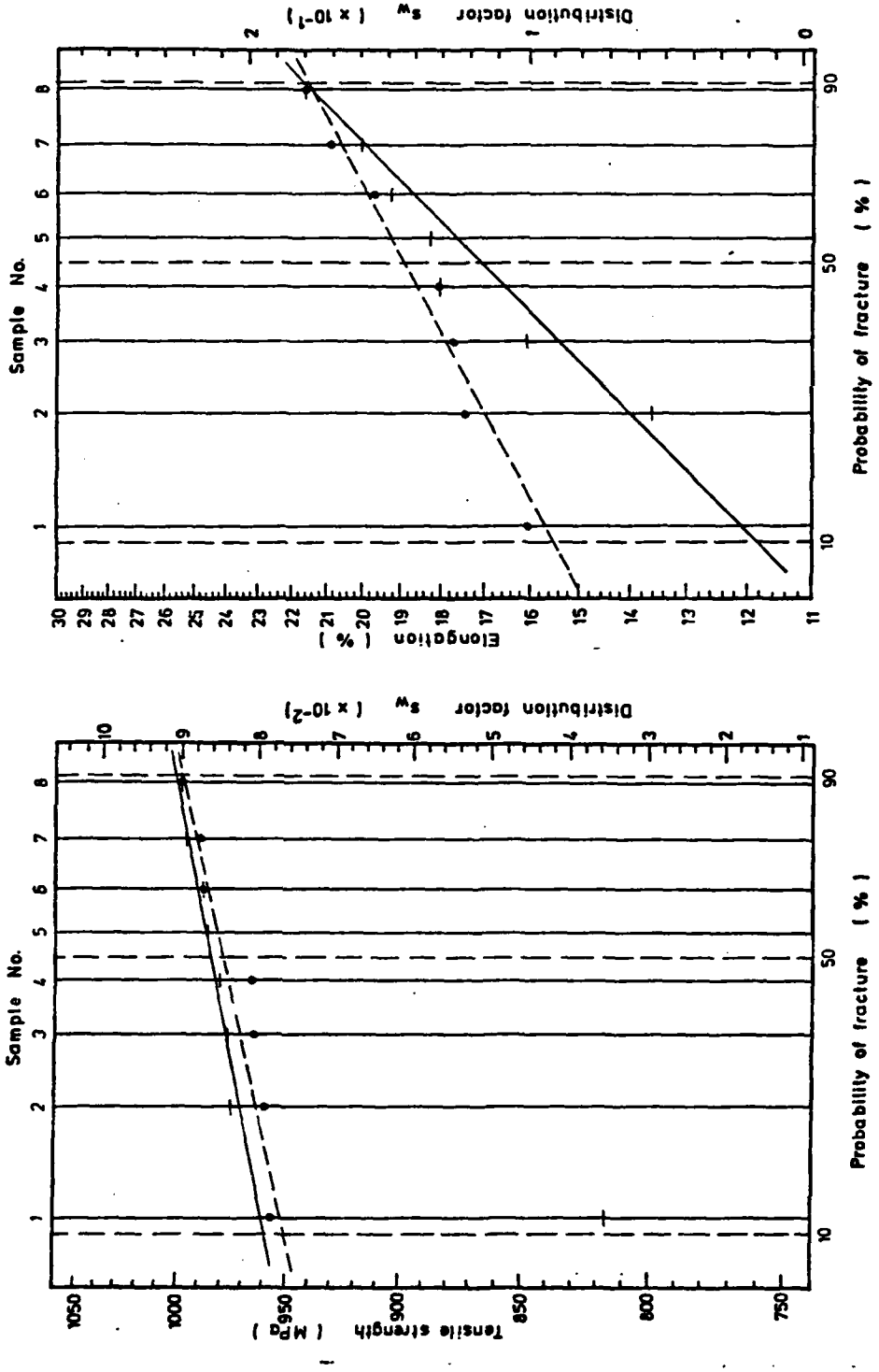

Fig.93: Weibull-diagrams for E71W (——) and W640/81 (- - -)

Powder E 79

Table 27: Mechanical properties of the samples prepared from E 79 and of the reference sample from E 640/81

E 79			640/81		
ϱ	σ	δ	ϱ	σ	δ
18,3113	857	6,80	18,3151	945	12,00
18,2824	932	8,80	18,3049	925	12,00
			18,3172	950	9,8
18,2665	962	10,80	18,3543	972	13,6
18,3457	969	12,0	18,9458	972	11,2
			18,3337	1004	20,2
			18,3400	994	19,6
18,3263	973	16,8	18,3268	998	14,6
18,2870	919	10,8	18,3160	988	10,0
			18,3215	1014	15,0
			18,3049	1034	18,8
18,3282	70	20,0	18,3225	979	18,8
18,3025	972	19,2	18,3510	981	15,2
			18,3205	980	19,0
			18,2987	976	19,5

Mean values ± standard deviations

E 79	18,3062 ± 0,0267	944 ± 41	13,2 ± 4,9
W 640	18,3249 ± 0,0170	981 ± 27	15,2 ± 3,7

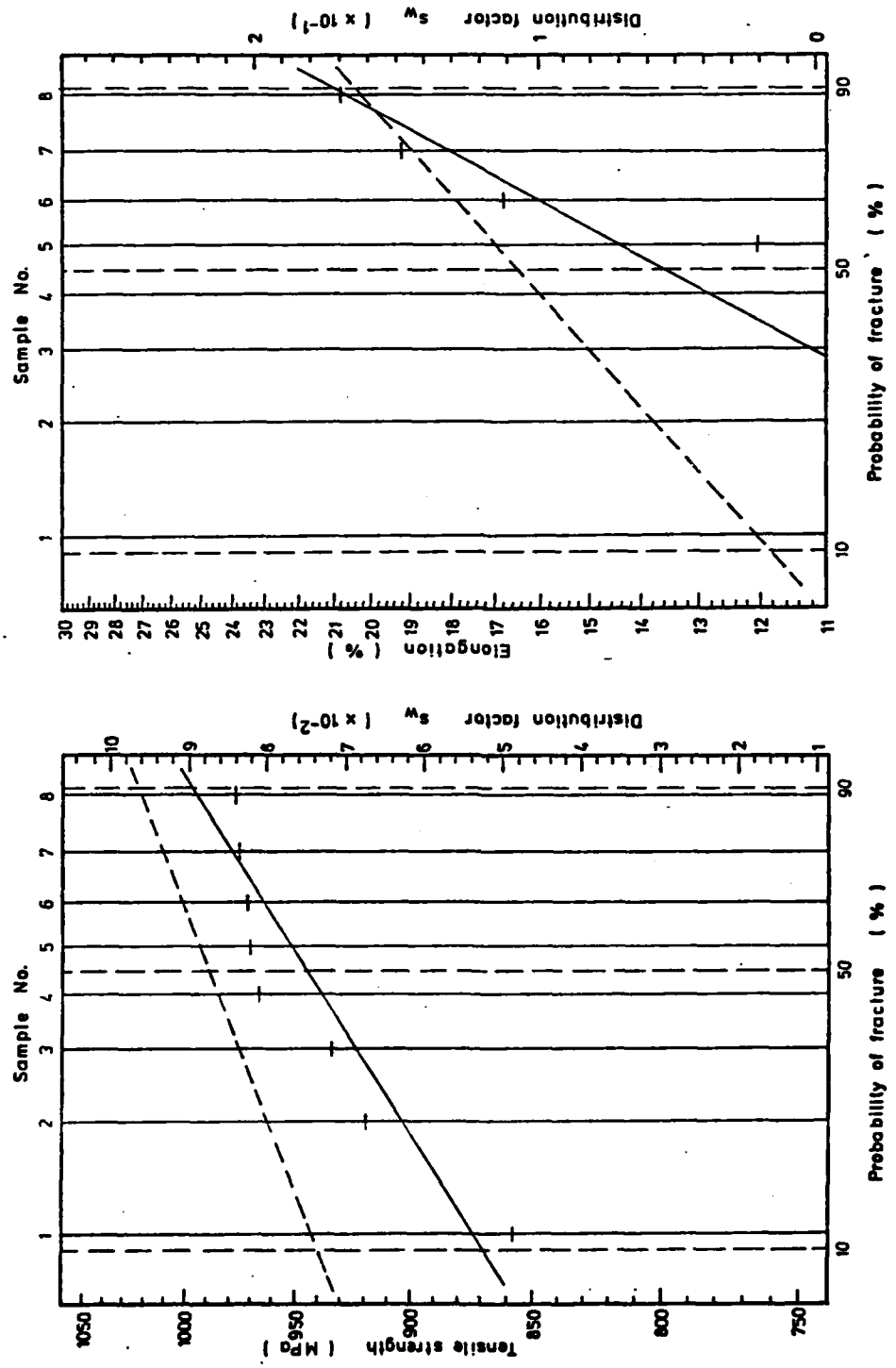

Fig. 94 : Weibull-diagrams for E79W (——) and W640/81 (- - -)

Powder E 83

Table 28: Mechanical properties of the samples prepared from E 83 and of the reference sample from W 640/81

E 83			W 640/81		
ϱ	σ	δ	ϱ	σ	δ
18,3482	983	18,2	18,3325	973	16,0
18,3391	949	14,6	18,3093	973	19,0
			18,3262	973	18,6
			18,3001	972	19,2
18,3484	950	16,0	18,322	975	19,2
18,3396	947	18,8	18,3198	965	20,6
18,3402	959	16,0	18,3333	975	15,2
18,3069	960	19,0	18,3295	958	20,4
18,3267	971	15,6	18,3325	967	19,6
18,3270	944	17,0	18,3150	959	17,6

Mean values $\pm$ standard deviations

E 83	18,3345 $\pm$ 0,0138	958 $\pm$ 13	16,9 $\pm$ 1,5
W 640	18,3220 $\pm$ 0,0111	969 $\pm$ 6	18,5 $\pm$ 1,8

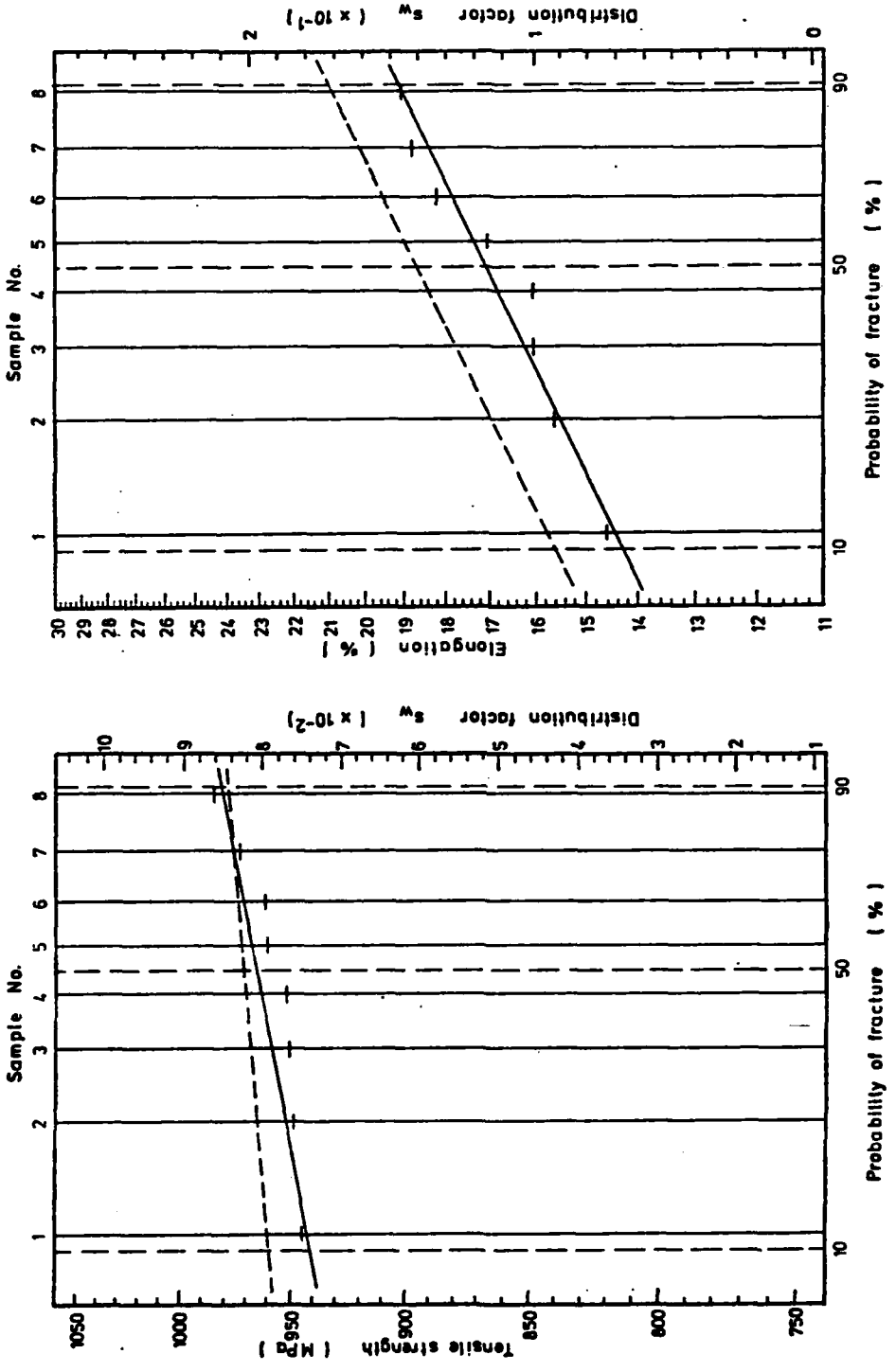

Fig. 95 : Weibull-diagrams for E83W (——) and W640/81 (- - -)

Powder E 87

Table 29: Mechanical properties of the samples prepared from E 87 and of the reference samples from W 640/81

E 87			W 640/81		
ϱ (g/cm^3)	σ_B(MPa)	δ(%)	ϱ (g/cm^3)	σ_B(MPa)	δ (%)
18,3058	949	12,4	18,3194	981	14,0
18,2940	981	17,0	18,3363	985	16,4
			18,3288	970	16,8
18,3084	953	16,0	18,2933	993	17,4
18,3151	1009	14,8	18,3500	1004	21,0
18,3077	1001	17,4			
18,3079	971	12,6	18,3618	977	20,0
18,3014	961	13,4			
18,3949	972	13,6			
18,3212	927	14,2	18,2960	941	14,6
18,2901	932	12,8	18,3502	948	19,0

Mean values $\pm$ standard deviations

E 87	18,3147 $\pm$ 0,0296	970 $\pm$ 28	14,4 $\pm$ 1,8
W 640	18,3295 $\pm$ 0,0253	975 $\pm$ 21	17,4 $\pm$ 2,5

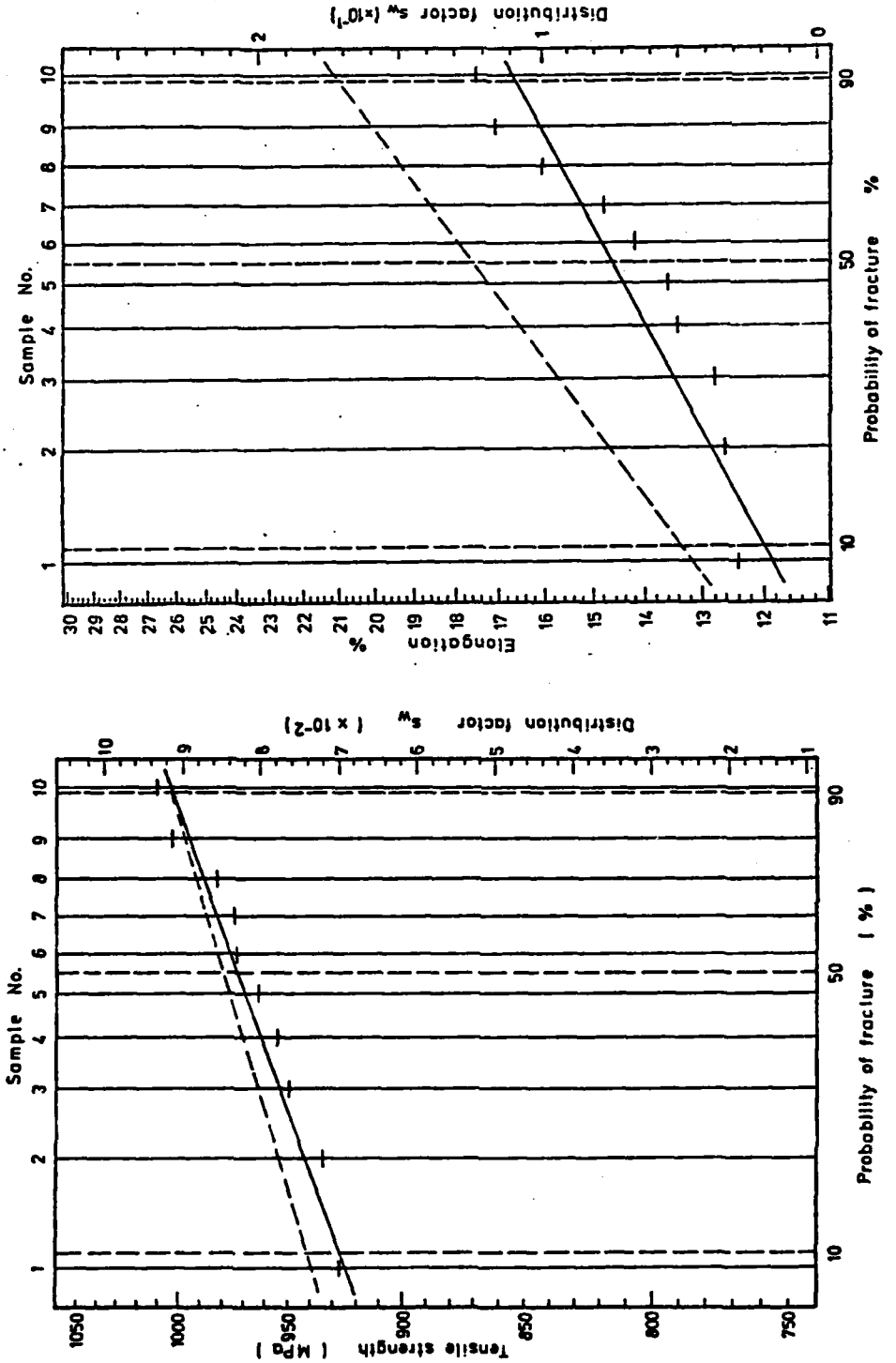

Fig. 96: Weibull-diagrams for E87W (——) and W640/81 (- - -)

Powder E 91

Table 30: Mechanical properties of the samples prepared from E 91 and of the reference samples from W 640/81

E 91			W 640/81		
ϱ	σ	δ	ϱ	σ	δ
18,2939	980	14,2	18,3194	981	14,0
18,2630	974	14,8	18,3363	985	16,4
18,2160	943	12,0	18,3288	970	16,8
18,2959	986	15,8	18,2933	933	17,4
18,2491	983	16,2	18,3500	1004	21,0
18,2628	960	17,0	18,3618	977	20,0
18,2252	952	12,6			
18,1745	954	12,2			
18,2756	918	11,6	18,2960	941	14,6
18,2852	918	12,8	18,3502	948	19,0

Mean values $\pm$ standard deviations

E 91	18,2541 $\pm$ 0,0388	957 $\pm$ 25	13,9 $\pm$ 1,9
W 640	18,3295 $\pm$ 0,0253	975 $\pm$ 21	17,4 $\pm$ 2,5

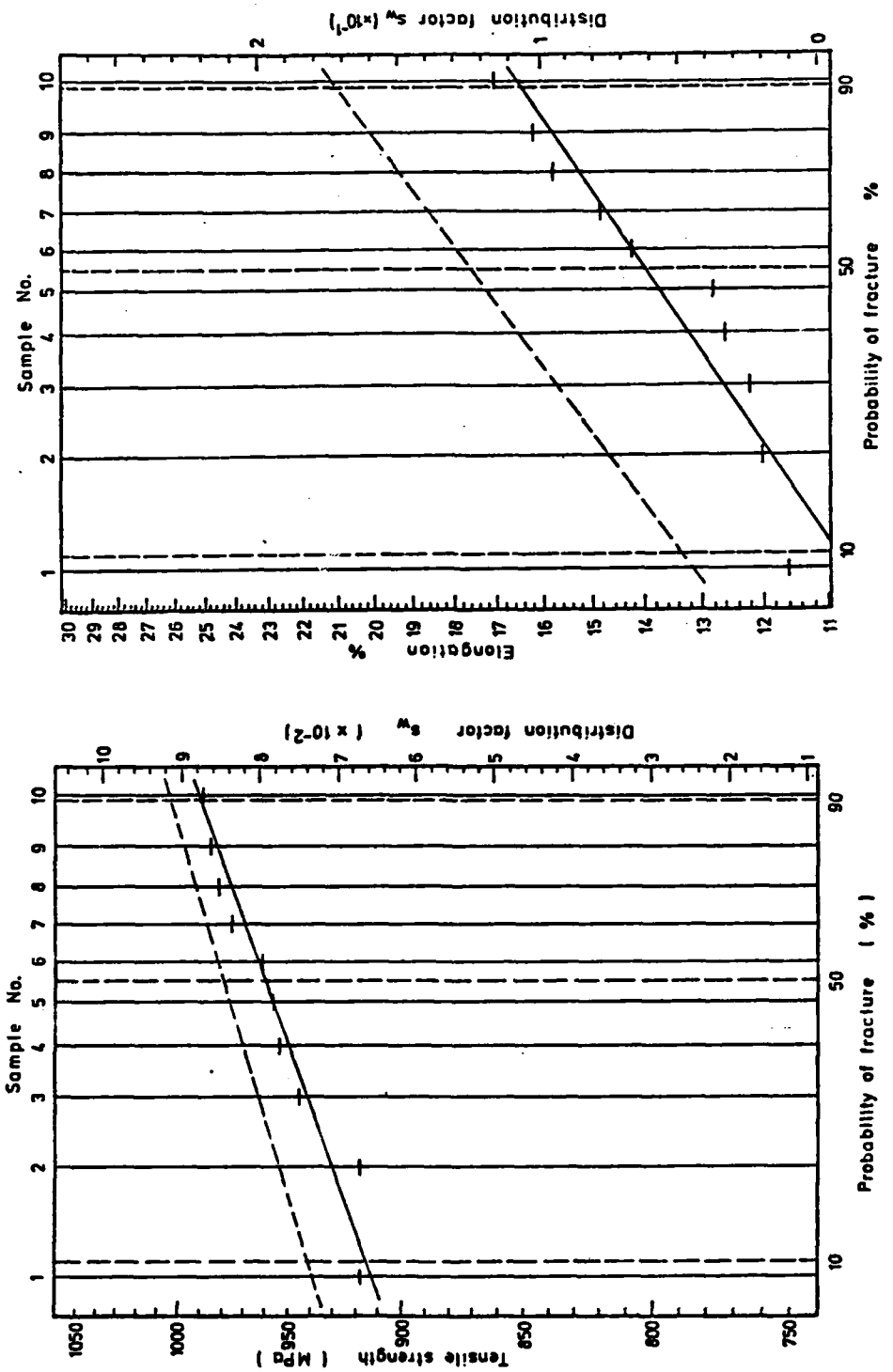

Fig. 97 Weibull-diagrams for E91W (——) and W640/81 (- - -)

Powder E 99

Table 31: Mechanical properties of the samples prepared from E 99 and of the reference samples from W 640/81

E 99			W 640/81		
ϱ	σ	δ	ϱ	σ	δ
18,3420	994	15,4	18,3194	981	14,0
18,3444	960	13,0	18,3363	985	16,4
			18,3288	970	16,8
18,2975	978	14,0	18,2933	993	17,4
18,3334	991	12,0	18,3500	1004	21,0
18,3468	994	13,4			
18,3255	1006	16,0	18,3618	977	20,0
18,3148	1000	14,8			
18,3522	989	14,0			
18,3565	924	13,1	18,2960	941	14,6
18,3450	938	15,4	18,3502	948	19,0

Mean values $\pm$ standard deviations

E 99	18,3358 $\pm$ 0,0184	977 $\pm$ 28	14,1 $\pm$ 1,3
W 640	18,3295 $\pm$ 0,0253	975 $\pm$ 21	17,4 $\pm$ 2,5

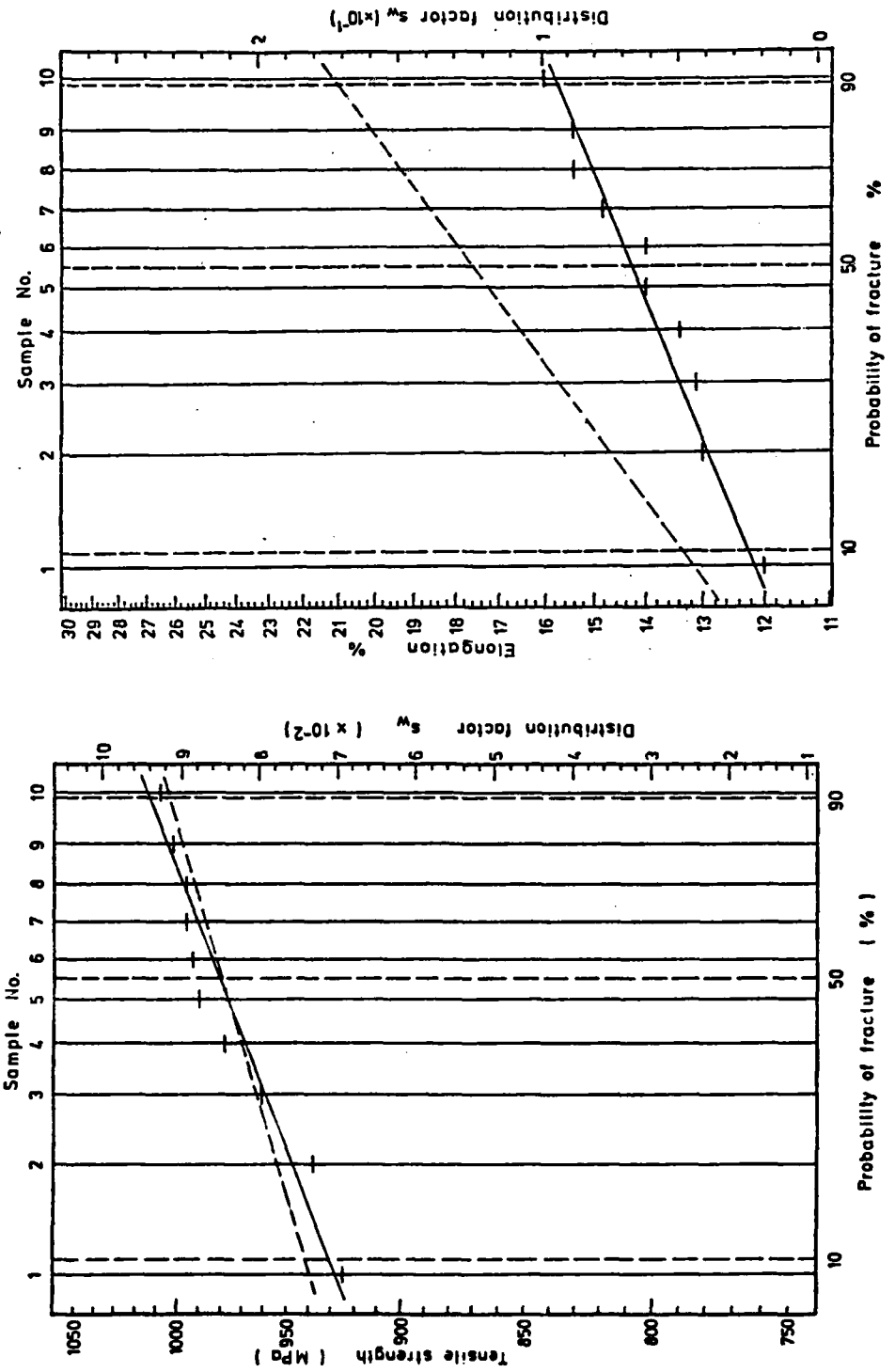

Fig. 98: Weibull-diagrams for E99W (——) and W640/81 (- - -)

Powder E 103

Table 32: Mechanical properties of the samples prepared from E 103 and of the reference samples from W 640/81

E 103			W 640/81		
ϱ	σ	δ	ϱ	σ	δ
18,3852	949	13,4			
18,3615	961	12,4			
18,3763	964	16,6			
18,3759	956	13,4			
18,3548	939	14,6			
18,3435	996	21,2	18,3352	984	22,8
18,3490	983	21,0	18,3387	1023	18,2
18,3522	982	20,6	18,3308	969	21,8
			18,3450	1003	20,6
			18,3369	1001	22,2
18,3431	963	15,2	18,3323	1050	17,6
18,3474	956	12,2	18,3387	985	21,2
			18,3403	989	19,0
			18,3380	984	19,4
			18,3294	988	19,2

Mean values $\pm$ standard deviations

E 103	18,3589 $\pm$ 0,0152	965 $\pm$ 17	16,4 $\pm$ 3,4
W 640	18,3365 $\pm$ 0,0047	997 $\pm$ 24	20,2 $\pm$ 1,7

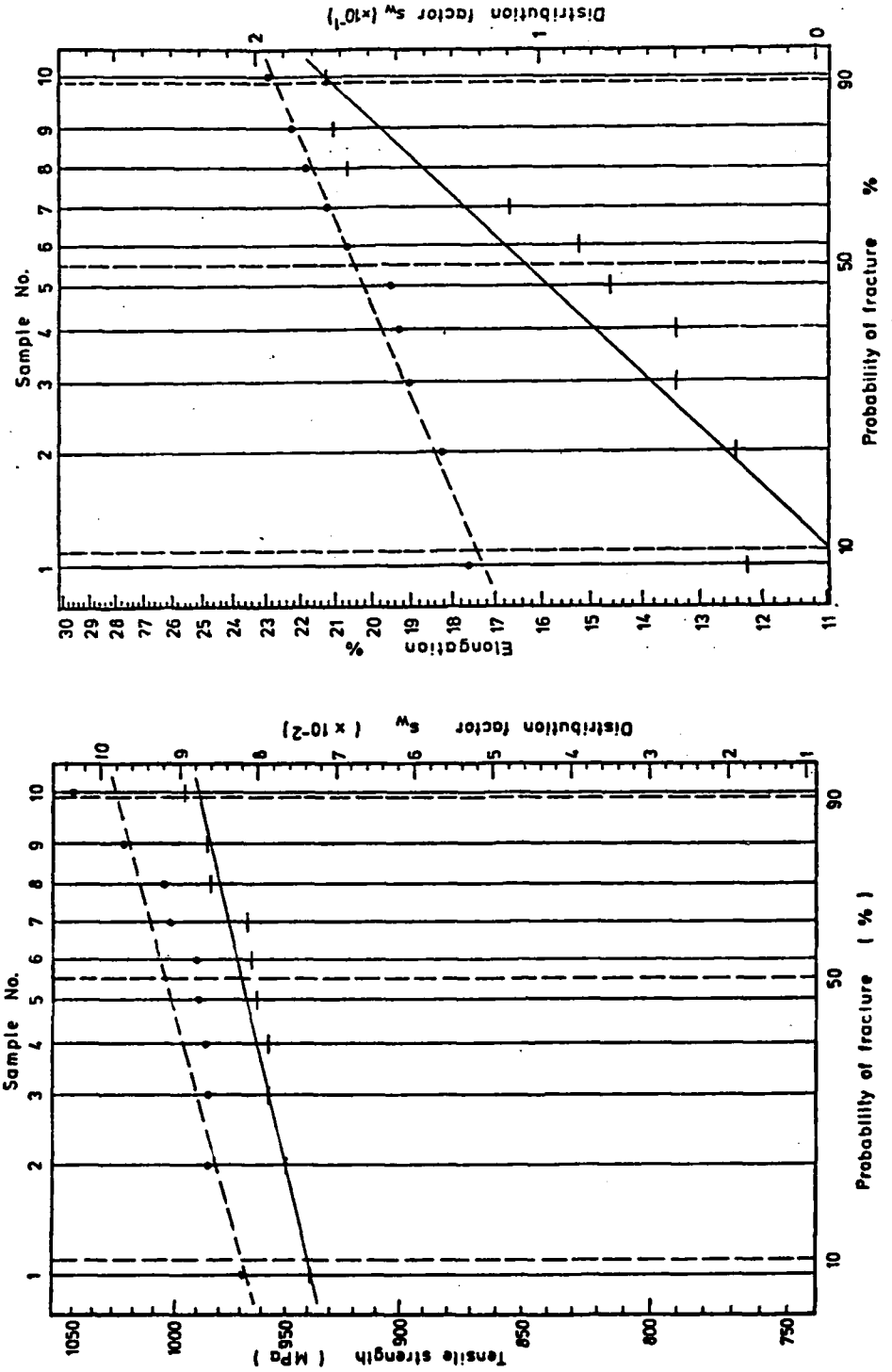

Fig. 99: Weibull-diagrams for E103W (——) and W640/81 (- - -)

Powder E 107

Table 33: Mechanical properties of the samples prepared from E 107 and of the reference samples from W 640/81

E 107			W 640/81		
ϱ	σ	δ	ϱ	σ	δ
18,3361	969	15,0			
18,3541	967	17,2			
18,3576	949	12,0			
18,3398	965	16,4			
18,3600	960	14,6			
			18,3352	984	22,8
18,3607	990	20,6	18,3387	1023	18,2
18,3374	986	18,8	18,3308	969	21,8
			18,3450	1003	20,6
			18,3369	1001	22,2
18,3564	981	14,4	18,3323	1050	17,6
18,3450	983	13,8	18,3387	985	21,2
18,3491	966	15,2	18,3403	989	19,0
			18,3380	984	19,4
			18,3294	988	19,2

Mean values $\pm$ standard deviations

E 107	18,3496 $\pm$ 0,0095	971 $\pm$ 13	15,8 $\pm$ 2,5
W 640	18,3365 $\pm$ 0,0047	998 $\pm$ 23	20,2 $\pm$ 1,3

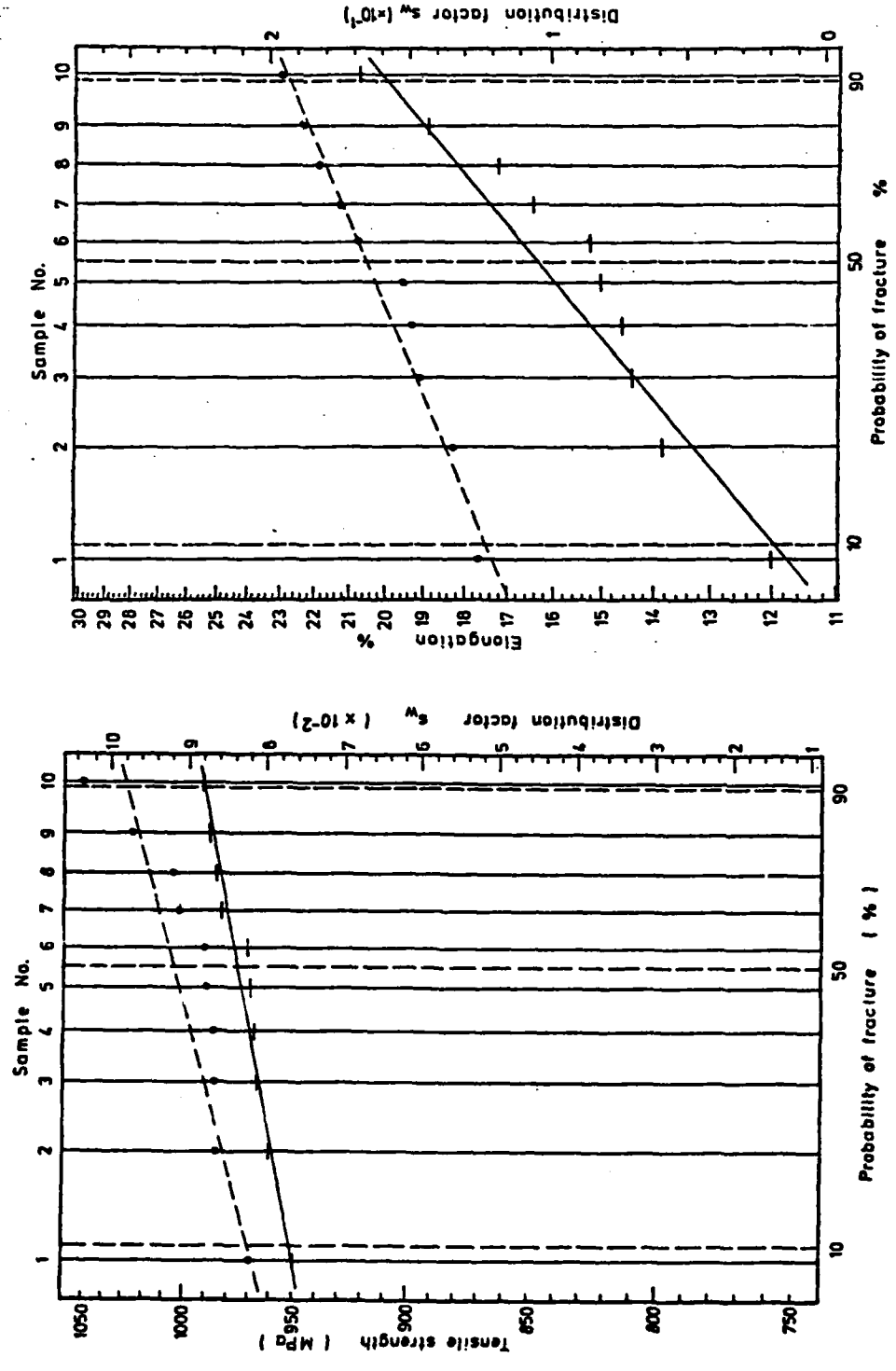

Fig.100: Weibull-diagrams for E107W (——) and W640/81 (- - -)

Powder E 111

Table 34: Mechanical properties of the samples prepared from E 111 and of the reference samples from W 640/81

E 111			W 640/81		
ϱ	σ	δ	ϱ	σ	δ
17,3363	945	11,2	18,2722	989	16,0
17,2927	867	8,0	18,2550	989	17,5
17,2151	877	11,2	18,2728	979	19,2
			18,2684	984	16,4
17,6825	882	10,8	18,2837	993	15,2
17,6632	883	10,2	18,2774	981	14,0
17,8032	908	14,0	18,2810	988	15,2
17,7224	900	12,0			
17,7254	836	9,2	18,2234	970	14,4
17,7308	836	6,0	18,3261	979	12,4
17,8090	762	2,4	18,3207	970	17,6
17,7592	816	6,6	18,3180	1007	17,6
17,8816	791	6,6			

Mean values $\pm$ standard deviations

E 111	17,6351 $\pm$ 0,2227	853 $\pm$ 64	9,0 $\pm$ 3,2
W 640	18,2817 $\pm$ 0,0305	984 $\pm$ 11	16,0 $\pm$ 2,1

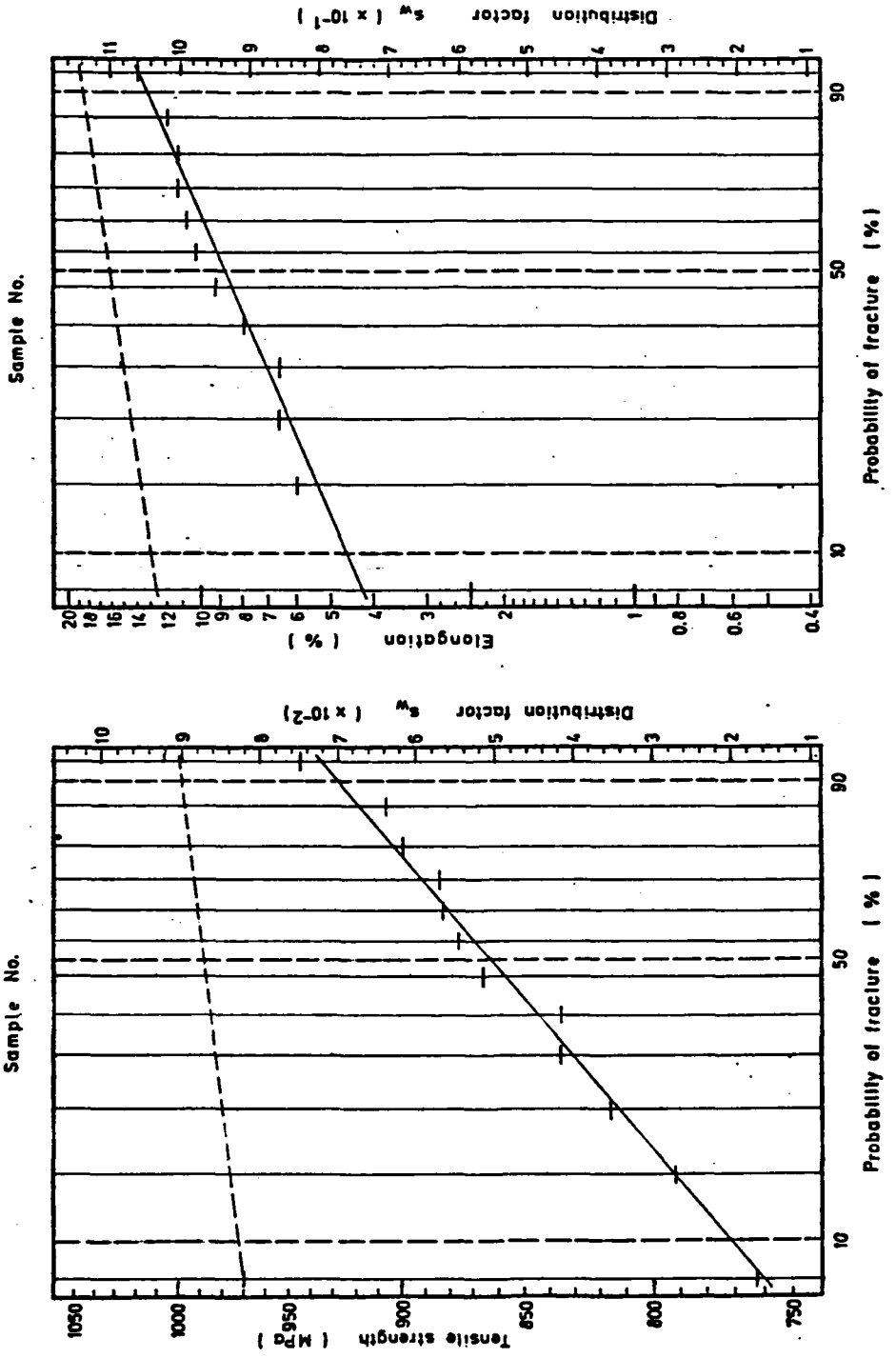

Fig.101: Weibull-diagrams for E111W (——) and W640/01 (- - -)

Powder E 115

Table 35: Mechanical properties of the samples prepared from E 115 and of the reference samples from W 640/81

E 115			W 640/81		
ϱ (g/cm^3)	σ_B (MPa)	δ (%)	ϱ (g/cm^3)	σ_B (MPa)	δ (%)
18,2400	943	10,4	18,3151	945	12,0
18,3310	899	8,8	18,3043	925	12,0
18,3147	999	15,0	18,3172	950	9,8
18,3271	985	14,6	18,3543	972	13,6
18,3414	1025	13,8	18,3458	972	11,2
			18,3337	1004	20,2
			18,3400	994	19,6
18,3176	969	19,0	18,3268	998	14,6
18,3478	964	17,6	18,3160	998	10,0
			18,3215	1014	15,0
			18,3049	1034	18,8
18,3196	994	19,0	18,3225	979	18,8
18,3137	980	20,0	18,3510	981	15,2
			18,3205	980	19,0
			18,2987	976	19,6

Mean values $\pm$ standard deviations

E 115	18,3170 $\pm$ 0,0312	973 $\pm$ 36	15,4 $\pm$ 3,9
W 640	18,3249 $\pm$ 0,0170	981 $\pm$ 28	15,3 $\pm$ 3,8

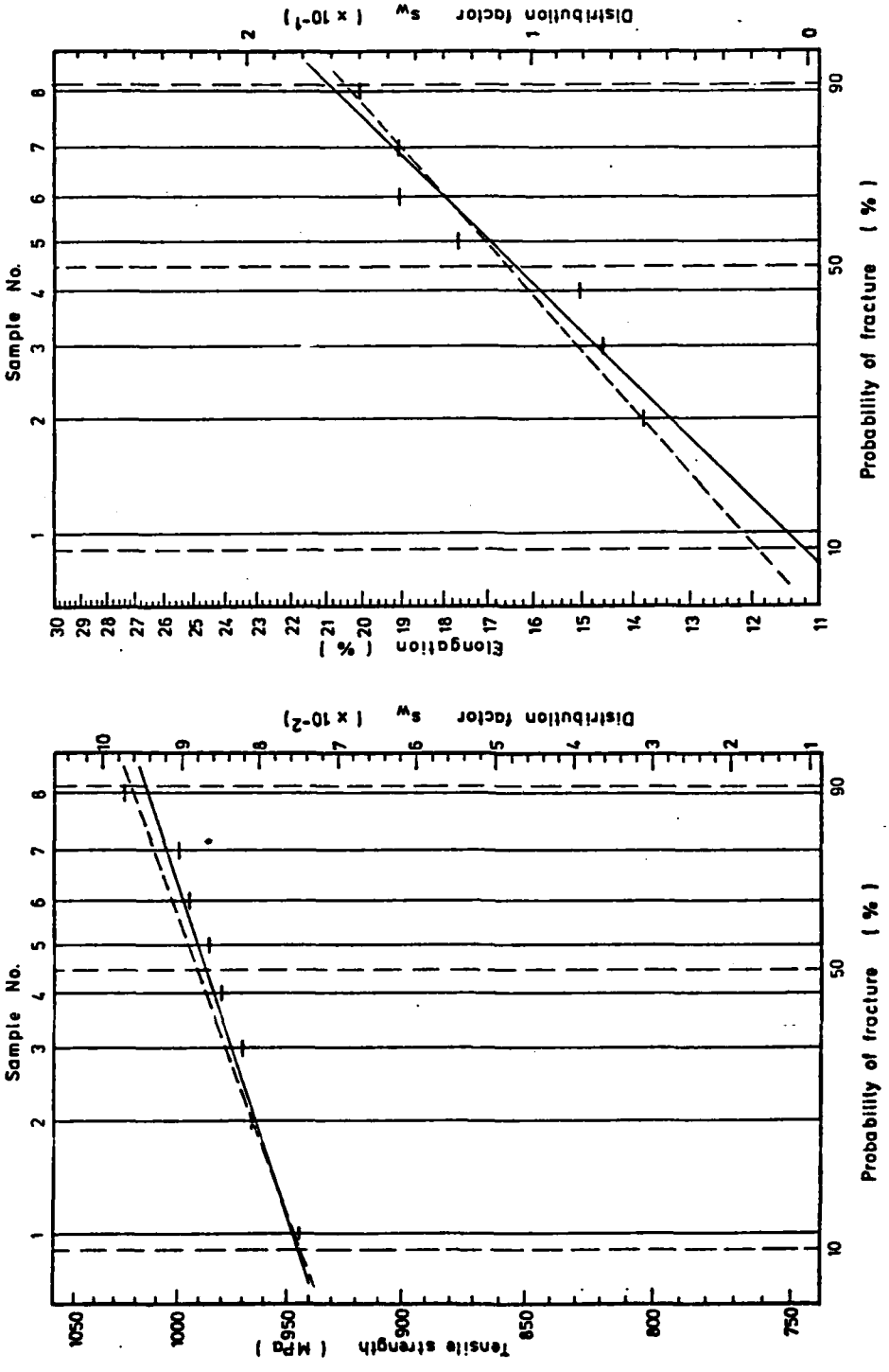

Fig.102: Weibull-diagrams for E115W (——) and W640/81 (- - -)

As with the samples containing 90% W, the most conspicuous phenomenon is the quite unsatisfactory sintering of those samples prepared from coarse powders, resulting in high residual porosity and correspondingly low mechanical properties. For the 96% W samples, however, the powders resulting in insufficientily sintered bars were not only E48 and E51 but virtually all those with average grain sizes >10 µm. As the amount of binder melt here is much lower, W grains must be sintered more closely together before the binder melts in order to enable uniform distribution of the binder phase. Apparently powder >10 µm cannot meet these sintering requirements. For example, the residual porosity in samples prepared from E 51 was 7% for 96% W content as compared to 1,3 for 90% W.

The degree of porosity is shown clearly by SEM photos: With the extremely coarse E48 and E51 there are only a few grains on each photo which have sintered together properly Most of the others are held together only by W-W- grain boundaries which, as described in Chapter 3, are inherently weak and unable to withstand higher degrees of deformation (Fig.103, 104). There are even some areas where no liquid phase sintering seems to have occurred at all (Fig.105) and the structure looks like that of solid state sintered W. Comparison with Fig.41, depicting an only prereduced sample, shows the striking similarity; understandably, the mechanical properties are equally unsatisfactory.

E 61, with a starting powder size of ~18 um, yielded somewhat better results, although the typical rounded shapes of W grains which had not undergone liquid phase sintering are visible in several places (Fig.106), and there are also many W-W grain boundaries in the fracture surface. E 56 with a medium grain size of ~12 µm resulted in largely sound compacts, as also indicated by its density value, although the SEM photo (Fig.107) reveals numerous large W-W- grain boundaries indicating somewhat defective sintering. Fig.103-107,

arranged according to their elongation, closely resemble the sequence Fig.41-45, better ductility being associated with more satisfactory liquid phase sintering. In Fig. 108 the elongation of equally sintered 96% W samples is plotted against the starting powder size.

It is evident that the fine powders are closely grouped together, while all samples with elongations <10% have been prepared from coarse W powders (>10 um). Even the extremely porous samples prepared from E111 are more ductile than the almost fully dense products from E56, an observation which also stresses the importance of proper liquid phase sintering, a factor apparently much more important than the particular purity of the starting powder.

The second type of pore formation observed with 90% W content, i.e. pore formation during liquid phase sintering, is not as pronounced with the 96% W samples.
This somewhat surprising result can be explained by the more efficient sintering cycle particularly the much higher temperature for sintering and pre-reduction. As pore closure occurs at considerably higher temperatures, the pre-reduction is more complete and leaves less oxide to be reduced during the liquid phase sintering. The only powder that exhibited really pronounced pore formation and blisters was E111, which behaved exactly as the sample with 90% W. Most of the large pores are situated near the surface rather than in the centre of the test bars. Most other powder also exhibited a few pores in the fracture surface, even those with very high ductility; the pores are quite different in size and shape and therefore also in their effect on the mechanical properties (compare Fig.109, 111). The basic structure however seems to be sound, as indicated by the fracture surface outside of the pores (Fig.110, 112); if there is even one pore in the whole test bar, it will probably be found in the fracture surface, as it is a weak point in the structure. Even in the fracture surface of a reference bar (Fig.113) that showed an elongation of 21,6%, a small pore is discernible in the

lower right corner of the photo. Pore closure or at least shrinkage might be achieved by hot isostatic pressing of the sintered samples, although this process is rather expensive and recommendable only for the highest standards.

Generally, with the modified sintering cycle the sintering of the heavy metals with high W content has reached a surprisingly high standard, Elongations >15% can be attained with satisfactory reproducibility. Heating the samples more slowly from 1400°C to sintering temperature brings a further increase in ductility as the slower heating apparently promotes reduction of the above mentioned oxides. If fine W powder (< 5 um) is used for production, and if the sintering is performed following the optimum sintering cycle, the heavy metals are not very sensitive to the trace impurities, commonly present in commercial W powders.

In Fig.114 and 115 the tensile strength and elongation of the doped heavy metals, with both 90 and 96% W are compared to those of the standard samples. The powders E51, E48, E61 and E56 exhibit the lowest mechanical properties due to their insufficient sintering can effect which is particularly pronounced with 96% W. With 90% W there is a continuous increase in both tensile strength and elongation, while with 96% W the remaining powders are grouped closely together, only the porous E111 (rare earth) lying between the two groups. Although the tensile strength is relatively independent of the type of doped powders, the standard powder W640/81 has proved to be generally superior both for heavy metals with 90 and 96% W.

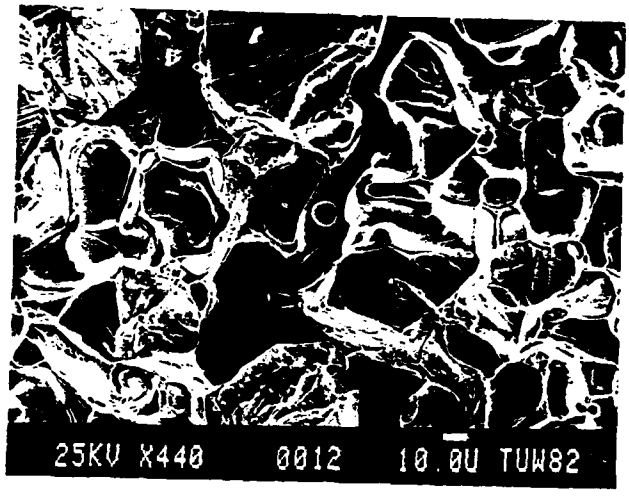

Fig.103
Heavy metal (96%W) sintered from E48W (200ppm Na); insufficient sintering

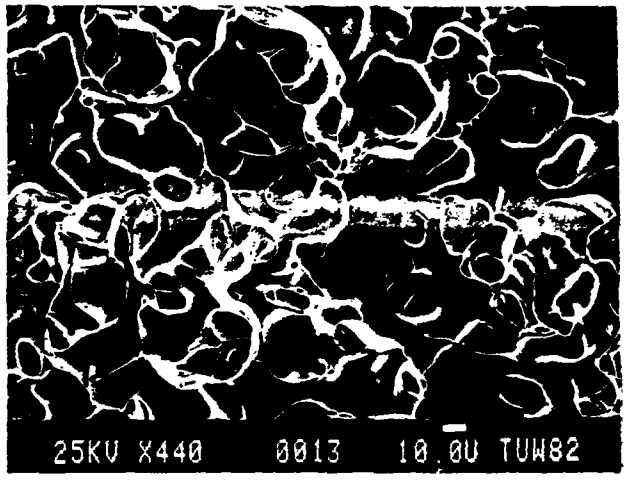

Fig.104
As Fig.10 ; only solid state sintering

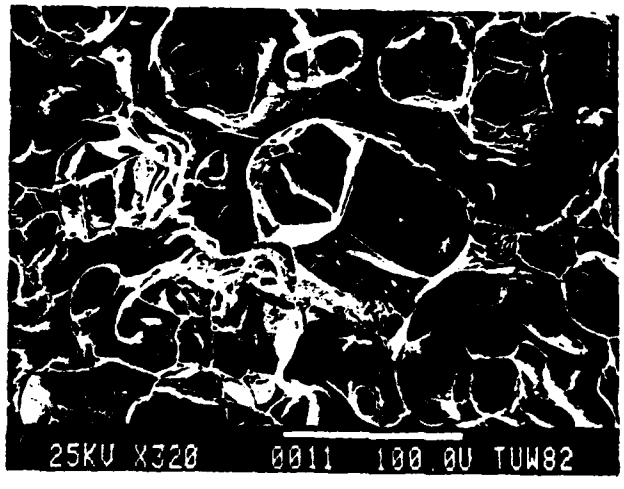

Fig.105
Heavy metal prepared from E51W; fracture surface similar to E48W material

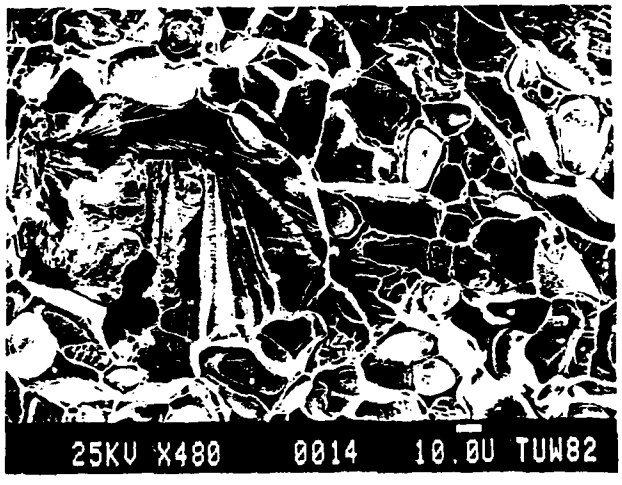

Fig.106
Heavy metal (96%W) sintered from E61W; inhomogeneous distribution of the binder

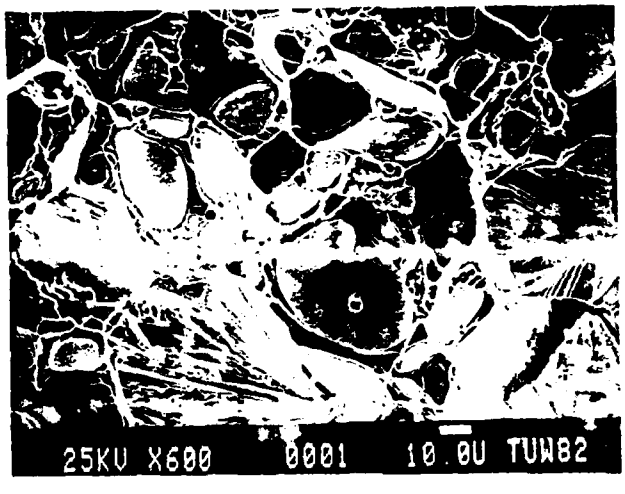

Fig.107
Heavy metal prepared from E56W (doped with Al); intergranular fracture predominant

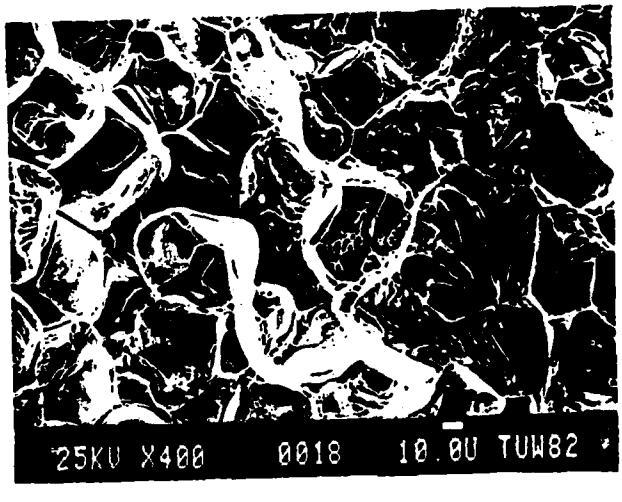

Fig.109
Heavy metal prepared from E71W (50ppm K); isolated pore

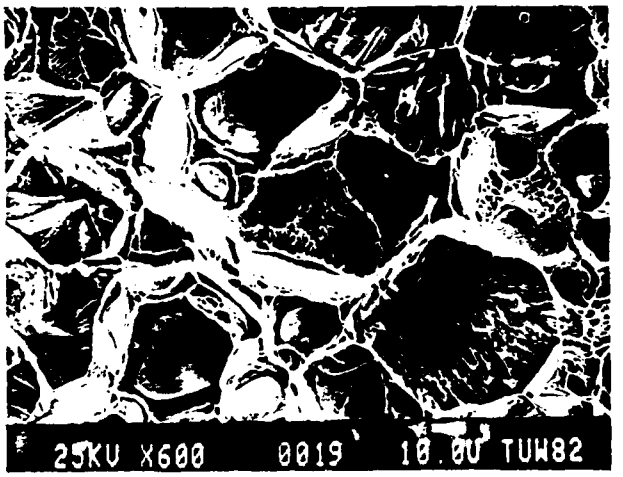

Fig.110
Same surface as on Fig.115; no pores visible

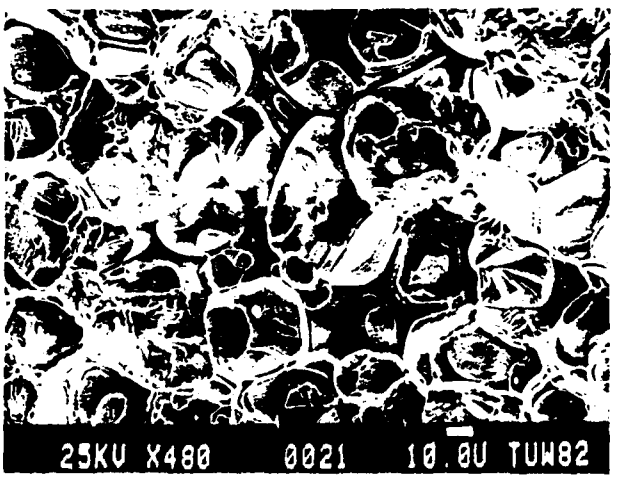

Fig.111
Heavy metal prepared from 1.83W; small pore

Fig.112
Same surface as on Fig.117; apparently satisfactory structure

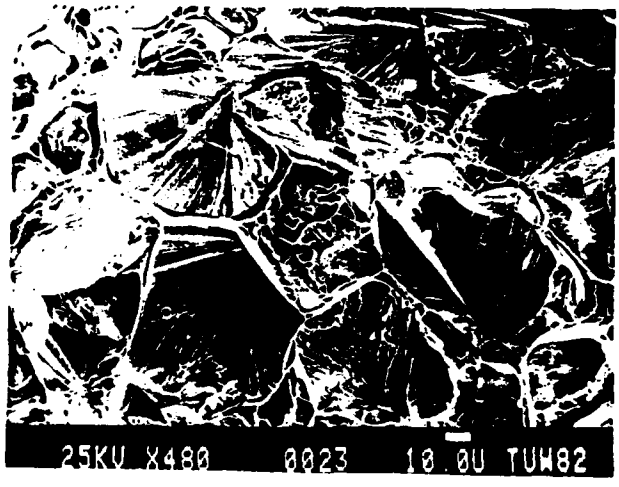

Fig.113
Heavy metal (96%W) prepared from standard W powder W640/81; trans-granular fracture and excellent ductility

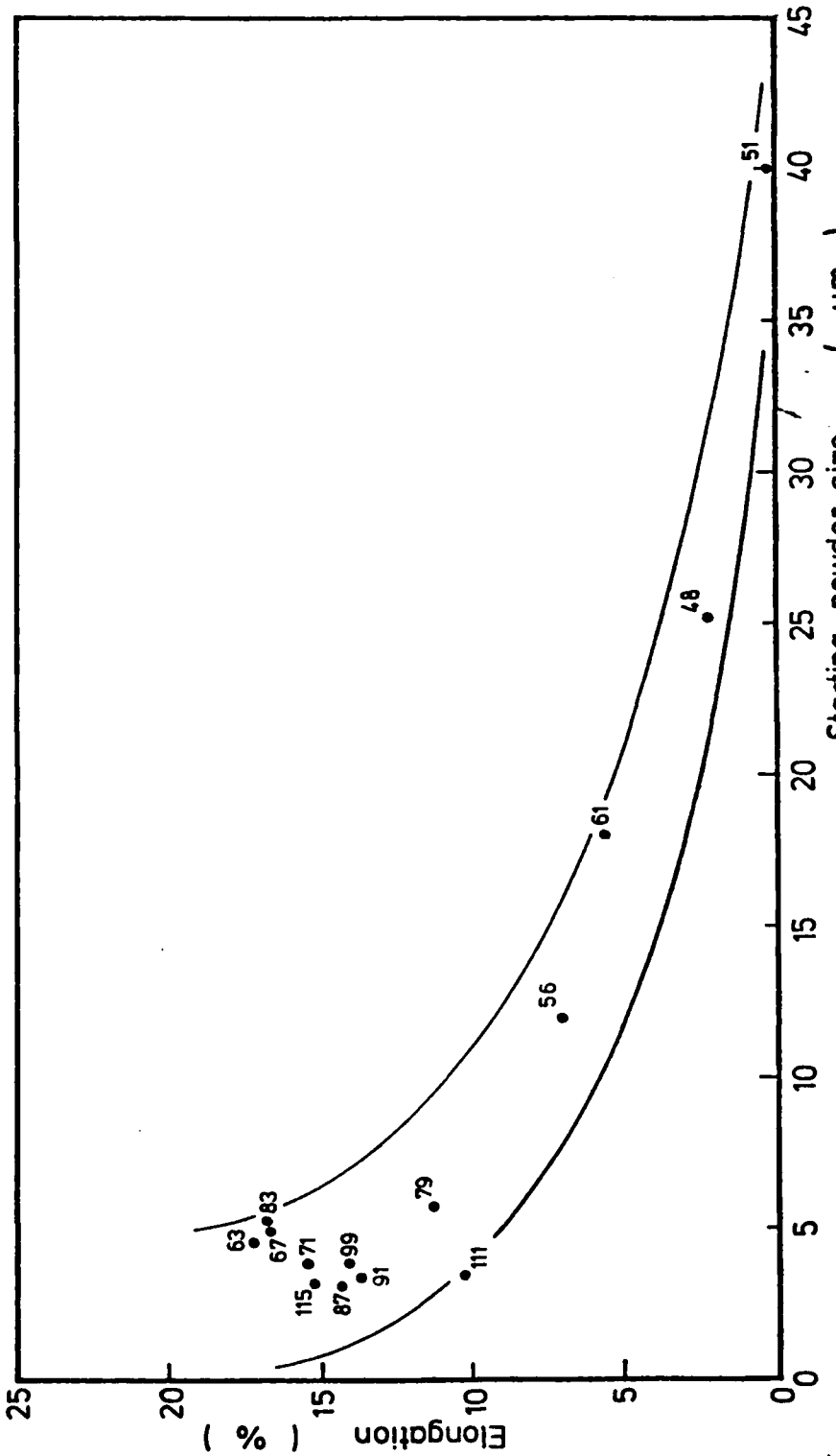

Fig.108: Influence of the starting W powder size on the ductility of heavy metals (96%W) uniformly sintered 30 min at 1580°C.

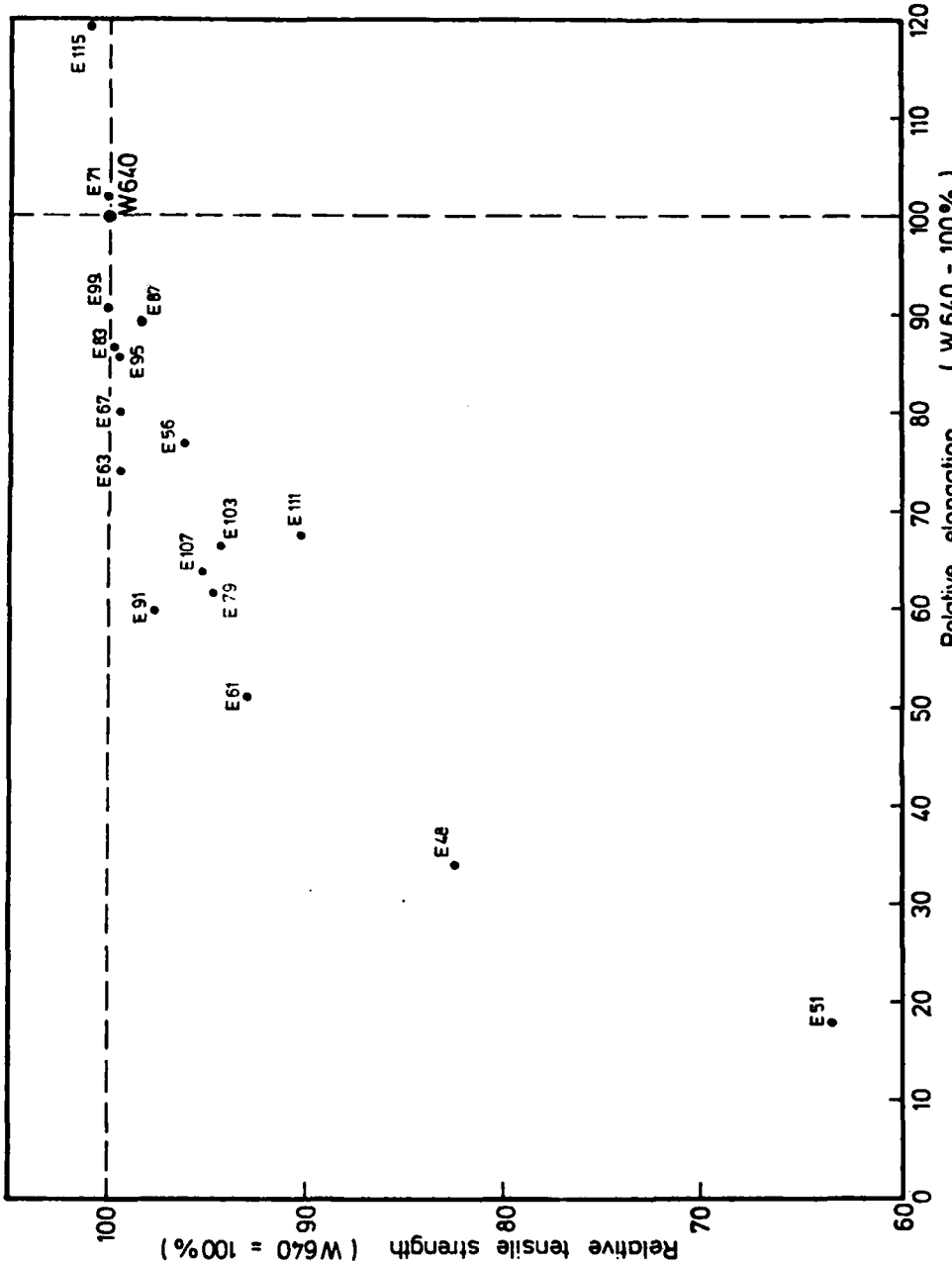

Fig.114: Relative tensile strength and elongation of various W heavy metals
(90W - 6,7Ni - 3,3Fe)

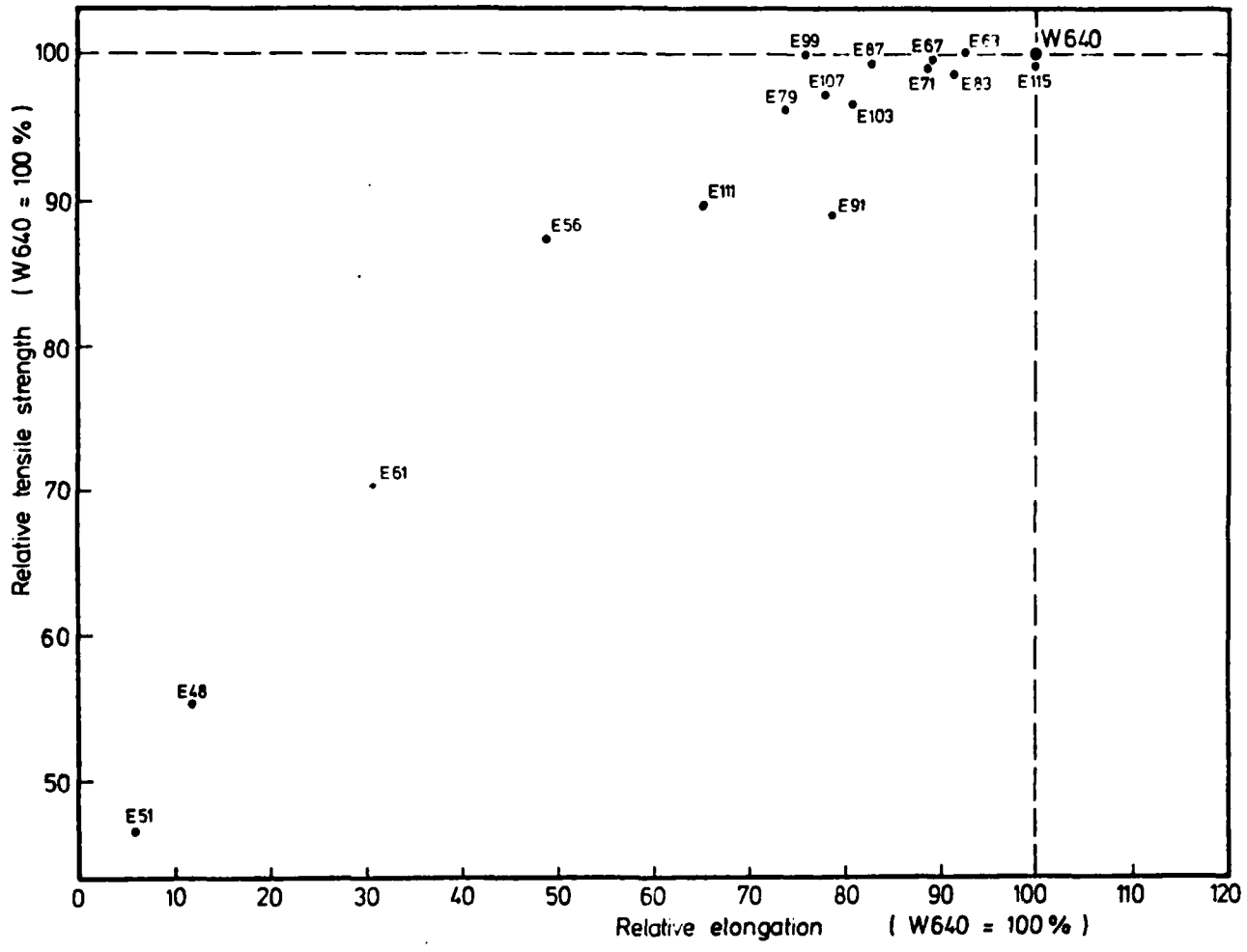

Fig.115: Relative tensile strength and elongation of various heavy metals
(96%W - 2,7%Ni - 1,3%Fe)

5. Heavy metals doped with carbon

From the production process, W and esp. the carbonyl powders Ni and Fe contain considerable amounts of carbon (219 ppm in Fe, 707 ppm in Ni), and furthermore, traces of pressing lubricant not removed during dewaxing may also contaminate the heavy metals. Therefore it was decided to investigate the effects of C addition on the heavy metals. By adding the carbon as very fine WC (0,7 µm) and mixing the powders carefully, homogeneous distribution was expected. The C concentrations selected were 50, 100 and 500 ppm; to keep the effect of the carbon contained by Ni and Fe as low as possible, the experiments were carried out with samples containing 96% W. This type of heavy metals had been shown by earlier experiments to be more sensitive towards impurities than heavy metals with higher binder content. The results of the tests are shown in Tables 36-38.

Table 36: Mechanical properties of W heavy metals (composition 96% W - 2,7% Ni - 1,3% Fe) doped with various amounts of C and sintered 30 min. at 1580°C.

50 ppm C			100 ppm C			500 ppm C			reference samples (undoped)		
ϱ (g/cm)	σ_B (MPa)	δ (%)	ϱ (g/cm)	σ_B (MPa)	δ (%)	ϱ (g/cm)	σ_B (MPa)	δ (%)	ϱ (g/cm)	σ_B (MPa)	δ (%)
18,2998	994	19,2	18,3244	998	18,8	18,2960	990	14,0	18,3239	993	23,0
18,2978	957	14,0	18,3170	1011	19,0	18,3352	985	13,6	18,2982	1007	19,0
18,3158	1009	21,2							18,2993	988	16,0
18,3019	998	13,8	18,3147	998	20,4	18,3244	988	22,8	18,3026	1018	21,6
18,3197	966	16,2	18,3090	999	22,0	18,3336	969	14,4	18,3243	975	16,8
18,3677	965	16,2	18,3421	986	21,6	18,3329	984	15,0			
18,3298	985	19,0	18,3220	994	20,8	18,3382	831	5,4	18,3125	984	21,2
						18,3262	927	10,8	18,3218	967	16,2
									18,3223	964	21,2
18,3690	969	22,2	18,3418	936	12,0						
18,3418	966	14,8	18,3231	959	15,8	18,3539	976	17,8	18,3314	969	20,2
18,3381	979	19,4	18,3486	979	15,0	18,3159	705	3,6	18,3021	944	12,8
18,3375	984	18,4	18,3185	976	20,6	18,3495	964	18,8	18,3558	978	18,2
18,3237	951	15,0	18,3065	967	19,2	18,3395	944	12,6	18,3310	972	23,6
			18,3285	956	16,0						

Table 36 continued

Mean values ± standard deviation

500 ppm C:	18,3314 ± 0,016	993 ± 88	13,5 ± 5,6
100 ppm C:	18,3243 ± 0,013	979 ± 21	18,2 ± 3,0
50 ppm C:	18,3278 ± 0,022	976 ± 16	17,4 ± 2,7
standard (undoped)	18,3188 ± 0,017	980 ± 20	19,2 ± 3,2

As shown by the experiments, 50 and 100 ppm C do not cause a significant deterioration of the mechanical properties, neither of tensile strength nor , which is more important, elongation. The tensile strength values do not show any difference to those of standard samples, and the decrease in elongation is so small that it is really within the range of the natural scatter. Only in case of 500 ppm C both tensile strength and elongation are considerably lower, and esp. the scatter of the values is much higher, which indicates that the distribution of C within the samples is of critical importance. This hypothesis is supported by C analyses carried out with samples of different elongation; no significant correlation between elongation and C content could be found. For technological purposes, therefore, contamination of heavy metals with C due to insufficient dewaxing seems to be not extremely harmful, although care must be taken to avoid excessive C residue in the material.

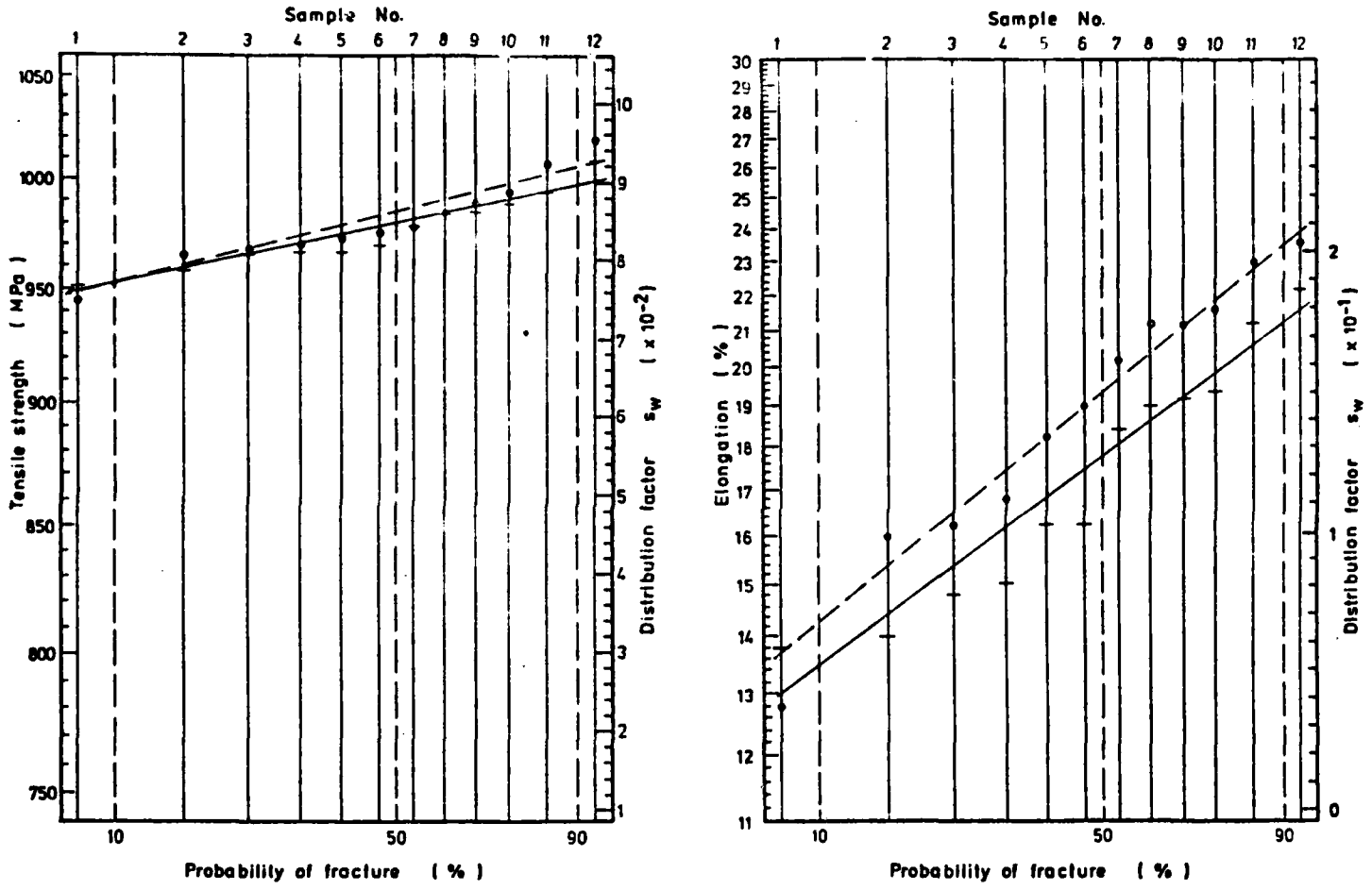

Fig.116: Weibull-diagrams for heavy metal doped with 50ppm C and undoped standard samples

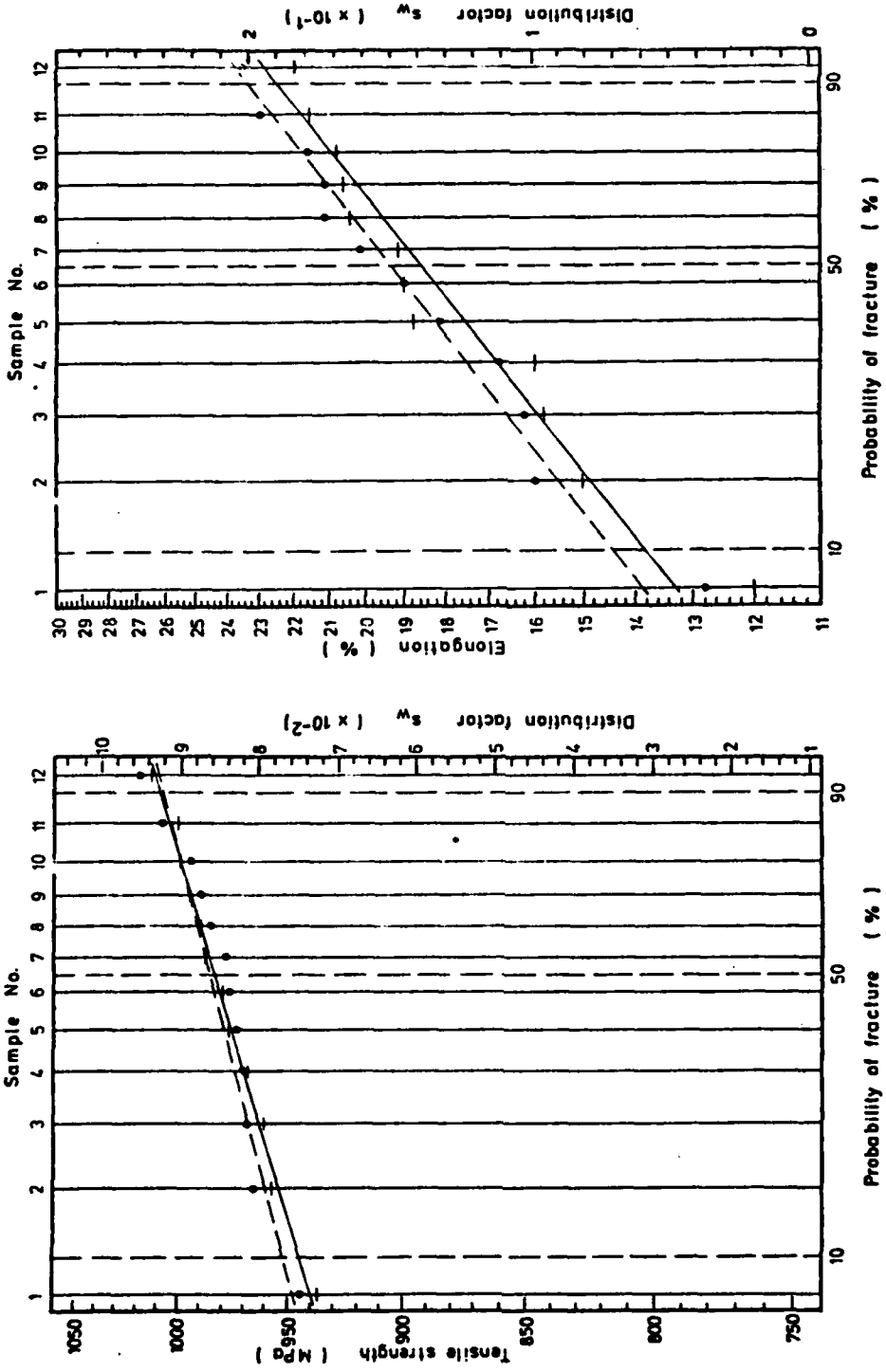

Fig.117: Weibull-diagrams for heavy metal doped with 100ppm C and undoped standard samples

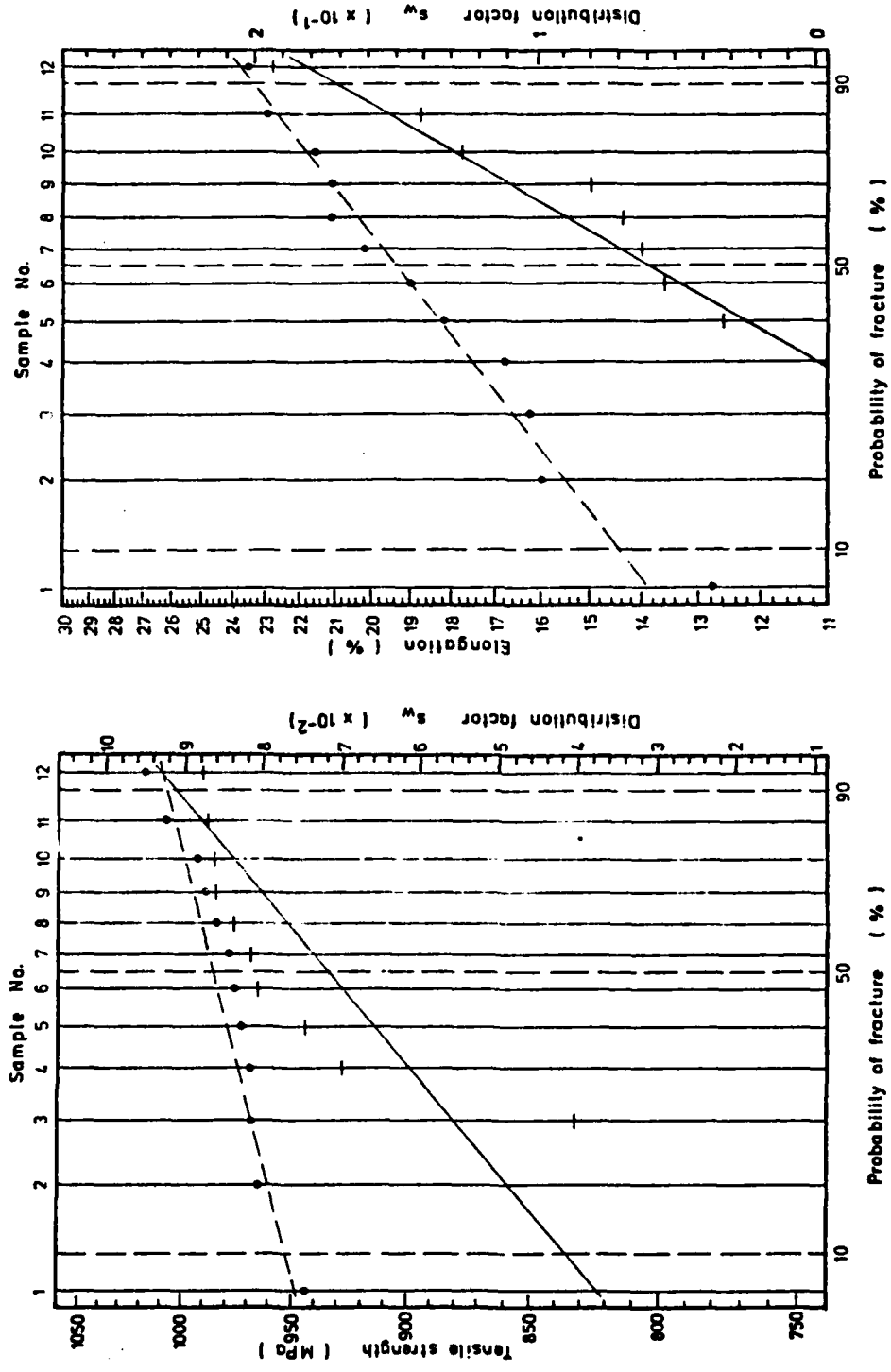

Fig.118: Weibull-diagrams for heavy metal doped with 500ppm C and undoped standard samples

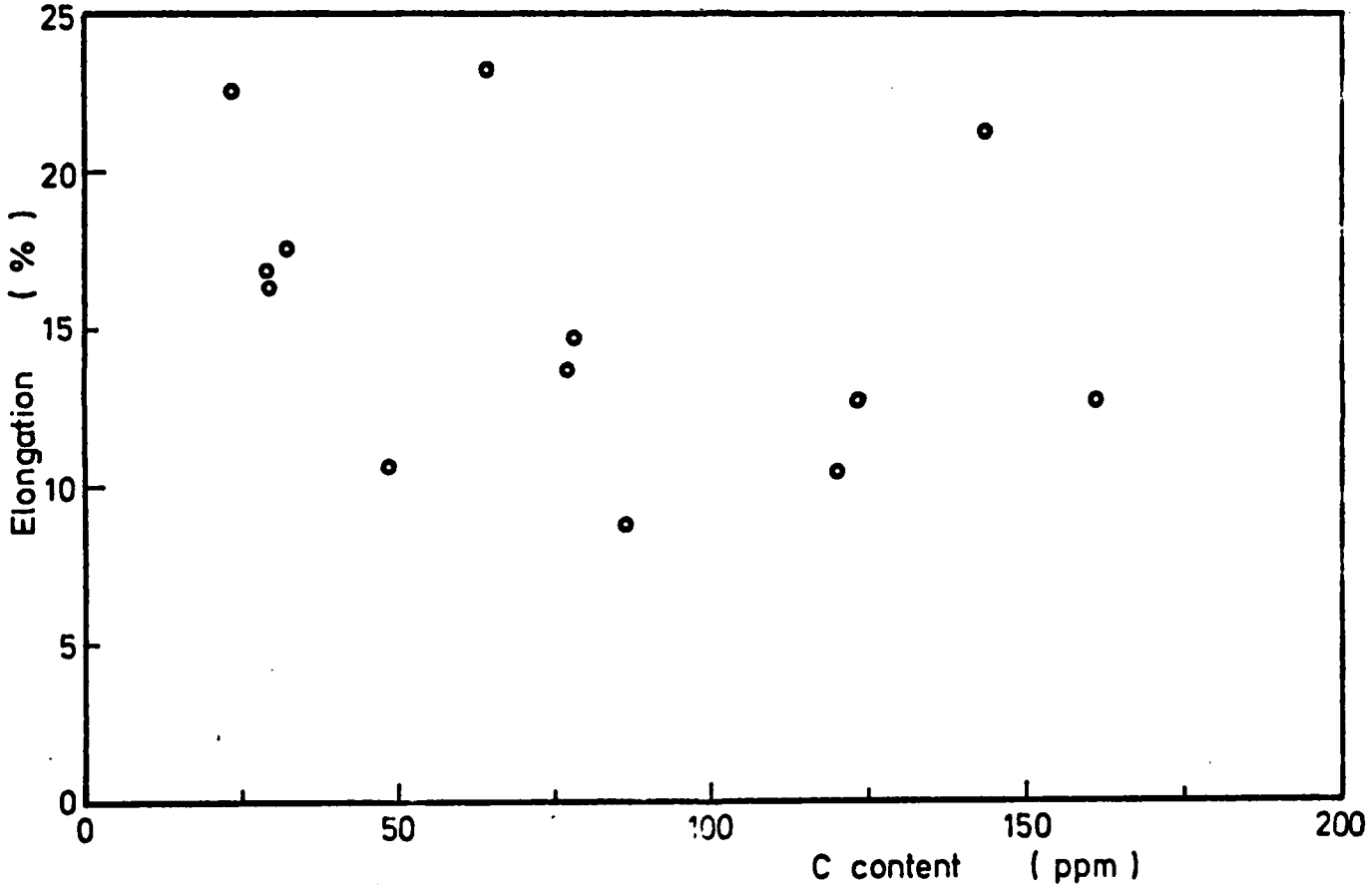

Fig.119: Elongation of W heavy metals (96%W) plotted against the C content; evidently no correlation

6. Summary

The work carried out in the last year concentrated on the investigation of the effects of trace impurities in the starting W powder on the sintering behavior and the resulting properties of the heavy metals. To explain possible effects of the impurities on the sintering process, a thorough investigation of the sintering process with standard (undoped) samples was regarded necessary. These experiments were carried out by sintering heavy metals of uniform composition (90W, 6,7Ni, 3,3Fe) at constant temperature but for different length of time. It was shown that a fundamental change occures in the microstructure of the heavy metals during sintering, which changes are necessary to obtain the mechanical properties desired. After prereduction (slow heating up to 1400°C), the samples are almost fully dense, and their tensile strength is surprisingly high, but as their microstructure is quite similar to that of pure W, the elongation is accordingly low. During liquid phase sintering the tensile strength improves rapidly; the elongation rises much slower, following the rounding of the grains and the homogeneous distribution of the binder. After 15 - 20 min. the typical microstructure of heavy metals has developed, with resulting high tensile strength and elongation. At longer sintering times however, the mechanical properties decrease sharply, as pores are formed in the structure, apparently by slow reduction of remaining oxides by hydrogen dissolved in the binder. The micropores grow through Ostwald-ripening untill they are sufficiently large to weaken the structure and to cause failure at low degrees of deformation.

The investigations carried out with doped W powders were based on these results. Generally, it was shown that the least satisfactory materials were obtained when using coarse W powders (>10 µm). SEM-photos revealed that these samples had not sintered properly, the liquid phase sintering being confined to a few areas, while in other parts of the samples only solid

state sintering had occurred, the resulting microstructure being similar to that observed with only prereduced samples. Apparently the uniform distribution of the binder melt in the W skeleton is not afforded in these materials, the capillary forces being too low, as the pores left after prereduction are still too large to surge the binder melt into them. This phenomenon was more pronounced with samples containing 96% W than with those with 90% W, which is logical because of the much lower amount of binder available in the former type of heavy metals.

This type of porosity is quite different, and easily discernible, from that observed with heavy metals prepared from several other powders. In the latter case, pore formation occurs during liquid phase sintering, in areas that have already been filled with binder melt. This second type of porosity is similar to that observed with heavy metals sintered for too long times, indicating that reduction of oxides is responsible for the porosity in these cases, too. Pore formation was observed with powders containing several elements that form rather stable oxides (e.g. Na, Si, rare earths) which may be reduced to some extent during sintering, but most probably act as oxygen transporters and thus accelerate pore growth, pore formation thus being observed at fairly short sintering times at which the standard (undoped) samples are still pore-free. Surprisingly, this type of porosity is more pronounced in heavy metals containing 90% W than with 96% W. If the dopants themselves were reduced, the reverse would be expected, but as probably the reduction of W, Ni and Fe oxides is responsible for pore formation, this effect can easily be explained, because the more effective prereduction in case of 96% W (up to much higher temperatures) leaves less oxide to be reduced during liquid phase sintering.

The investigations carried out with carbon doped heavy metals showed that up to considerable C contents in the starting materials ($\geq$100 ppm) no deterioration of the mechanical properties occurs; apparently the carbon reacts with oxides

covering the powder particles already during prereduction and is thus largely removed as CO. Only with 500 ppm of C added, a marked decrease of tensile strength and elongation was observed, the wide scatter of the individual values indicating that the distribution of C rather than the overall content determines the resulting properties. Under technical conditions, however, C contamination of the heavy metals due to incomplete dewaxing is largely eliminated during prereduction, which explaines the low sensibility of heavy metals towards changes of the dewaxing process observed in earlier investigations.

Conclusively it must be stated that both careful control of the sintering process and selection of the starting materials are of decisive importance for the production of heavy metals. Improper sintering may cause embrittlement by oxygen or hydrogen and/or pore formation in the material; selection of unsuitable starting W powders may result in insufficiently sintered or at least porous heavy metals, which both are unsatisfactory for most applications. Although the effects of several nonmetallic (e.g. O,H) and metallic impurities (Na,K,Al,...) have been shown to advantage, there is still a lot of investigation to be done to gain overall knowledge about the mechanisms through which the impurities influence the sintering behaviour and thus the properties of heavy metals.

Literature:

1) Contract No. DAJA-80-C-008, First Annual Report

2) Contract No. DAERO-78-G-086, First Annual Report

3) Contract No. DAERO-78-G-086, Final Technical Report

4) R.V.Edmonds, D.N.Jones: Met.Transactions AIME 10A(1979)289

5) L.Ekbom: Scand.J.Metallurgy 5(1976) 179

6) H.Danninger, G.Jangg, E.Lassner, B.Lux: high temp., high press. 1981, vol.13, 541

7) R.V.Minakova, A.N.Pilyankevich, O.K.Theodorovich, I.N.Frantsevich Poroshkovaya Met. 6(66)(1968) 61

8) H.Mayer, E.Lassner, M.Schreiner, B.Lux: high temp., high press. 1981, vol.13, 529

9) E.Lassner, H.Petter, B.Tiles: Planseeber.Pulvermet.23(1975)86

10) S.Jamazaki, I.Koseki, S.Ogura, R.Akijama: Planseeber.Pulvermet. 22(1974)279

11) J.Neugebauer: Planseeber.Pulvermet. 23 (1975) 77

12) G.Petzow, W.J.Huppmann: Z.Metallkde. 67 (1976) 579

13) E.G.Zukas, P.S.Z.Rogers, R.S.Rogers: Z.Metallkde. 67 (1976) 591

14) C.Agte: Hutnicke Listy 8 (1953) 227

15) W.A.Kaysser, F.Puckert, G.Petzow: Powder Met.Int.12, No.4 (1980) 188

16) K.S.Churn, D.N.Yoon: Powder Met. 1979, No.4, 175

17) H.Kostron: Z.Metallkde. 43 (1952) 269,373

18) S.N.Tiwari, J.Beek: Metal Sci. 1978 , 356

19) W.Weibull: Appl.Mech.Rev. 1952, 449

20) H.E.Exner: Materialprüf. 7 (1956) 357

21) W.A.Kaysser, O.J.Kwan, G.Petzow: Int.Powder Met.Conf.1982, Florenz

22) V.Smolej, S.Pejovnik, W.A.Kaysser: Powder Met.Int.14 (1982) 34

END

DATE
FILMED

7 83

DTIC